A Novel Approach to the Strain Based Analysis of Dented Pipelines

by

Chike Okoloekwe

A thesis submitted in partial fulfillment of the requirements for the degree of

Master of Science
in
Structural Engineering

Department of Civil and Environmental Engineering
University of Alberta

Abstract

Pipelines form an integral component of the distribution network of oil and gas products, which have to be transported from production sites to markets far off where there is need for them. Pipelines thus have to traverse long distances and as any other structure are susceptible to damages with use. A common cause of damage is the mechanical damage in pipeline in the form of dents, which are caused by a host of factors ranging from, but not limited to construction errors, ground movement and third-party interactions. While some dents in a pipeline might be dormant features, some have the potential to affect the structural integrity of the pipeline thus resulting in the immediate or delayed failure of the pipeline. It becomes necessary that some measure be put in place for accessing the severity of dents in order to prioritize allocation of the resources in the implementation of management strategies. The codified stipulation of the Canadian pipeline code, CSA Z662-16, proposes the depth based criterion as a measure of the severity of dents in pipelines. History and research have however shown that this approach fails to accommodate other factors such as the localized strain and stress distribution because of the geometry of the dent, as a dent might fall below the codified deformation limits while violating the localized plastic strain or stress limits. As an alternative to the traditional depth based approach, the American Society of Mechanical Engineers Standard for gas pipelines, ASME B31.8-16, presents a set of non-mandatory closed form expressions for evaluating the strains in pipelines in a bid to generate the strain state of the dented region based on the dent profile. This technique has, however, been criticized for inaccuracies in its assumptions. Well aware of the pitfalls of existing analytical evaluation techniques for the strains in dented pipeline, some pipeline operators subscribe to the numerical modeling via Finite Element Analysis (FEA) of dents as assessment technique, a procedure regarded to be computationally demanding and

resource intensive. The work presented herein is a novel technique for evaluating the strains in dented pipelines based solely on data obtained from inline inspection devices. This study discusses two ideas. The first proposes a new technique for the strain analysis of thin walled structures through a combination of B-Spline interpolation and deformation discretization. This technique allows for the evaluation of all the components of the strain tensor that defines the strain state of the dented pipeline. The second novel approach is extending the proposed technique and the existing ASME B31.8-16 equations into a three-dimensional continuum, thus allowing for a more elaborate analysis without loss in the generality of the procedure.

Preface

This thesis is an original work by Chike Okoloekwe. The following academic articles are presented in chapters, 2, 3 and 4 respectively;

1. **Okoloekwe, C**., Kainat, M., Langer, D., Hassanien, S., Cheng, R. and Adeeb, S. (2017). Deformation Analysis of Dented Pipelines via Surface Interpolation. Proceedings of the Pressure Vessels and Piping Conference (PVP), Waikoloa, Hawaii, USA

2. **Okoloekwe, C**. Aranas, N., Kainat, M., Langer, D., Hassanien, S., Cheng, R. and Adeeb, S (2017). Improvements on the ASME B31.8 Dent Strain Equations. Under review with the Journal of Pressure Vessel Technology.

3. **Okoloekwe, C**., Kainat, M., Langer, D., Hassanien, S., Cheng, R. and Adeeb, S. (2017). Three-Dimensional Strain Based Model for the Severity Characterization of Dented Pipelines. Under review with the Journal of Nondestructive Evaluation, Diagnostics and Prognostics of Engineering Systems.

For the above mentioned studies, Okoloekwe, C., Cheng, R. and Adeeb, S. developed the methodology, Okoloekwe, C. performed the numerical analysis, analyzed the results and produced the manuscripts, Aranas, N. assisted with validating the numerical models and the results of the investigation were reviewed by Kainat, M., Langer, D. and Hassanien, S.

Dedication

Dedicated to my family, Vincent, Rose, Marian, Cecelia and Mary

Acknowledgements

I will begin by thanking my supervisor, Dr. Samer Adeeb for providing me with the right mentorship and believing in me. His constant support and patience helped me throughout the course of the program. I have been able to learn a lot under his supervision both in and out of the classroom and our academic meetings. I indeed feel privileged to have obtained my Master's degree under his tutelage.

I would like to thank the Faculty of Graduate Studies at the University of Alberta, for providing me with the Graduate Recruitment Scholarship.

I would also want to acknowledge Enbridge Liquid Pipelines for providing supporting funds, the opportunity for onsite training and access to valuable information that enhanced the speed and the rigor of the study.

I am also thankful to my colleagues at the University of Alberta especially Diana Abdulhammed, Nikko Aranas, Akash Bajaj, Jonelle Jn. Baptiste and Onyekachi Ndubuaku for the invaluable help received from them in the course of the research, I could not ask for a better set of colleagues.

I would like to appreciate the efforts of the industrial collaborators at the Pipeline Integrity and Reliability group, Enbridge Liquid Pipelines, Edmonton, in particular, Doug Langer and Muntaseer Kainat for the technical advice and mentorship which went a long way in improving the quality of the academic publications produced from the study.

Finally, I would also want to extend my appreciation to my Parents for the constant prayers, emotional and financial support during my studies. I hope this degree makes you proud.

Table of Contents

List of Figures

List of Tables

Chapter1- Introduction

1.1 Background and Problem Statement

Oil and gas pipelines are a demonstrably safe means of transporting hydrocarbons (Macdonald and Cosham, 2005) and typically are used to transport oil and gas products from production sites to far off markets where they are required. Pipelines are left exposed, buried, or laid on the seabed depending on the geography of the region, environmental condition, safety concerns and as a means to optimize the financial implications of operating the pipeline. However, like any other infrastructure, pipelines are subjected to different loading and environmental conditions and as such there are always risks and uncertainties associated with them. Mechanical damages (dents, gouges and corrosion) have been identified as a common cause of the failure of the pipeline (Cosham and Hopkins, 2004). Mechanical damage in the form of dents in pipelines could be because of an imperfection in the pipeline during the forging process, influenced by human activities in the process of the transportation and laying of the pipelines or natural actions such as ground excitation. Dents have been defined as inward plastic deformations in pipelines (Cosham and Hopkins, 2003) and are typically classified under the following categories:

1. Smooth-Dents leading to a smooth change in the curvature of the pipe wall;
2. Kinked-Dents resulting in an abrupt change in the curvature of the pipe wall;
3. Plain-Dents without stress concentrations and wall thickness reductions;
4. Constrained-Dents prevented from rebounding and re-rounding due to the constant surface to surface contact with the indenting body; and
5. Unconstrained-Dents allowed elastic rebounding and inelastic re-rounding when the indenting body is removed.

The presence of dents in pipelines has the potential to lead to serviceability or integrity concerns (Rosenfeld et al., 1998, Panetta et al., 2001, Dinovitzer et al., 2002, and Hanif and Kenny, 2014). The failure of pipeline structures can be severe, leading to the loss of lives, property and perturb the balance in the ecosystem.

As not all pipelines can be easily accessed via visual inspection as they may be buried underground or be laid on a seabed, pipeline inspection gauges (PIGs) are thus commonly used to inspect pipelines. The PIGs are equipped with calipers or sensors through the circumference of the tool. PIGs run through pipelines and reports the geometry of the pipeline from which geometric anomalies along the pipe's span can be identified. These inspection tools also collect precise data regarding the location and the orientation of these anomalies. The data obtained from such inspections is used to reconstruct the anomaly and make a decision on structural integrity state of the pipeline. In many countries of the world, pipeline regulations not only demand inspections or monitoring of structural integrity at certain intervals, but a continuous process of verification of pipeline integrity and fitness-for-purpose (Barbian and Beller, 2012). It thus becomes necessary that pipeline operators are well versed in the concepts of pipeline mechanical damage.

Various studies have been performed to fully understand the effect of mechanical damage on the structural integrity of pipelines. Ong et al., (1992) performed full scale experimental studies and FEA in investigating the elastic strain distribution in plain dented pipelines. The study revealed that the peak stresses developed in dented surface is a function of the indenter shape and for the cases studied, the burst strength of the pipeline was insensitive to the presence of localized dents and the thinning of the pipe wall during the deformation posed a greater threat. Fowler et al., (1993) investigated the effect of the $\frac{D}{t}$ ratios (where D is the diameter of the pipeline and t is the

thickness of the pipe wall) on the fatigue behavior of dented pipelines using full-scale tests. Several of the geometric ratios were considered and the dented pipelines were fatigue cycled. This study revealed that the fatigue life of a dent decreased with increasing $\frac{D}{t}$ ratios, which implies that dents in thin walled pipelines are more susceptible to fatigue cycling when compared to thick walled pipelines. The work by Rosenfeld, et al. (1998) on evaluating the strains in defected pipelines identified three strain components required to properly define the strain state of a dented pipeline. These components are the longitudinal bending strain, longitudinal membrane strain, and circumferential bending strain. Once all three strain components were obtained, it was assumed that the strain components occur at the peak of the dent. With these strain components evaluated, the peak strain values at the external and the internal surface of the pipeline can be easily evaluated as an algebraic combination of the obtained directional strain components.

Various attempts have been made by independent bodies to characterize dents in the order of severity by setting acceptability limits. The most common premise for the characterization of the severity of a dent is the depth of the dent. The dents are deemed to be potential threats if the depth is greater than a fraction of the outer diameter (OD) or the nominal pipe size (NPS) at a particular operating condition, usually the Specified Minimum Yield Strength (SYMS). Table 1-1 shows various stipulations regarding the acceptability limit for plain dents set by different standards.

Table 1-1. Acceptability limits for plain dents (Race, et al., 2010).

	PLAIN DENTS	
	Constrained	**Unconstrained**
ASME B31.8	Up to 6% OD or strain level up to 6%	
ASME B31.4	Up to 6% OD in pipe diameters > NPS4” Up to 6 mm in pipe diameters < NPS 4”	
API 1156	Up to 6% OD but > 2% OD requires a fatigue assessment	
EPRG	≤ 7% OD at a hoop stress of 72% SMYS	
PDAM	Up to 10% OD	Up to 7% OD
CSA Z662	Up to 6 mm for ≤ 101.61 mm OD, or < 6% OD for > 101.6 mm OD	

Although the depth of the dent could be indicative of a potential concern with a dent, it has been noted that the depth of the dent is not sufficient to characterize the severity of the dent (Baker, 2004, Dawson et al., 2006 and Rafi et al., 2012). An advisory (Erikson, 2010) was released by the National Energy Board of Canada to pipeline operators under its jurisdiction regarding incidents where the codified stipulations as regarding the dent depth failed to identify the impending failure of pipelines. This was to serve as an indication of the need to revise the current pipeline integrity management and assessment strategies as the depth alone does not provide sufficient information for judging the severity of a defect.

A strain based criterion tends to be more informative regarding the severity of a deformation along the pipeline as it takes into consideration the localized distortion of the regions around the dent and the curvature of the profile of the dent rather than the global overlook of the dent

topology. The ASME B31.8-2003 provides the non-mandatory strain equations that allow for the evaluation of the strains in a dented pipeline by discretizing the strains into the directional components and algebraically combining these directional components to evaluate the equivalent strain on the surface of the dented pipeline, similar to the work done by Rosenfeld et al. (1998). There is, however, no codified explicit guideline on the implementation of these equations (as to how to obtain the variables) and as such its use is often subjected to the expertise of the operator. The works by Noronha et al. (2010), Baker (2004) and Rafi et al. (2012) identified lapses in the codified strain equations and focus areas for a more elaborate technique for evaluating the strains on the dented segment. One of which were addressed in the ASME B31.8-2007 edition.

Well aware of the shortcomings of the codified techniques, some operators opt for the use of numerical modelling for the integrity assessment of defects in pipelines via FEA. The nonlinear numerical modelling with FEA allows for the simulation of the indentation of the pipeline and as such the residual stresses and strains associated with the deformation can be obtained for well-defined pipeline geometric and material models (Belanger and Narayanan, 2008). These solutions can be computationally demanding and expensive as it might require numerous simulation trials to be run in order to achieve a geometric match with the reported dent profile. The accuracy of the numerical modelling technique is hinged on the representation of the actual reported dent with a numerical model as described in (Woo et al., 2017) and this increases the complexity of the procedure and subsequently the technical expertise required for the analysis of the deformation. With the large number of dents reported by PIG's, the numerical modelling approach with FEA becomes a relatively expensive option. Analytical evaluation of the deformation and associated stresses and strains would be a more efficient technique for the severity characterization of dents.

The work presented herein is aimed at improving the utilization of the existing codified expressions for evaluating strains and introduce a novel approach to the evaluation of the strains in a dented pipeline based on the data reported by PIGs.

In this study, we propose two improvements to the strain analysis of dented pipelines. The first is a modification to the use of codified equations for evaluating the strains in dented pipelines. The codified closed form expressions are currently implemented on the dent profile with the maximum dent depth. This might, however, be counterproductive, as the depth of the dent is not the only governing factor. Dents in pipelines affect the three-dimensional continuum of the pipeline and as such there might be a profile having a deformation contour with high strain concentrations which is not aligned with the dent profile having the maximum depth. A three-dimensional representation of the dent topology would thus be more descriptive of the strain state of the pipeline.

The second focus of this study is developing a technique for evaluating the strains in dented pipeline from the directional displacement of the pipeline. While the PIGs report the radial displacement of the pipeline, one would intuitively expect the radial displacement to be associated with displacements in the longitudinal and the circumferential directions. However, these components cannot be measured easily. The investigation performed as part of this thesis evaluates the directional displacements associated with the radial displacement reported from in-line inspections within the confines of continuum mechanics. With the directional displacements (longitudinal, circumferential and radial) evaluated, the gradients of the displacements can be calculated and subsequently, the directional strains associated with the said displacements. By discretizing the deformation into the respective components, it would be possible to account for strain components initially ignored in the current implementation of the codified dent strain

equations. This technique provides a flexible model for the strain analysis of dented pipelines that allows the operators the choice of the strain measure and also comes equipped with the ability to account for the geometric and material nonlinearities associated with the indentation of the pipe. This novel approach to the strain analysis of dents is also extended to a three-dimensional continuum, which provides the global strain state of the pipeline.

1.2 Organization of Thesis

The thesis is divided into five chapters. Chapters two to four are based on peer reviewed publications that discuss the various studies carried out in achieving the global objective of this thesis of improving the analytical strain analysis of dented pipelines.

Chapter two is from a scientific paper published in the proceedings of the 2017, Pressure Vessels and Piping Conference. The paper discusses the concepts of the proposed deformation discretization technique for the strain analysis of dented pipelines. The governing equations of this novel approach are discussed and a typical case of a dented pipeline is investigated. The predictions of this approach are benchmarked against the predictions of a numerical model and the codified dent strain expressions.

Chapter three is a scientific paper prepared for submission to the International Pressure Vessels and Piping Journal. It discusses the extension of the codified strain evaluation equations to the three dimensional continuum and benchmarks the strain predictions of the modified closed form expressions to the predictions of numerical models developed using nonlinear FEA.

Chapter four is a scientific paper prepared as a submission to the Journal of Nondestructive Evaluation, Diagnostics and Prognostics of Engineering Systems. This paper focuses on extending the deformation discretization technique to the third dimension and comparing the

predictions of the proposed three-dimensional analysis to the predictions of numerical models generated using nonlinear FEA.

Chapter five summarizes the results obtained in this study and recommends the direction for future work.

References

ASME 2003, B31.8-2003: Gas Transmission and Distribution Piping Systems. ASME International, New York, NY.

ASME 2007, B31.8-2007: Gas Transmission and Distribution Piping Systems. ASME International, New York, NY.

Baker, M., 2004. Integrity Management Program–Dent Study. Department of Transportation, Office of Pipeline Safety, TTO Number 10.

Barbian, A. and Beller, M., 2012. In-line Inspection of High Pressure Transmission Pipelines: State-of-the-Art and Future Trends. Proceedings of the 18th World Conference on Nondestructive Testing, Durban, South Africa.

Belanger, A.A. and Narayanan, R., 2008, Direct Strain Calculation of Pipe Line Dent from Knot Migration using a Kinematic Model Free of Material Properties. Proceedings of the International Pipeline Conference, Calgary, Alberta, Canada.

Cosham, A. and Hopkins, P., 2003. The Pipeline Defect Assessment Manual (PDAM) – A Report to the PDAM Joint Industry Project. Newcastle, UK.

Cosham, A. and Hopkins, P., 2004, The Effect of Dents in Pipelines – Guidance in the Pipeline Defect Assessment Manual. International Journal of Pressure Vessels and Piping, 81(2), pp.127-139.

CSA Z662, Oil and Gas Pipeline Systems 2016.

Dawson, S.J., Russel, A. and Patterson, A., 2006. Emerging Techniques for Enhanced Assessment and Analysis of Dents", Proceedings of the International Pipeline Conference, Paper No. ASME, IPC2006-10264, Calgary, Alberta, Canada.

Dinovitzer, A., Lazor, R., Carroll, L.B., Zhou, J., McCarver, F., Ironside, S., Raghu, D. and Keith, K., 2002, Geometric Dent Characterization. 4th International Pipeline Conference (pp. 1589-1598). Calgary, Canada.

Erickson, A., 2010. Fatigue Crack Failure Associated with Shallow Dents on Pipelines. NEB. File of-Surv-Inc-02.

Fowler, J.R., 1993, Criteria for Dent Acceptability in Offshore Pipeline. Offshore Technology Conference. Offshore Technology Conference, Houston, Texas, USA.

Hanif, W. and Kenny, S., 2014, Mechanical Damage and Fatigue Assessment of Dented Pipelines using FEA. Proceedings of the 10th International Pipeline Conference, Calgary, Canada.

Macdonald, K.A. and Cosham, A., 2005. Best Practice for the Assessment of Defects in Pipelines – Gouges and Dents. Engineering Failure Analysis, 12(5), pp.720-745.

Noronha, D.B., Martins, R.R., Jacob, B.P. and de Souza, E., 2010. Procedures for the Strain Based Assessment of Pipeline Dents. International Journal of Pressure Vessels and Piping, 87(5), pp.254-265.

Ong, L.S., Soh, A.K. and Ong, J.H., 1992. Experimental and Finite Element Investigation of a Local Dent on a Pressurized Pipe. The Journal of Strain Analysis for Engineering Design, 27(3), pp.177-185.

Panetta, P.D., Diaz, A.A., Pappas, R.A., Taylor, T.T., Francini, R.B. and Johnson, K.I., 2001. Mechanical Damage Characterization in Pipelines. Pacific Northwest National Lab. Richland WASA35467

Race, J.M., Haswell, J.V., Owen, R. and Dalus, B., 2010. UKOPA Dent Assessment Algorithms: A Strategy for Prioritising Pipeline Dents. Proceedings of the 8th International Pipeline Conference, Calgary, Alberta, Canada.

Rafi, A.N.M., Das, S., Ghaednia, H., Silva, J., Kania, R. and Wang, R., 2012. Revisiting ASME Strain-Based Dent Evaluation Criterion. Journal of Pressure Vessel Technology, 134(4).

Rosenfeld, M.J., Porter, P.C. and Cox, J.A., 1998. Strain Estimation using Vetco Deformation Tool Data. International Pipeline Conference, Calgary, Alberta, Canada.

Woo, J., Muntaseer, K. and Adeeb, S. 2017. Development of A Profile Matching Criteria to Model Dents in Pipelines using Finite Element Analysis Pressure Vessels and Piping Conference, Hawaii, USA.

Chapter 2- Deformation Analysis of Dented Pipeline via Surface Interpolation

2.1 Abstract

Advances in the interpolation techniques of discrete data points and their application to monitoring the displacement of physical infrastructure have led to improved analytical strain evaluation procedures. In order to generate a detailed mathematical model of the strain state of a dented pipeline, it is necessary to decompose the deformation data obtained from monitoring devices into the corresponding radial, longitudinal and circumferential components. In this paper a technique for analytically evaluating the strains in dented pipelines, based on the coordinates of the geometric profile of the dent, is investigated; and the strains predicted from the said method are benchmarked against the strains predicted from a numerical model generated using nonlinear finite element analysis (FEA) and the codified equations for evaluating strains in dented pipes. This novel technique to strain analysis is an application of the principles of shell theory to a deformed pipeline in order to evaluate the components of the displacements in the cylindrical coordinate system. The coordinates of the deformed profile are obtained from the FEA model and interpolated with B-Splines curves, equipped with second order continuity. The resulting strain distribution along the thickness of the pipe wall is evaluated analytically by performing derivatives on the spline functions. The good agreement obtained in the strains predicted by the developed model and FEA indicates a possibility of conducting in-depth strain analysis of thin-walled structures.

Keywords – Shell Theory-Spline, Dents, Pipeline and FEA

2.2 Introduction

Cylindrical thin shell structures are used in many engineering structures, examples being water tanks, ships, domes, aircraft, pressure vessels, and pipelines. A shell structure comes equipped with the mechanical advantage of having high strength to weight ratio and efficient load bearing characteristics owing to its curvature (Foroughi et al., 2014). The typical response of these structures is governed by a set of partial differential equations or a minimized functional that predicts the resulting stresses and displacements arising from a loading scenario (Ciarlet and Mardore, 2008). The first publication on the linear elastic theory of shells discussed in (Love, 1888) established the relationship between the strain and displacement and the constitutive relationship between the stresses and the strains developed during deformation. This formed the platform for numerous studies on both linear and nonlinear shell theories (Reissner, 1952, Naghdi and Nordgren, 1963, Sanders, 1963 and Koiter, 1970). Linear elastic thin shell theories have formed the foundation for our current understanding of the dynamic response of pipelines (Bitter and Shephard, 2003) with the Kirchhoff–Love's hypothesis of straight normal being the most common premise in its formulation (Ventsel and Krauthammer, 2001). This hypothesis imposes a few constraints on the applicability of the theory as normals to the undeformed mid-surface remain straight and normal in the deformed configuration. The thickness of the pipe wall should also be a lot smaller than any other dimension and the out-of-plane strains are considered to be negligible. These constraints on the geometry and the deformation path of the shell reduce a three-dimensional deformation problem of shell to a two-dimensional case.

Pipelines, which form an integral component of the distribution and transmission network for oil and gas, like any other infrastructure are susceptible to mechanical damage, dents being a common mechanical defect having the potential to adversely affect the structural integrity of the pipeline (Dawson et al., 2006, Wu and Han, 2013 and Ghadenia, et al., 2015). Information

regarding the dent severity is of utmost importance to pipeline operators for the proper allocation of resources for management strategies. The current approach for a thorough dent analysis is via FEA, which provides a medium for predicting the stresses and strains from the material properties and shape functions of the mechanical numerical model of a pipe defect of similar geometry. This procedure is, however, computationally demanding and it can be prohibitive to perform full-scale numerical modeling of all reported dents (Belanger and Narayanan, 2008), thus the need for a tool for rapid dent severity characterization. The ASME B31.8-2016 provides a set of non-mandatory equations for the evaluation of strains in dented pipelines. However, there have been concerns about the underlying assumptions used in its derivation (Noronha, et al., 2010, and Rafi, et al., 2012). The codified stipulations also do not provide definite directions on how to evaluate some of the variables used in estimating the strain components. This paper seeks to devise a technique for the analytical evaluation of strains by assigning a thin shell model to a deformed pipeline in a bid to provide an approximate deformation path and the resulting strain state of the pipeline.

2.3 Methods

The deformation field of a dented pipeline is defined by approximating its geometrical shape using a thin shell as described in Noronha, et al. (2010) and assuming that the thin shell structure is governed by the kinematic displacement equations established in the linear shell theory. The key components of the proposed technique are discussed below.

2.3.1 Spline Interpolation

The deformation field of the dented pipe is interpolated from the coordinates of the reported dented surface using B-Spline functions discussed in Roger and Adams (1990). The generated curves have the advantage of allowing for the smooth transitions between the position vectors in

deformation fields as they are non-global and are applied in a piecewise fashion along the dented section of the pipeline. This results in a continuous and differentiable contour surface of the dent. Equation (1) presents the mathematical representation of a typical n^{th} order spline interpolation function,

$$P(v) = \sum_{i=1}^{n+1} B_i \, N_{i,k}(t) \tag{1}$$

where P(v) is the position of a vector along the internal-surface of the dented pipeline; v represents a set of variables, which in this setting are the angular position of the internal surface of the pipeline θ with interval $(-\pi \leq \theta \leq \pi)$ and Z the longitudinal distance of the pipeline with interval $(-L \leq Z \leq L)$ where L is the longitudinal distance from either side of the dent apex, B_i represents the position vectors of the vertices of the curves, $N_{i,k}$ are the normalized basis functions, and k represents the degree of the function. Cubic spline functions, which provide second order continuity, are used to interpolate the dent profile investigated in this study, as unique values for the changes in the slope at each point along the dent profile can be obtained from such functions. The basis function can be defined by the Cox –de-Boor recursion formulas (Roger and Adams, 1990) shown in equations (2) and (3)

$$N_{i,1}(v) = \begin{cases} 1 \text{ if } v_i \leq v \leq v_{i+1}) \\ 0 \text{ Otherwise} \end{cases} \tag{2}$$

and

$$N_{i,k}(v) = \frac{(v - v_i) N_{i,k-1}(v)}{v_{i+k} - v_i} + \frac{(v_{i+k} - v) N_{i+1,k-1}(v)}{v_{i+k} - v_{i+1}} \tag{3}$$

The formulation is such that the relationship ($v_i \leq v_{i+1}$) is satisfied. The splines follow the shape of the control polygon, which is defined by the coordinates of the dent, and does not oscillate about any straight line. The first and second derivatives of neighboring spline functions

are equal at the nodes they meet. With these conditions, a tridiagonal equation is formed from which the constants of interpolation are obtained. Depending on the degree of precision of the inline inspection tool used to extract the dent profile, it is common for such reported data to contain noise. Thus, becomes pertinent the need for some filtering technique such as the Fast Fourier Transform to be employed to remove the oscillations and produce smoothened coordinates of the dent profile. A detailed description of the filtering algorithms is outside the scope of this study. Figure 2-1 below is a typical cubic B-Spline spline function fitted over data points that defines a deformed profile.

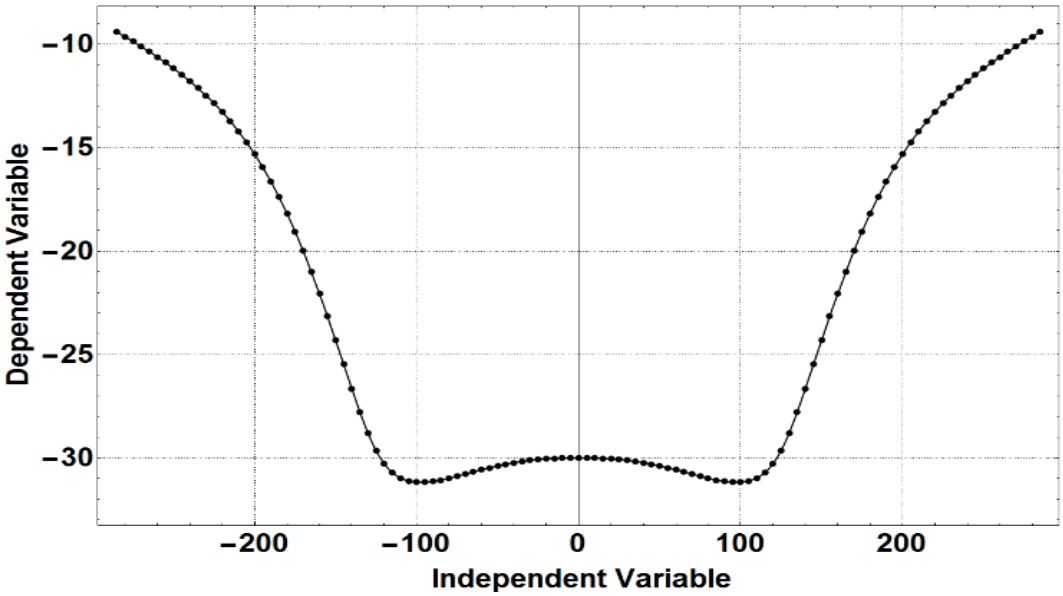

Figure 2-1: B-Spline interpolation curves fitted on a deformed profile

2.3.2 Deformation Analysis

The axisymmetric nature of pipelines makes the cylindrical coordinate system a more suitable base for defining the displacements rather than the Cartesian coordinate system. The obtained coordinates of the deformed profile in the Cartesian coordinate system are transformed into the

cylindrical coordinate system such that a vector position in the Cartesian coordinate system characterized by the coordinates (x, y, z) is transformed to the cylindrical coordinate system (R, θ, Z) using the set of expressions shown in equation (4)

$$\begin{Bmatrix} R = \sqrt{x^2 + y^2} \\ \theta = tan^{-1}\frac{y}{x} \\ Z = z \end{Bmatrix} \tag{4}$$

The basis vector in the cylindrical coordinate system can be obtained using the transformation matrix shown in equation (5).

$$\begin{Bmatrix} e_r \\ e_\vartheta \\ e_z \end{Bmatrix} = \begin{Bmatrix} Cos\theta & Sin\theta & 0 \\ -Sin\theta & Cos\theta & 0 \\ 0 & 0 & 1 \end{Bmatrix} \begin{Bmatrix} e_x \\ e_y \\ e_z \end{Bmatrix} \tag{5}$$

where e_r, e_ϑ and e_z are the unit vectors in the cylindrical coordinate system and e_x, e_y and e_z are the unit vectors in the Cartesian coordinate system. The unit vectors e_r and e_θ vary with the angular position θ while e_z remains constant. It is such that the equalities shown in equation (6) hold;

$$\left\{\frac{\partial e_r}{\partial \theta} = e_\theta, \frac{\partial e_\theta}{\partial \theta} = -e_r, \frac{\partial e_r}{\partial r} = \frac{\partial e_\theta}{\partial r} = 0\right\} \tag{6}$$

The inline inspection yields the internal radius of the deformed pipeline, R_i, and the corresponding angular position, θ_{def}, at each monitored point. These obtained coordinates define the geometry of the dented region. The radius of the mid-surface of the pipe wall, R_m, is evaluated as a summation of the internal radius of the pipeline and the directional component of the thickness of the pipeline assuming there is no reduction in the pipe wall thickness during deformation. This radius is evaluated using equation (7) below.

$$R_m = R_i + \frac{t}{2} Cos\left(ArcTan\left(\frac{\partial R_i}{R_i \partial \theta_{def}}\right)\right) \quad (7)$$

The circumferential displacement is obtained by assuming the pipeline is inextensible in the circumferential axis. This assumption implies the governing mode of deformation in the circumferential direction is the bending rather than the extension of its circumference and as such the total length of the deformed section of the pipe remains $2\pi R_0$, where R_0 is the initial radius of the undeformed pipeline. However, as the exact radius of a cross section of the pipe is not known, a radius R_{omest} is estimated such that the equality described in equation (8) below holds at the mid-surface of the pipe wall.

$$\int_{-\pi}^{\pi} R_m \partial\theta_{def} = \int_{-\pi}^{\pi} R_{omest} \partial\theta_{un} = 2\pi R_{omest} \quad (8)$$

where R_m is the radius of the mid-surface of the deformed pipeline and θ_{un} and θ_{def} represent the angular positions in the undeformed and deformed configurations of the pipeline respectively. The left-hand side of equation (8) can be evaluated using the data describing the geometry of the dent and thus an estimate for R_{omest} can be evaluated. However, this might lose its validity for deep dents as the change in length in the circumferential direction tends to be significant for such dents. The orientation of the pipe is such that the negative interval $(-\pi \leq \theta_{un} \leq 0)$ represents the bottom half of the pipeline which remains fairly unstrained throughout the indentation process and the positive interval $(0 < \theta_{un} \leq \pi)$ represents the top half of the pipe which is strained during indentation. In the numerical procedure proposed, the dent's peak was approximately at $\theta_{def} = \frac{\pi}{2}$ radians and for every angular position in the deformed configuration, θ_{def}, the corresponding angles in the undeformed configuration, θ_{un}, can be evaluated analytically as in equation (9).

$$\theta_{un} = \frac{1}{R_{omest}} \int_{-\pi}^{i} R_m \partial\theta_{def} \quad \text{for } (-\pi \leq i \leq \pi) \tag{9}$$

The difference between the circumferential angles of a vector position in the deformed and the original configuration ϕ as a result of the deformation is used to form a trigonometric relationship that defines the circumferential and the radial displacement of the mid-surface of the pipeline. Figure 2-2 is a representation of a section of the undeformed and the deformed pipeline in the R-θ plane. The associated circumferential displacements and radial displacements of the mid-surface are evaluated with respect to the original configuration as shown in equations (10) and (11).

$$u_{\theta m} = R_m Sin[\phi] \tag{10}$$

$$u_{rm} = R_m Cos[\phi\,] - R_{omest} \tag{11}$$

The obtained displacements of the mid-surface of the pipeline are made into a function of the pipe wall's thickness by including the displacement components as a result of the variable thickness of the pipe wall t_v of range $(-\frac{t}{2} \leq t_v \leq \frac{t}{2})$, with t being the thickness of the pipeline; the negative component of the interval refers to the region of the pipe wall between the mid-surface of the pipe wall and the internal surface of the pipeline, and the positive component of the interval refers to the region between the mid-surface of the pipe wall and the external surface of the pipeline.

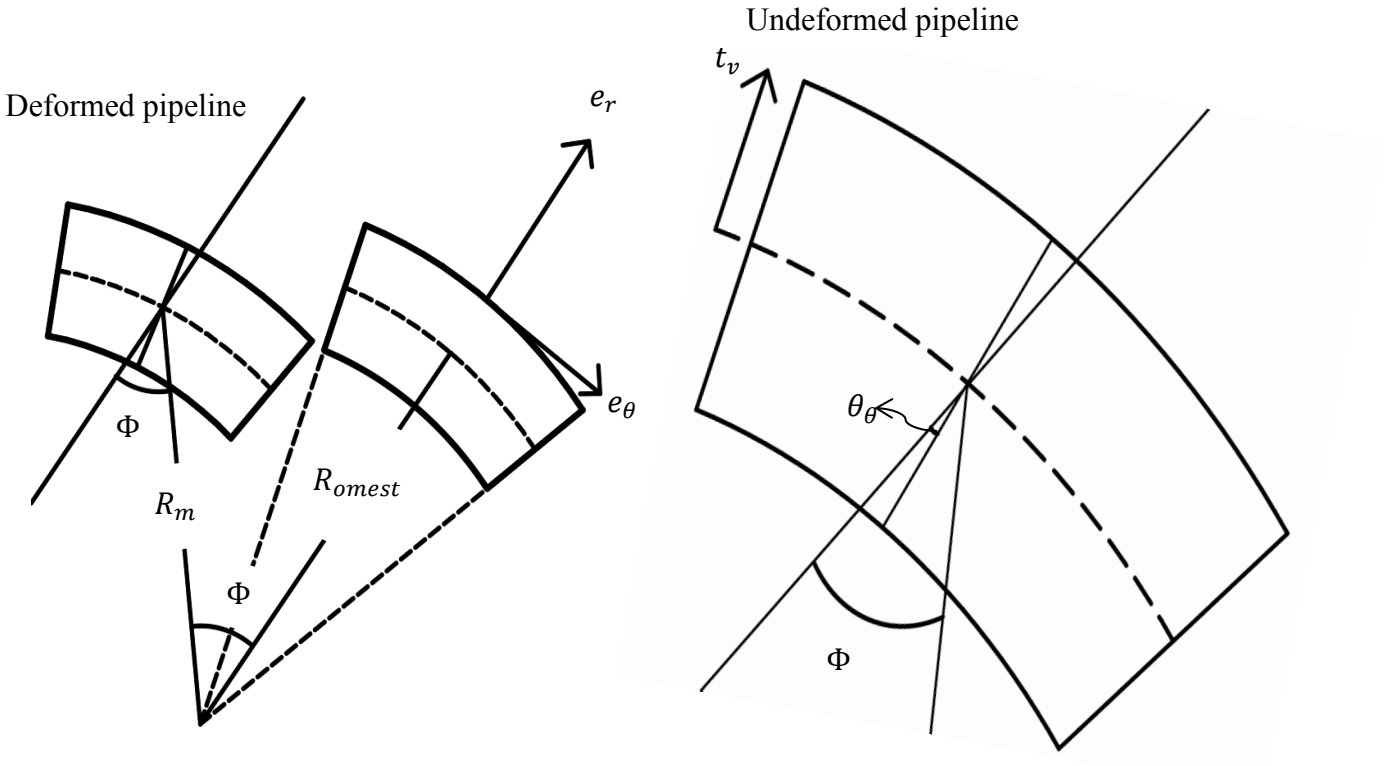

Figure 2-2: Schematic representation of the deformed pipeline in the R-θ plane

The distribution of the circumferential displacement along the thickness of the pipe wall is a function of both the angular distortion ϕ and the slope of the pipe wall in the circumferential axis, θ_θ. The slope in the circumferential axis is developed as a result of the localized distortion of the pipe wall and is evaluated as shown in equation (12).

$$\theta_\theta = ArcTan\left(\frac{\partial R_m}{R_m \partial \theta_{def}}\right) \tag{12}$$

The variable circumferential displacement along the thickness of the pipe wall is evaluated as per equation (13).

$$u_\theta = u_{\theta m} - t_v Sin(\phi - \theta_\theta) \tag{13}$$

The variable radial displacement along the thickness of the pipe wall is evaluated as per in equation (14).

$$u_r = u_{rm} - t_v + t_v Cos(\phi - \theta_\theta) \tag{14}$$

The slope of the mid-surface of the deformed pipeline in the longitudinal direction θ_z is evaluated using equation (15).

$$\theta_z = ArcTan\left(\frac{\partial u_r}{\partial z}\right) \tag{15}$$

The longitudinal displacement along the thickness of the pipe wall, which is a function of the obtained longitudinal slope, is evaluated using equation (16).

$$u_z = -t_v Sin(\theta_z) \tag{16}$$

It has also been assumed that the deformations and resulting slopes are significant and as such the trigonometric approximations of the Euler-Bernoulli beam theory as discussed in Adeeb (2011) do not hold.

It is worth noting that at the mid-surface of the pipeline, the longitudinal displacement u_{zm} is zero and owing to the linear distribution of the longitudinal displacement as enforced by the shell theory, the maximum longitudinal displacement is experienced at the surfaces of the pipeline. Figure 2-3 is a representation of a deformed pipeline in the R-Z plane.

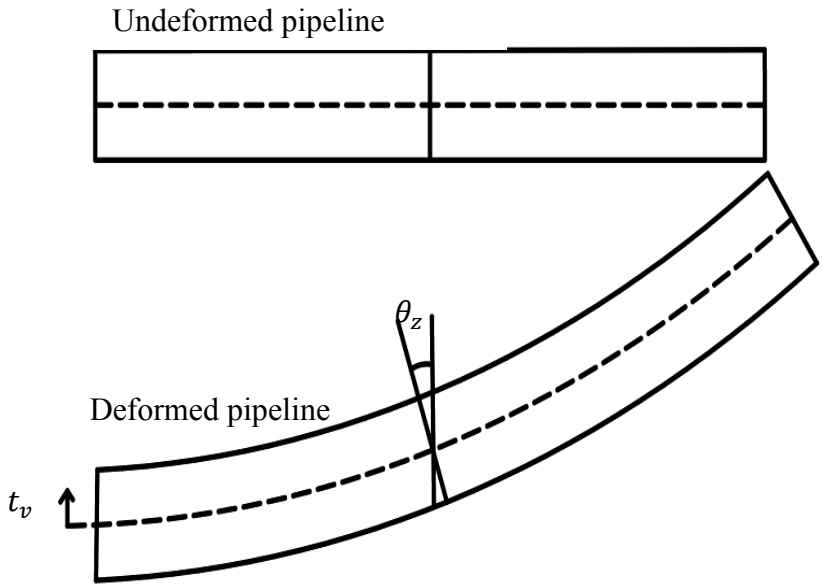

Figure 2-3: Schematic representation of the deformed pipeline in the R-Z plane.

The total displacement field of the dented pipeline U is defined as shown in equation (17);

$$u = u_r e_r + u_\theta e_\theta + u_z e_z \tag{17}$$

The Jacobian determinant, ∇u which is the gradient of the displacement vector, is a second order tensor that relates the undeformed and the deformed configurations of the pipeline is defined by performing the derivatives shown in equations (18-20).

$$\frac{\partial u}{\partial r} = \frac{\partial u_r}{\partial r} e_r + \frac{\partial u_\theta}{\partial r} e_\theta + \frac{\partial u_z}{\partial r} e_z \tag{18}$$

$$\frac{\partial u}{r\partial \theta} = \frac{\partial u_r}{r\partial \theta} e_r + \frac{u_r}{r} e_\theta + \frac{\partial u_\theta}{r\partial \theta} e_\theta - \frac{u_\theta}{r} e_r + \frac{\partial u_z}{r\partial \theta} e_z \tag{19}$$

$$\frac{\partial u}{\partial z} = \frac{\partial u_r}{\partial z} e_r + \frac{\partial u_\theta}{\partial z} e_\theta + \frac{\partial u_z}{\partial z} e_z \tag{20}$$

The term R represents the variable radius of the pipeline which is the sum of the estimated mid surface radius of the pipeline and the variable thickness.

The resulting matrix which maps vector position of the material component of the pipeline from the original to the deformed configuration is shown in equation (21).

$$\nabla u = \begin{Bmatrix} \frac{\partial u_r}{\partial r} & \frac{\partial u_r}{R\partial\theta} - \frac{u_\theta}{R} & \frac{\partial u_r}{\partial z} \\ \frac{\partial u_\theta}{\partial r} & \frac{u_r}{R} + \frac{\partial u_\theta}{R\partial\theta} & \frac{\partial u_\theta}{\partial z} \\ \frac{\partial u_z}{\partial r} & \frac{\partial u_z}{R\partial\theta} & \frac{\partial u_z}{\partial z} \end{Bmatrix} \tag{21}$$

2.3.3 Strain Analysis

The methodology being proposed in this study allows some flexibility in the choice of the strain measure employed. The Linear and the Lagrangian strain formulations which are based on the additive and the multiplicative decomposition of the Jacobian determinant respectively as discussed in Adeeb (2011) are employed to evaluate the strains in the deformed pipeline with the deformations measured relative to the original configuration of the pipeline. The generalized form of the strain state of a three-dimensional body is a 3 by 3 strain tensor with the normal strains aligned along the diagonal of the tensor and the shear strains as off-diagonal components. The Linear strain measure assumes small deformations while the nonlinear Lagrangian strain measure creates a distinction between deformed and undeformed configurations of the pipeline and contains quadratic extensions to account for large rotations and deformations. A combination of the different strain measures is used to define the strain state of the pipeline. In the longitudinal direction, the Lagrangian strain measure is used to evaluate the strains since there is a considerable extension of the middle surface of the pipe in this axis when the pipeline is subjected to a denting force. The mathematical representation of the nonlinear Lagrangian longitudinal strain is shown in equation (22).

$$\varepsilon_{zz} = \frac{\partial u_z}{\partial z} + \frac{1}{2}\left(\left(\frac{\partial u_r}{\partial z}\right)^2 + \left(\frac{\partial u_\theta}{\partial z}\right)^2 + \left(\frac{\partial u_z}{\partial z}\right)^2\right) \tag{22}$$

The circumferential strains are evaluated using the linearized strain measure as the assumption of in-extensionality imposes a small rotation and deformation condition on the pipe in this axis and the mathematical expression for this is shown in equation (23)

$$\varepsilon_{\theta\theta} = \frac{u_r}{R} + \frac{\partial u_\theta}{R\partial\theta} \tag{23}$$

The shear strain components are not covered in this study but can also be evaluated by a combination of derivatives as the strain components discussed.

The codified equations for the circumferential and the longitudinal strains are shown in equations (24) and (25) respectively.

$$\varepsilon_1 = \frac{t}{2}\left(\frac{1}{R_0} - \frac{1}{R_1}\right) \tag{24}$$

$$\varepsilon_2 = -\frac{t}{2}\left(\frac{1}{R_2}\right) + \frac{1}{2}\left(\frac{d}{L}\right)^2 \tag{25}$$

where R_0, R_1 and R_2 are the radius of the undeformed pipeline, the radius of curvature in the circumferential direction and the radius of curvature in the longitudinal directions respectively. d is the depth of the dent and L the length of the dent.

In this study, the radius of curvature of the dent profile is obtained as a mathematical function along the longitudinal and the circumferential directions of the deformed pipeline. This allows for evaluating the unique strain values at any point along the dent profile. A provision which will be useful when the maximum strains in the circumferential and the longitudinal directions do not coincide or the maximum strain developed during the indentation does not occur at the apex of the dent. The radii of curvature are evaluated mathematically using the expressions shown in equations (26) and (27).

$$R_1 = \frac{\left(R_i{}^2 + \left(\frac{dR_i}{d\theta}\right)^2\right)^{\frac{3}{2}}}{\left|R_i{}^2 + 2\left(\frac{dR_i}{d\theta}\right)^2 - R_i\frac{d^2R_i}{d\theta^2}\right|} \tag{26}$$

$$R_2 = \frac{\left(1 + \left(\frac{du_r}{dz}\right)^2\right)^{\frac{3}{2}}}{\left|\frac{d^2u_r}{dz^2}\right|} \tag{27}$$

2.4 Numerical Example

A deformed shell simulation is conducted by simulating a shell structure subjected to indenting force. The modeled shell in form of a pipeline is developed in the commercially available numerical solver, ABAQUS 6.14. The numerical model has nonlinear capabilities so as to account for the anticipated large displacements and rotations associated with the indentation. The meshing algorithm employed discretizes the entire structure into a series of 8- node linear brick elements with reduced integration and equipped with hour glass control. A quarter symmetry of the pipe is developed and the meshing scheme is such that dense meshes are used in the dented region and this is softened further away from the dented region so as to reduce computation time. The pipeline model is 2000mm long with an external radius of 203mm and the indenter is a spherical rigid surface with a diameter of 60 mm and the material model for the pipeline is an isotopic elastoplastic material with the elastic regime governed by a Young's Modulus of 200 GPa, Poisson's ratio of 0.3 and plastic regime governed by the true stress-true strain curve of a typical X-52 pipeline as predicted using the Ramberg-Osgood model. The stress-strain relationship used in modelling the pipeline's plasticity is shown in figure 2-4.

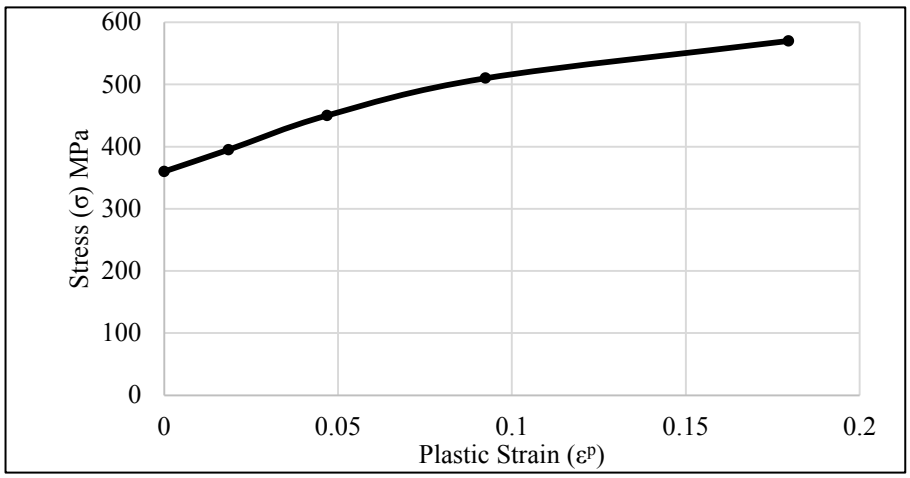

Figure 2-4: True-stress-strain relationship for the material model

The modelled pipeline is 2000 mm long to ensure that in comparison to the length of the pipeline, the dent formed can be considered to be a localized deformity. The chosen length of the pipeline which is approximately 10 times the radius of the pipeline also prevents the interaction between the boundary conditions at the ends of the pipe and the dent. The pipeline is restricted from translations and rotations at the ends and a boundary condition that prevents the vertical displacement at the base of the pipeline is created to idealize the support provided by the underlying soil as present in buried pipelines. The simulation is displacement controlled and as such the indenter is displaced towards the pipelines surface to create the dent of 50 mm which is about 12% of the pipelines outer diameter. Figure 2-5 shows a longitudinal cross section of the pipe structure with the corresponding displacement contours obtained from the numerical model.

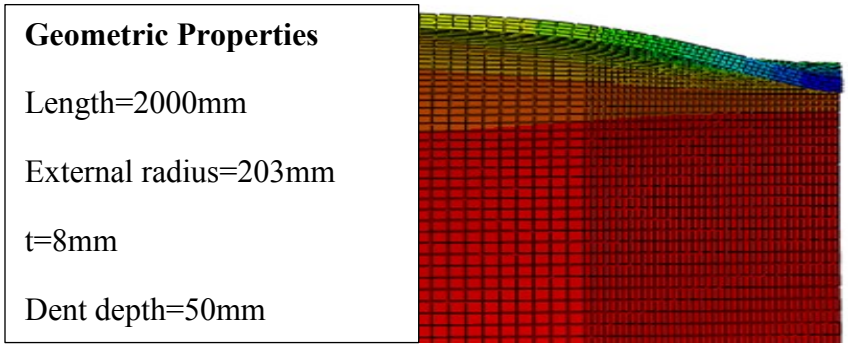

Figure 2-5: Longitudinal cross section of the numerical model of the dented pipeline

The coordinates of the deformed profile are extracted and used as the input for the mathematical model created for our procedure. By fitting the coordinate of the deformed profile with B-Spline functions, a continuous and differentiable dent surface is generated on which the analytical calculations are performed. The cross section corresponding to the maximum dent depth is analyzed in this study. Figure 2-6 is a sectional view of the mid-surface of the pipeline before and after the indentation.

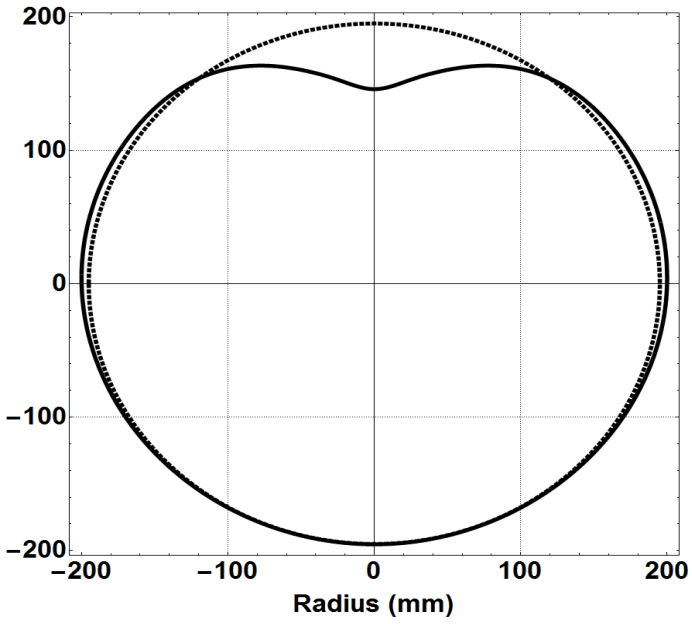

Figure 2-6: Cross-sectional view of the pipeline

2.4.1 Longitudinal Displacement Distribution

The displacement in the longitudinal direction at the internal surface of the pipeline is evaluated as per equation (16) and its distribution obtained along the longitudinal length of the pipeline is shown in figure 2-7.

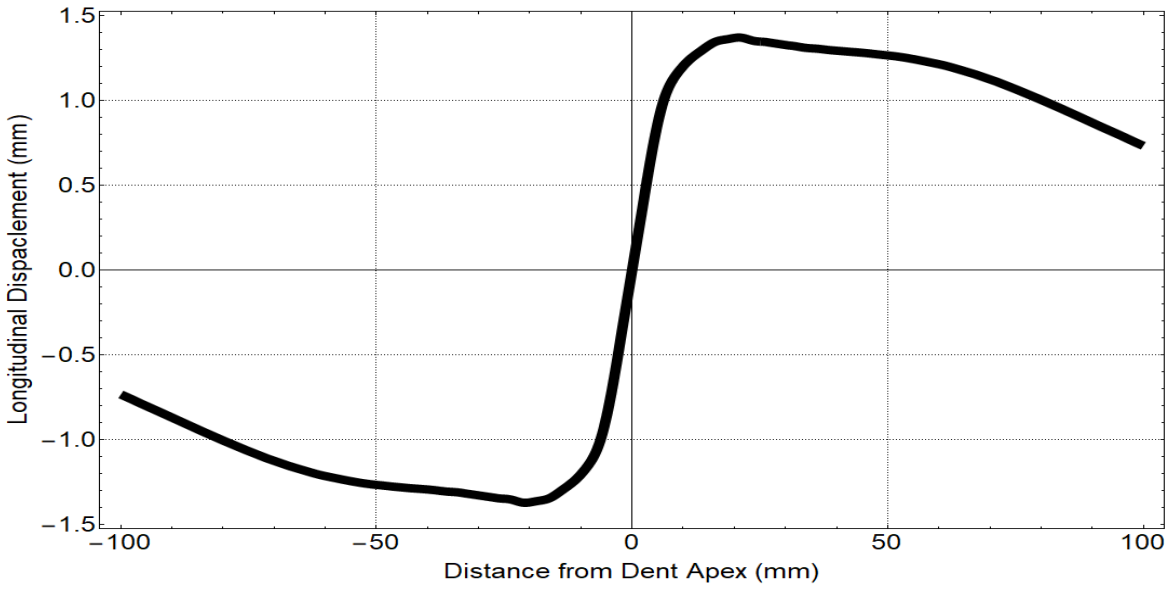

Figure 2-7: Longitudinal displacement distribution at the internal surface of the pipe wall

From figure 2-7, it can be observed that there are no longitudinal displacements at the apex of the dent which corresponds to the zero mark on the horizontal axis. The maximum value of the slope occurs approximately 20 mm away from the apex of the dent on both directions owing to the symmetry of the dent profile. The longitudinal strains associated with the obtained displacement are then evaluated using equation (22). The strain contour predicted by the proposed formulation is benchmarked against the integrated strain contours from the nonlinear FEA model and the codified equations in ASME B31.8-2016.

The Lagrangian strain distribution along the thickness of the pipe wall predicts non-uniform bending as the neutral axis does not pass through the centroid of the pipe wall and the strain

distributions at the compressive and tensile zones are dissimilar as shown in the strain contour in figure 2-8.

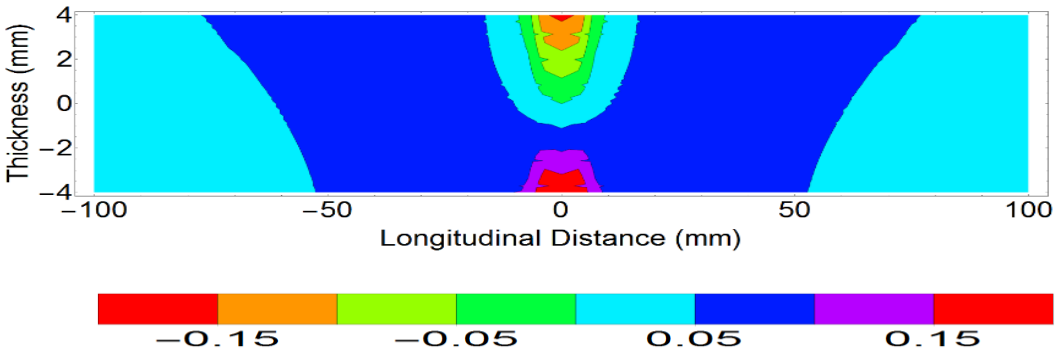

Figure 2-8: Lagrangian longitudinal strain distribution

From figure 2-8, it is observed that the maximum strains are developed around the peak of the dent, which is the zero mark on the horizontal axis of the contour plot. The strains switch orientation from tensile in the internal surface of the pipeline to compressive at the external surface of the pipeline but do not vanish at the mid-surface of the pipeline owing to the membrane extension. The distribution obtained is similar to the distribution predicted from FEA shown in figure 2-9.

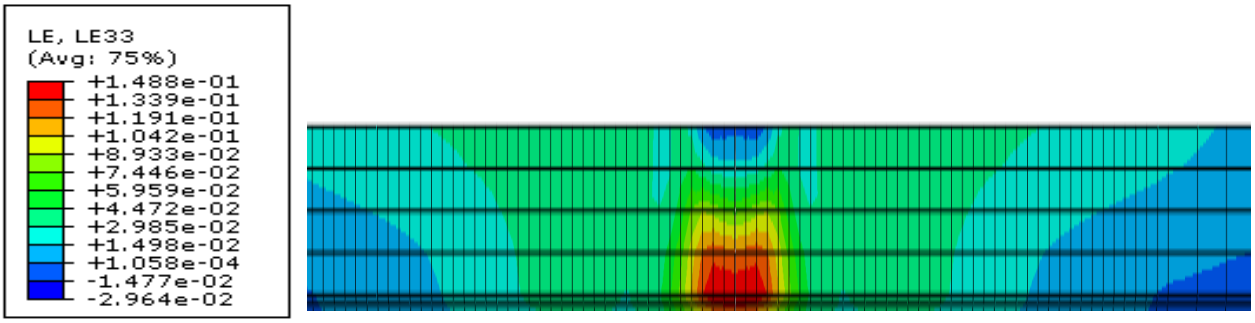

Figure 2-9: Integrated logarithmic strain distribution

The contour plots presented above show strain concentrations at the peak of the dent with a maximum tensile strain value of 15%. The strains predicted by the codified equations are also similar in terms of magnitude, orientation and location as seen in figure 2-10.

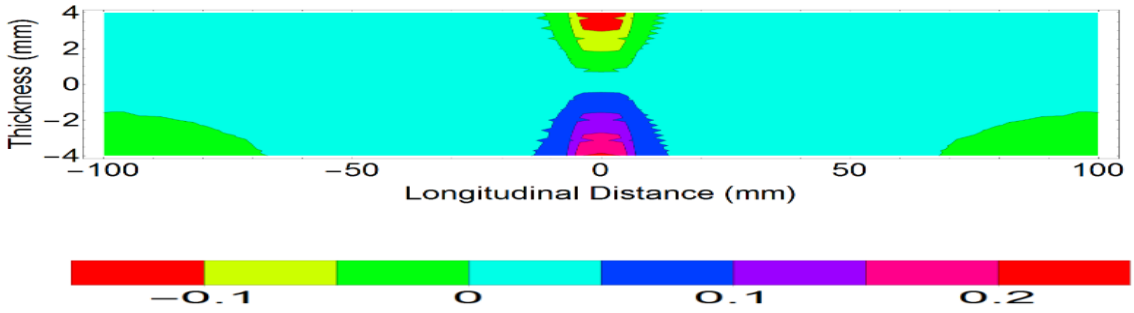

Figure 2-10: Longitudinal strains as per ASME B31.8 equations

The codified equation predicts a nonlinear distribution of the strains along the thickness of the pipe wall and like the previous strain measures; it predicts strain concentration around the apex of the dent. An overlay plot of the critical strains which are the tensile strains at the pipeline's internal surface predicted using the investigated strain measures is presented in figure 2-11. The strains predicted by all the strain measures investigated are symmetric on both sides of the dent. However, owing to the limited degrees of freedom of the analytical strain models, conservative strain magnitudes are predicted when compared to the results from FEA. The procedure proposed, however, performs better than the codified stipulations for this case investigated as the longitudinal strains predicted by the proposed method are more comparable to the strains predicted by FEA.

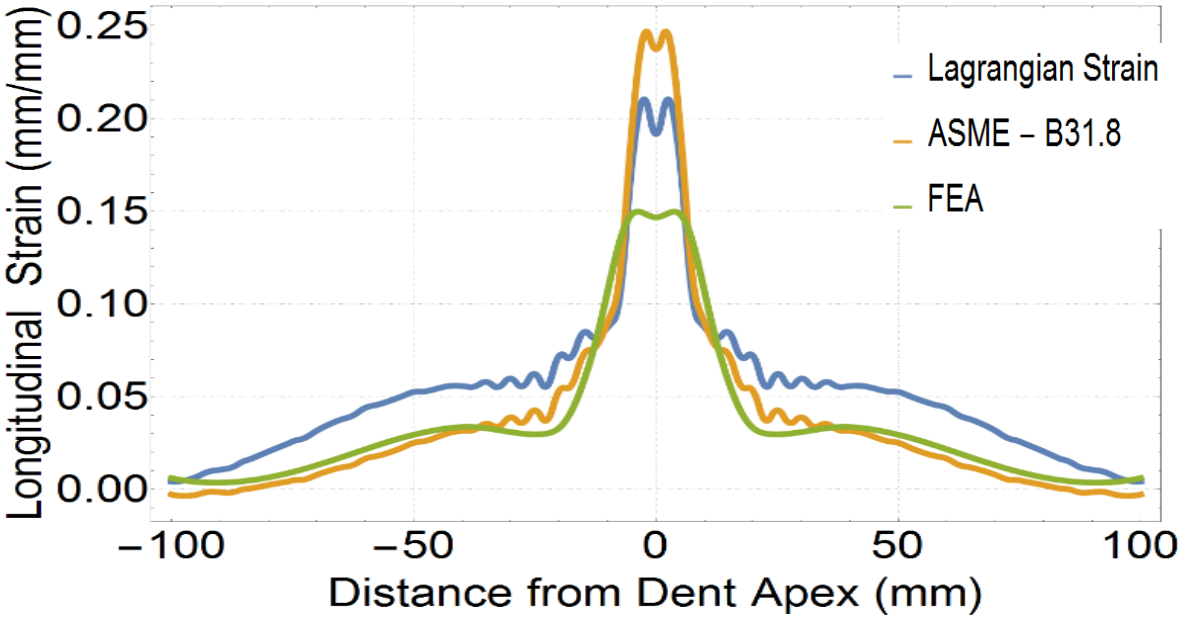

Figure 2-11: Longitudinal strains at the internal surface of the pipeline

2.4.2 Circumferential Displacement and Strain Distribution

To evaluate the circumferential displacement of the mid-surface of the pipeline, an interpolation function relating the angular position of vector positions in the deformed and the undeformed profiles is developed such that for every angular position of the deformed pipeline obtained from inline inspections, a corresponding angular position in the undeformed profile is evaluated. Figure 2-12 shows a plot of the function that relates the angular positions in the deformed and the undeformed configurations of the pipeline.

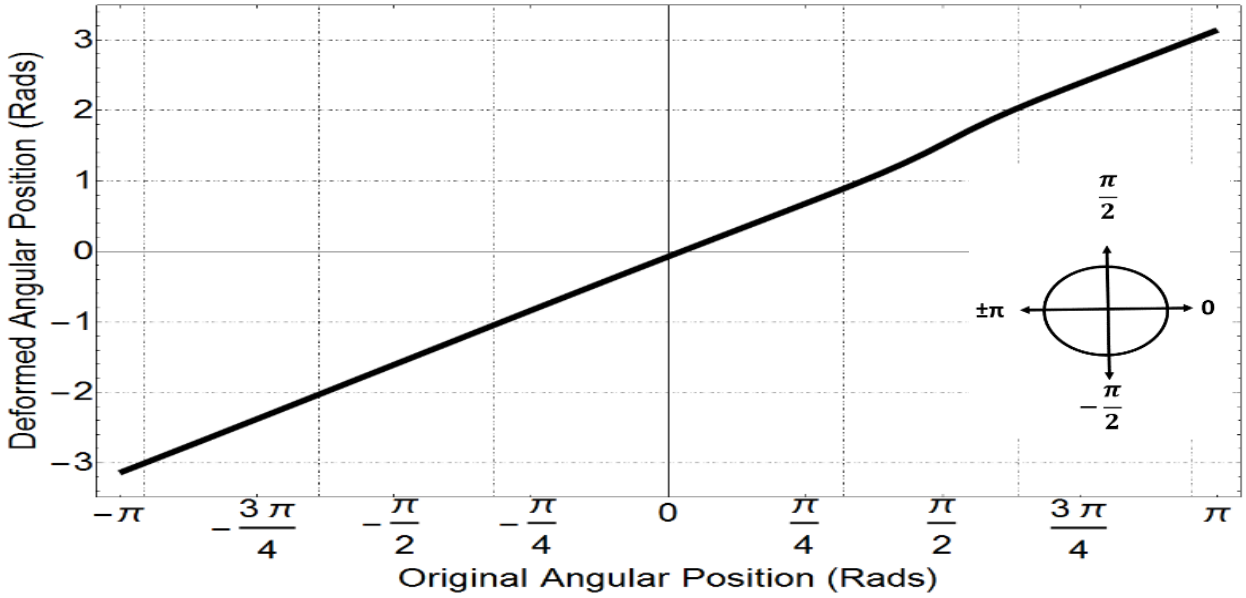

Figure 2-12: Interpolating function relating the angular positions in the deformed to the undeformed configurations

The circumferential displacement at the mid-surface of the pipe wall is also obtained as per equation (13) and the obtained response shown in figure 2-13.

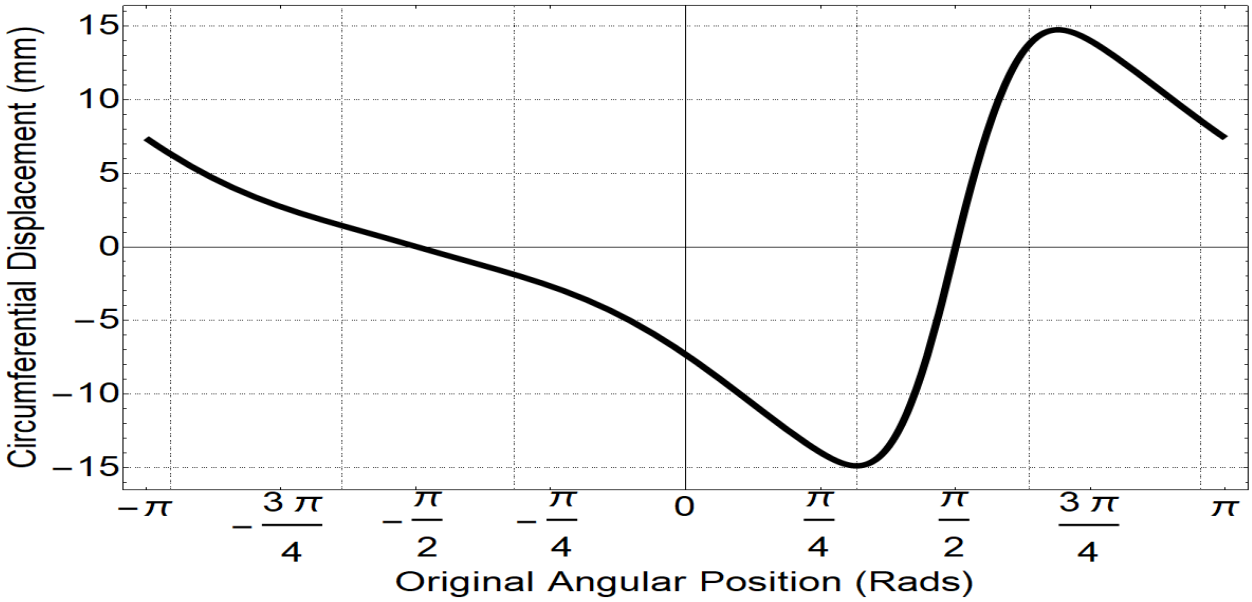

Figure 2-13: Circumferential displacement distribution

From the figure 2-13, it can be observed that at the apex of the dent which corresponds to the $\frac{\pi}{2}$ radians mark, the circumferential displacement is constrained to zero as it is assumed that the deformation experienced at the peak of the dent is purely radial and the circumferential displacement at both ends of the pipe corresponding to the angular positions $\pm\pi$ radians is similar. The rate of change of the circumferential displacement with respect to the angular position can be evaluated and the corresponding strains in the circumferential direction evaluated as per equation (23). The obtained strain contour using the linearized strain measure is presented in figure 2-14.

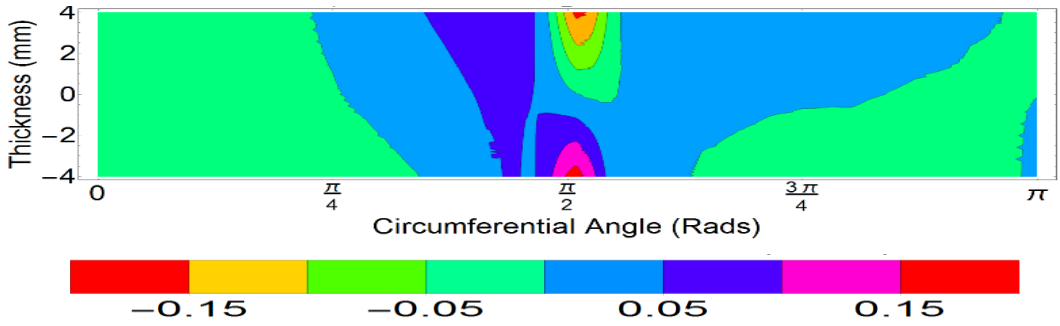

Figure 2-14: Linear circumferential strains

The strain contour in figure 2-14 shows that the maximum circumferential strain occurs at the peak of the dent. The deformations and slopes used in this formulation of the circumferential strains are evaluated assuming large deformations and as such the linear strain measure also predicts non-uniform bending with the distribution of strains similar as in the longitudinal direction. From the circumferential strain contours, it can be observed that while the magnitudes of the tensile and the compressive strain zones are similar, the neutral plane does not pass through the centroid of the pipe wall. Figure 2-15 presents the strain contours predicted using the ASME B31.8 equations. It can be observed that this measure predicts a state of pure bending in

the pipeline as the neutral plane which neither extends nor contrasts can be identified at the mid-surface of the pipe wall and the strains increase linearly away from this neutral surface. The magnitudes of the compressive and tensile strains are same which implies that the interaction between possible torsional, shear and axial deformations are ignored.

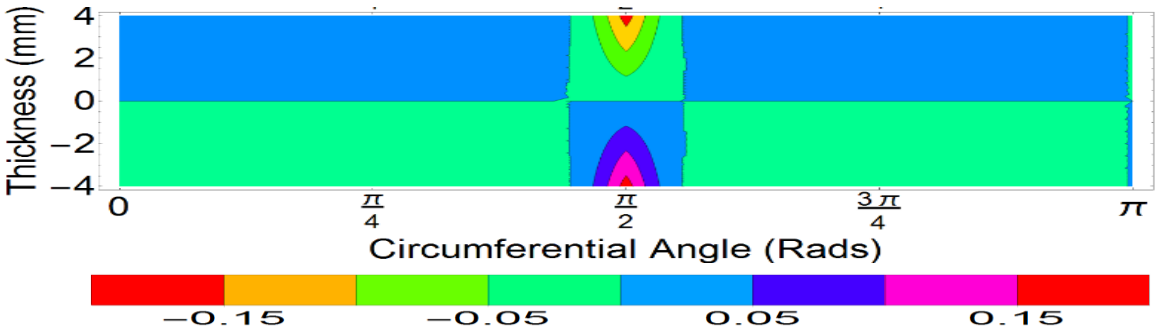

Figure 2-15: Circumferential strains as per ASME B31.8 equations

The nonlinear FEA predicts similar strain magnitudes with our formulation and the ASME B31.8 equations. The contour plots of the integrated circumferential strains predicted by FEA are presented in figure 2-16 below

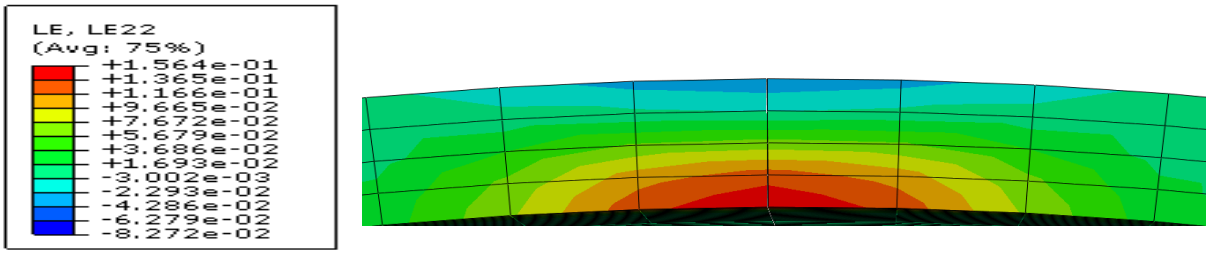

Figure 2-16: Integrated circumferential strain distribution

It can be observed that all strain measures predict a maximum tensile strain value of 15% at the internal surface of the dent.

The strain distribution predicted by the investigated strain measures at the critical section of the pipeline is presented in figure 2-17 below.

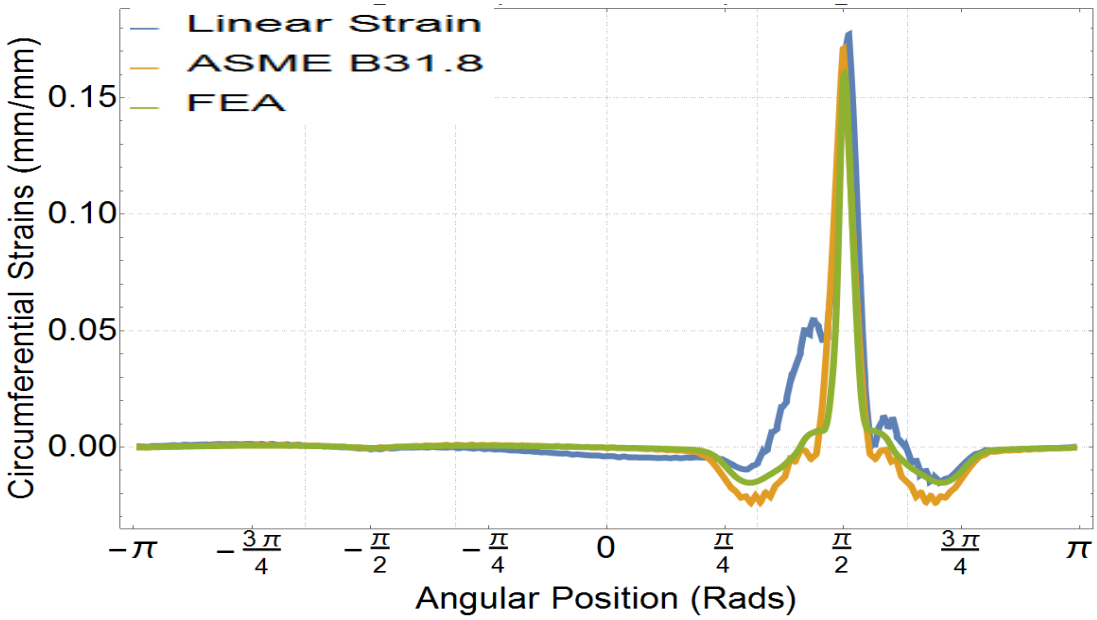

Figure 2-17: Circumferential strains at the internal surface of the pipeline

From figure 2-17 above it can be observed that the maximum strain value is similar for all the models with the proposed technique having some asymmetrical distribution of strains which is as a result of the errors associated with the estimated radius to enforce the inextensibility of the pipeline's circumference.

2.5 Conclusions

The technique proposed predicts a similar strain distribution to nonlinear FEA, provides flexibility in the strain measure to be employed and allows for the concise strain analysis of thin-walled structures. The angular distortion makes it difficult to relate vector positions in the deformed and the original pipeline and as no simplified model has been proposed for accounting for this response. Therefore, neglecting the extensional strains on the mid-surface in the

circumferential direction allows for this mapping to be done between the deformed and the undeformed configurations. With the method proposed, the total strain state of the dented region of the pipeline which will include the shear strain components that are currently ignored in codified existing strain based equations can be developed. A sensitivity analysis will be required to assert the validity of this procedure.

In this paper, the shell theory was also applied within the confines of finite continuum mechanics to establish the deformation field and associated strain field of a cylindrical shell based on the consistent kinematic assumption of straight normal in order to develop a technique for evaluating the strains in deformed shell structures. The introduced method can be easily extended to a three dimensional continuum and the entire strain state of deformed pipeline evaluated.

2.6 Acknowledgments

The authors acknowledge the financial support from Enbridge Liquid Pipelines Inc. and the technical support from the University of Alberta, Canada.

References

Adeeb, S.,2011. Introduction to Solid Mechanics and Finite Element Analysis Using Mathematica. Kendall Hunt.

ASME 2016, B31.8-2016: Gas Transmission and Distribution Piping Systems. ASME International, New York, NY.

Belanger, A.A. and Narayanan, R., 2008. Direct Strain Calculation of Pipe Line Dent from Knot Migration using a Kinematic Model Free of Material Properties. In Proceedings of the International Pipeline Conference, Calgary, Alberta, Canada.

Bitter, N.P. and Shepherd, J.E., 2013. On the Adequacy of Shell Models for Predicting Stresses and Strains in Thick-Walled Tubes Subjected to Detonation Loading. Pressure Vessels and Piping Conference, Paris, France.

Ciarlet, P.G. and Mardare, C., 2008. An Introduction to Shell Theory. Differential Geometry: Theory and Applications, 9, pp.94-184.

Dawson, S.J., Russell, A. and Patterson, A., 2006. Emerging Techniques for Enhanced Assessment and Analysis of Dents. Proceedings of the International Pipeline Conference, Calgary, Alberta, Canada.

Foroughi, H., Moen, C.D., Myers, A., Tootkaboni, M., Vieira, L. and Schafer, B.W., 2014. Analysis and Design of Thin Metallic Shell Structural Members-Current Practice and Future Research Needs. in Proc. of Annual Stability Conference Structural Stability Research Council, Toronto, Canada.

Ghaednia, H., Das, S., Wang, R. and Kania, R., 2015. Safe Burst Strength of a Pipeline with Dent–Crack Defect: Effect of Crack Depth and Operating Pressure. Engineering Failure Analysis, 55, pp.288-299.

Koiter, W.T., 1970. The Stability of Elastic Equilibrium. Stanford Univ Ca Dept. of Aeronautics and Astronautics.

Love, A.E.H., 1888. The Small Free Vibrations and Deformation of a Thin Elastic Shell. Philosophical Transactions of the Royal Society of London. A, 179, pp.491-546.

Naghdi, P.M. and Nordgren, R.P., 1963. On The Nonlinear Theory of Elastic Shells under the Kirchhoff Hypothesis. Quarterly of Applied Mathematics, 21(1), pp.49-59.

Noronha, D.B., Martins, R.R., Jacob, B.P. and de Souza, E., 2010. Procedures for the Strain Based Assessment of Pipeline Dents. International Journal of Pressure Vessels and Piping, 87(5), pp.254-265.

Rafi, A.N.M., Das, S., Ghaednia, H., Silva, J., Kania, R. and Wang, R., 2012. Revisiting ASME Strain-Based Dent Evaluation Criterion. Journal of Pressure Vessel Technology, 134(4), p.041101.

Reissner, E., 1952. Stress-Strain Relations in the Theory of Thin Elastic Shells. Studies in Applied Mathematics, 31(1-4), pp.109-119.

Rogers, D.F. and Adams, J.A., 1990. Mathematical Elements for Computer Graphics, McGraw-Hill Book Co. New York.

Sanders Jr, J.L., 1963. Nonlinear Theories for Thin Shells. Quarterly of Applied Mathematics, 21(1), pp.21-36.

Ventsel, E. and Krauthammer, T., 2001. Thin Plates and Shells: Theory: Analysis and Applications. CRC press.

Wu, Y.Z.P. and Han, X., 2013. Analysis of Pipe Size Influence on Pipeline Displacement with Plain Dent Based on FE Calculation. International Journal of Computer Science Issues, 10(1), pp.507-510.

Disclaimer

Any information or data pertaining to Enbridge Employee Services Canada Inc., or its affiliates, contained in this paper was provided to the authors with the express permission of Enbridge

Employee Services Canada Inc., or its affiliates. However, this paper is the work and opinion of the authors and is not to be interpreted as Enbridge Employee Services Canada Inc., or its affiliates', position or procedure regarding matters referred to in this paper. Enbridge Employee Services Canada Inc. and its affiliates and their respective employees, officers, director and agents shall not be liable for any claims for loss, damage or costs, of any kind whatsoever, arising from the errors, inaccuracies or incompleteness of the information and data contained in this paper or for any loss, damage or costs that may arise from the use or interpretation of this paper.

Chapter 3- Improvements to the ASME B31.8 Dent Strain Equations

3.1 Abstract

Pipelines used to transport oil and gas products are often subjected to external interferences forces. These external interferences can result in the formation of dents in a pipeline which has the potential to reduce the burst strength of the pipeline, lead to the ovalization of the pipeline and increase the susceptibility to fatigue fracture. The repair of defected pipeline can be cost intensive and as such it becomes good practice to have a screening measure to properly allocate resources for the implementation of repairs. Various pipeline codes have stipulations on how these threats should be assessed in order to prioritize repairs. The most prominent being the depth based criterion which determines the severity of a dent in the pipeline by the depth of the dent. The depth of the dent is limited in its scope as it fails to consider the fact that the geometry of the dent can lead to strain concentration and eventually the failure of the pipeline at the dented section. A non-mandatory set of equations in the ASME B31.8-2016 standards is used to evaluate the strains at the dented region of the pipeline. This tool serves its purpose as a good indication of strain concentrations along the profile of the dent, however, the peak strains are not always developed at the apex of the dent especially when the dent is asymmetrical. The current implementation of the ASME B31.8 equations might fail to capture the strains that are not aligned with the most severe profile of the dent and as such a global view of the strain distribution of the dented profile would be a good indication of the locations of the strain concentrations. The study presented herein is a detailed implementation of ASME B31.8 formulations together with the suggested modifications to evaluate the three-dimensional strain state of the dented pipeline. The strain distributions obtained are compared against the strains predicted by a nonlinear finite element analysis (FEA) model. The correlation in the prediction of the strains by this model indicate the possibility of evaluating the strains of the dented region

of a pipeline and would go a long way in advancing the rapid characterization of dented pipelines based on the reported coordinates of identified anomalies

Keywords-ASME B31.8, Strains, FEA

3.2 Introduction

Dents as a form of mechanical damage in pipelines are characterized by the inward deformation of the pipe wall. The presence of such damage is well-known to have adverse effects on the pressure integrity of the pipe and to serve as initiators of cracks which may fail immediately or delayed with pressure cycle (Maxey, 1986). Pipeline dents are usually caused by external forces acting on the surface of the pipeline ranging human errors like poor construction practices to natural events in the form of landslides. Dents are classified by the response to internal pressure cycles and the change of the curvature of the pipeline as discussed in (Cosham and Hopkins, 2003). The dents with a smooth change in the curvature of the pipe wall and not interacting with other features are referred to as plain dents and the dent profiles with sharp curvatures are termed kinked dents. For the internal pressure classification, dents prevented from fatigue cycling by the indenter having contact with the surface of the pipeline are referred to as constrained dents and dents which are allowed to rebound and reround under the effect of internal pressure cycles are referred to as unconstrained dents. Some work has been done on investigating the effects on dents on the pipeline's integrity. Ornyak and Shlapak (2001) investigated the ultimate load for ductile fracture for defects in pipelines and also developed an analytical model of the plastic state of a deformed pipeline. Iflefel et al. (2005) performed numerical investigation using FEA to investigate the capacity of dented pipeline to withstand different loading scenarios. It is evident from these various studies that these geometric anomalies could have adverse effects the performance of a pipeline. The potential of a dent feature to lead to failure of a pipeline is

intuitively governed by the severity of the dent. It is thus pertinent that dents be ranked in order of severity to identify potentially severe features. The depth of the dent which is a precedent for many pipeline codes including the Canadian CSA Z662-2016 stipulates a threshold of 6% of the outer diameter (OD) for pipes with diameters of 101.6 mm and greater, a 6 mm threshold for pipes with OD less than 101.6 mm. However, the depth of the dent is not usually the most effective technique for evaluating the severity of a dent as some dented pipelines could still sustain normal operation conditions even after violating the dent depth criterion while some pipelines have failed with relatively shallow dent depths which would have been flagged as safe by the depth based criterion. Therefore, the use of the depth as the sole governing factor can lead to both unnecessary excavations and can miss moderated dents that are severe owing to the sharpness and overall size, (Gao, et al., 2008).

As an alternative to the depth based criterion, the strain based approach to the assessment of a dent can be more informative as regards the severity of the dent feature (Dinovitzer et.al., 2002, Dawson et.al., 2006, and Rafi et al., 2012). The strain based approach involves evaluating the localized strain distributions around the dented region which takes into account the deformation contour of the dented pipelines, and as such the localized strain concentrations that can lead to potential failures can be identified.

The ASME B 31.8-2016, which is a safety code governing the design, construction, operation, and maintenance of gas transmission and distribution piping systems, acknowledges this concept and provides a set of non-mandatory closed form expressions for evaluating the strains. These set of equations can be used to evaluate the maximum strains at the peak of the dent. A close investigation of the ASME B31.8 dent strain equations shows that the implemented procedure

recognizes the multiaxiality of the strains in dented pipeline and discretizes the strains into the three components as shown in figure 3-1.

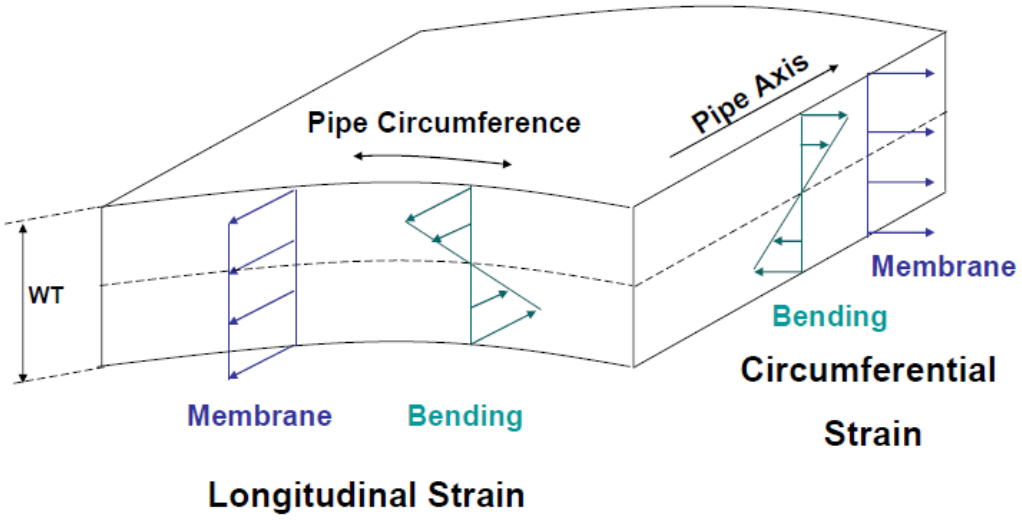

Figure 3-1: Strain components of a dented pipeline (Lukasiewicz et al., 2006)

From figure 3-1, it can be seen that the membrane strains are a result of the extension of the pipeline in the longitudinal direction and are uniformly distributed along the thickness of the pipe wall. The bending strains vary linearly along the thickness of the pipe wall (with tensile strains developed at the internal surface of the pipe wall and compressive strains at the external surface of the dented pipeline). The ASME B31.8-2016 expressions for evaluating the circumferential bending strain, ε_1, the longitudinal bending strain, ε_2 and the longitudinal membrane strain, ε_3 are shown in equations (1-3) respectively.

$$\varepsilon_1 = \frac{t}{2}\left(\frac{1}{R_0} - \frac{1}{R_1}\right) \quad (1)$$

$$\varepsilon_2 = -\frac{t}{2}\left(\frac{1}{R_2}\right) \quad (2)$$

$$\varepsilon_3 = \frac{1}{2}\left(\frac{d}{L}\right)^2 \quad (3)$$

where t is the pipe wall thickness, R_0 is the internal radius of the un-deformed pipeline, R_1 and R_2 are the radius of curvature of the dent in the circumferential and longitudinal directions respectively, d is the depth of the dent and L is length of the dent.

The ASME B31.8 equations ignore the effect of the circumferential membrane strains. A direct implication of this premise is that the pipeline remains inextensible in the circumferential axis during the deformation. This assumption can be taken to be valid as the pipeline is flexible in the circumferential direction and intuitively the deformation mode in this axis should be as result of the bending of the pipeline rather than the extension of the membrane. The circumferential extension may occur when deep dents are considered. However, this quantity cannot easily be obtained from the dent profile and its contribution to the entire strain state of the pipeline is assumed not to be significant owing to the ease of ovalization of the pipeline's cross section. In the longitudinal direction, the deflections are relatively large and as such, it is accompanied by the stretching of the membrane of the pipeline, hence the inclusion of equation (3) to the strain equations.

The evaluated directional strain components are then combined accordingly assuming a state of plane strain to evaluate an equivalent strain in the dented section as shown in equations (4) and (5) respectively.

$$\varepsilon_i = \sqrt{(\varepsilon_1)^2 + \varepsilon_2(\varepsilon_2 + \varepsilon_3) + (\varepsilon_2 + \varepsilon_3)^2} \quad (4)$$

$$\varepsilon_o = \sqrt{(\varepsilon_1)^2 + \varepsilon_1(\varepsilon_3 - \varepsilon_2) + (\varepsilon_3 - \varepsilon_2)^2} \quad (5)$$

where ε_i and ε_o are the strains in the inner and outer surfaces of the pipe wall respectively.

As seen in the equations above, the bending strains in a dented pipeline is hugely dependent on the magnitude of the radius of curvature of the dent profile. This parameter can be difficult to calculate from the dent profiles and the ASME B31.8 does not provide a definition on how this is to be estimated. A host of interpolation techniques can be employed in fitting the coordinates of the dent reported by inline inspection, Rosenfeld et al., (1998) proposes the use of the half point osculating circle method. However, the work by Noronha et al., (2010) states that the osculating circle method is not suitable for dent features having strain components that are not aligned in the principal axis and a B-Spline interpolation of the dent profile would be able to handle such scenarios. The B-spline interpolations introduced in their study were equipped with second order continuity and allowed for the analytical evaluation of the strains. Various mathematical techniques like the forward difference, backward difference and centered difference methods can also be used to evaluate the radius of curvature of the dented pipeline numerically on a point by point basis. The codified dent strain expressions have been criticized in recent times, some of the concerns in (Baker, 2004) include the fact that the longitudinal membrane strain equation is an empirical estimate benchmarked against a limited number of finite element runs, and a state of plane strain is assumed in the pipeline. The latter implies that the radial strain component is ignored, a condition that does not comply with deformation plasticity.

Another concern is the ASME B31.8 equations are employed assuming that the maximum strains are developed at the apex of the dent, (Noronha et al., 2005). This might be sufficient for "well

behaved" dents that are aligned with the principal axis and are symmetric in its geometric orientation. For real life cases, there might be some deviation from this assumption. For a more complete analysis of the strain state of the pipeline, the effect of the radial strain components should be considered. The work by Lukasiewicz, et al., (2006) presents an equation for the equivalent strains shown in equation (6) for the equivalent strain definition.

$$\epsilon_{eq} = \frac{2}{\sqrt{3}}\sqrt{\epsilon_x^2 + \epsilon_x\epsilon_y + \epsilon_y^2} \tag{6}$$

where, ϵ_x and ϵ_y are the longitudinal and circumferential strains respectively. These expressions are based on the premise that no volumetric strains are developed in the dented pipeline during the deformations and as such the radial strains can be evaluated as a function of the other directional strain components.

In this study, the predicting capabilities of the analytical expressions of strains are benchmarked against a three-dimensional numerical model. A three-dimensional view of the dented region of the pipeline might be more informative and will give a general view of the pipeline's strain state. This study focuses on plain dents, which are immured from fatigue cycling. While plain dents might not have such a detrimental effect on the structural integrity of the pipeline when considering the burst strength of the pipeline (Cosham and Hopkins, 2001), these defects can lead to the long-term degradation as seen in cases of rock-contact fatigue (in liquid pipelines only), punching shear and stress corrosion cracking, (Rosenfeld et al.,1998).

The presentation herein serves as a tool regardless of the equations employed for the rapid characterization of dent severity from a strain based standpoint.

3.3 Methodology

The procedure follows from the concept introduced in Noronha et al., (2005) on spline interpolation of dented pipelines in the evaluation of the strain state of the pipeline. In this study, piecewise spline functions are used to interpolate the dent topology. The B-spline functions generate a continuous and differentiable surface from the coordinates of the vector positions of the deformed pipeline on which mathematical operations can be performed. The radius of the curvature of the deformed pipeline can be evaluated analytically by performing derivatives on the interpolating functions. The corresponding strains can then be evaluated using the codified closed form expressions.

The deformation coordinates of the analyzed dents are generated from numerical models and the directional strains predicted by the numerical models are benchmarked against the directional strains predicted using the ASME B31.8 equations.

The dent surface is generated by extracting the radial displacements and the angular positions directly from the nodes of the numerical model. The resolution of the data points used to interpolate the dent surface was designed to correspond to that obtained from an inline inspection tool having 64 sensors in the circumferential direction and obtains data at every 10mm interval. The number of sensors along the circumference of the pipeline was varied to account for the different accuracies obtainable in inline inspection tools. The sensor numbers investigated were 32, 16 and 8 sensors along the circumference of the pipeline. With the interpolated profile, the radius of curvature in both the axial and the circumferential directions were evaluated. The associated normal strain components were then evaluated using the closed form expressions in the ASME codes and benchmarked against the strains predicted by the numerical model. The equivalent plastic strains were evaluated using the equations proposed in Lukasiewicz et al.,

2006). The strains compared are the circumferential strains (LE 22), longitudinal strains (LE33) and the equivalent plastic strains (PEEQ).

3.3.1 The Spline Interpolation

The interpolation of the dented surface is done using B-spline functions equipped with second order continuity. The B-spline curves used are polynomials between a pair of data points with components defined slightly "non locally" in order to obtain some level of smoothness up to a particular derivative. B-spline interpolation can be used to represent complex deformations (Deng and Denney, 2002). The generated curves have the advantage of allowing for the smooth transitions between the position vectors in deformation fields as they are non-global and are applied in a piecewise fashion along the dented section of the pipeline. This results in a continuous and differentiable contour surface of the dent. The developed B-spline functions are dependent on the angular position of the pipeline θ with interval $(-\pi \leq \theta \leq \pi)$ and Z the longitudinal distance of the pipeline with interval $(-L \leq Z \leq L)$, where L is the longitudinal distance from either side of the dent apex.

The radius of curvature is evaluated in the circumferential and the longitudinal direction using the classical expressions for the radius of curvature (Weisstein, 2005) shown in equations (7 and 8) respectively.

$$R_1 = \frac{\left(R^2+\left(\frac{dR}{d\theta}\right)^2\right)^{\frac{3}{2}}}{\left|R^2+2\left(\frac{dR}{d\theta}\right)^2-R\frac{d^2R}{d\theta^2}\right|} \tag{7}$$

where R is the inner radius of the pipeline as reported by the inline inspection device, θ is the angular position associated with each reported internal radius.

In the longitudinal direction, the radius of curvature is evaluated using equation (8)

$$R_2 = \frac{\left(1+\left(\frac{du_r}{dz}\right)^2\right)^{\frac{3}{2}}}{\left|\frac{d^2u_r}{dz^2}\right|} \quad (8)$$

where u_r is the radial displacement and z represents the axial direction.

With the radius of curvatures obtained, the associated strains can then be easily evaluated using the closed form expressions defined in equations (1-5). The computation of the strains employed in this study acknowledges the fact that the tensile strains are developed at the internal surface of the pipeline and the compressive strains at the external surface of the pipeline.

3.3.2 Numerical Modelling

The finite element models for this study were developed using the commercially available numerical solver, ABAQUS 6.14. The pipes modelled had a diameter of 140 mm, wall thickness of 8 mm and a length of 1100 mm. The pipeline was modeled as a deformable elastoplastic material having its elastic regime governed by a Young's Modulus of 200 GPa and a Poisson's ratio of 0.3. The plastic regime of the material model was defined using the post yield stress-strain curve of a typical X-60 pipeline. The dents analysed were restrained dents and as such the loading scenario was monotonic. The numerical simulation was such that an indenter was displaced into the pipe's surface a distance corresponding to a certain percentage of the OD and remained in place. The indenters used were modeled as rigid bodies and as such the pipelines deform relative to the indenters on contact. The contact surfaces in the models were defined with the master slave algorithm. The models were also allowed to account for large strains and rotations and the other nonlinearities associated with the deformation. The indenter had a length of 80 mm in contact with the pipe surface and fillets of 10 mm radius at the edges. The numerical models were meshed with three-dimensional 8-node brick elements. The computation time for

the simulation is reduced by introducing some bias in the meshing scheme such that the dented region of the pipeline was meshed with 5 mm element while the other regions were meshed with 15 mm elements. In total five numerical models were generated by varying the depth of the dent. The dent depths considered for the study were 2%, 4%, 6% 10% and 12% OD. Figure 3-2 shows the assembly of the numerical model developed for this study.

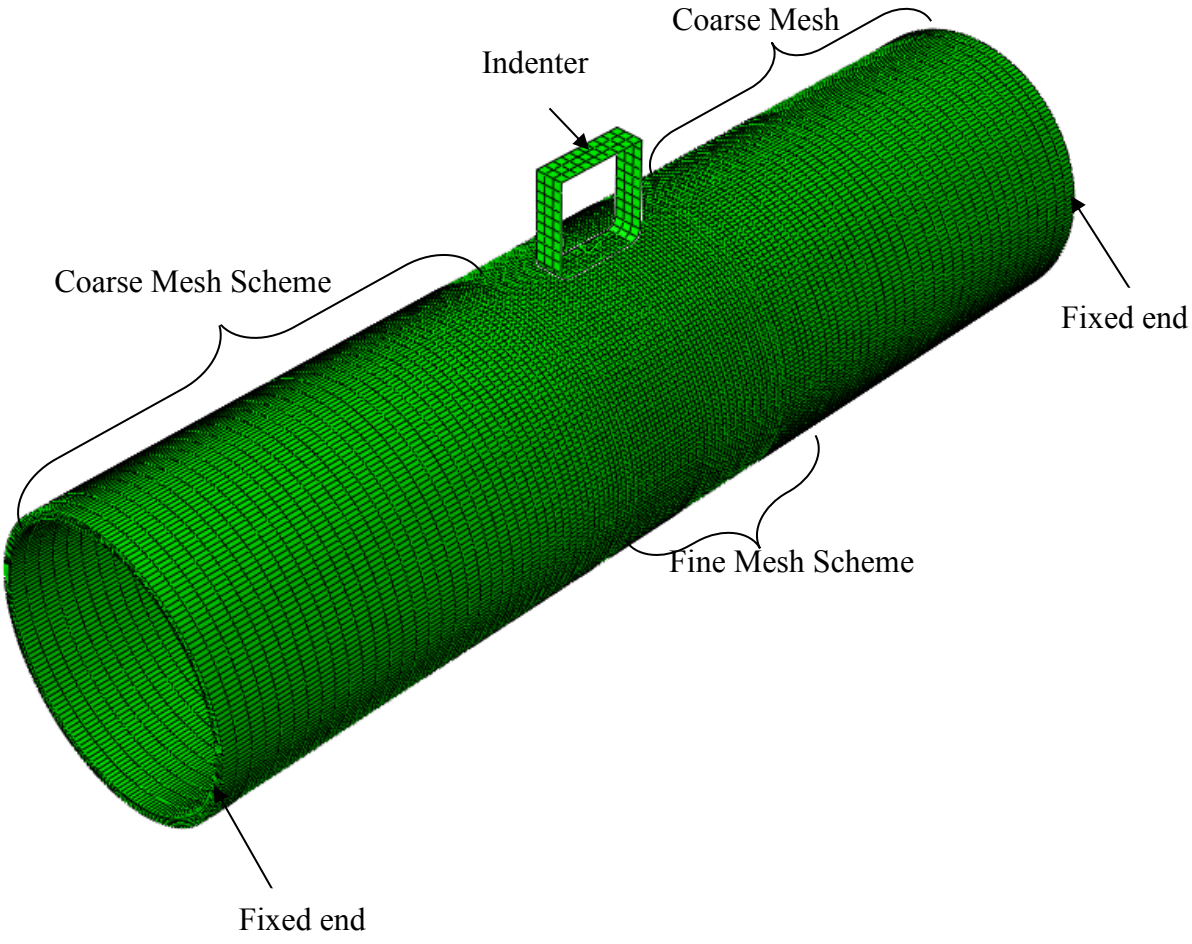

Figure 3-2: Finite element model of the deformed pipeline

3.4 Results

3.4.1 Numerical Modelling

The finite element models were generated as previously discussed with an average computation time of 60 minutes. The results from the simulation are the deformation coordinate, the deformation and the strain contours. Figure 3-3 below shows the displacement (U) contours obtained from the numerical models

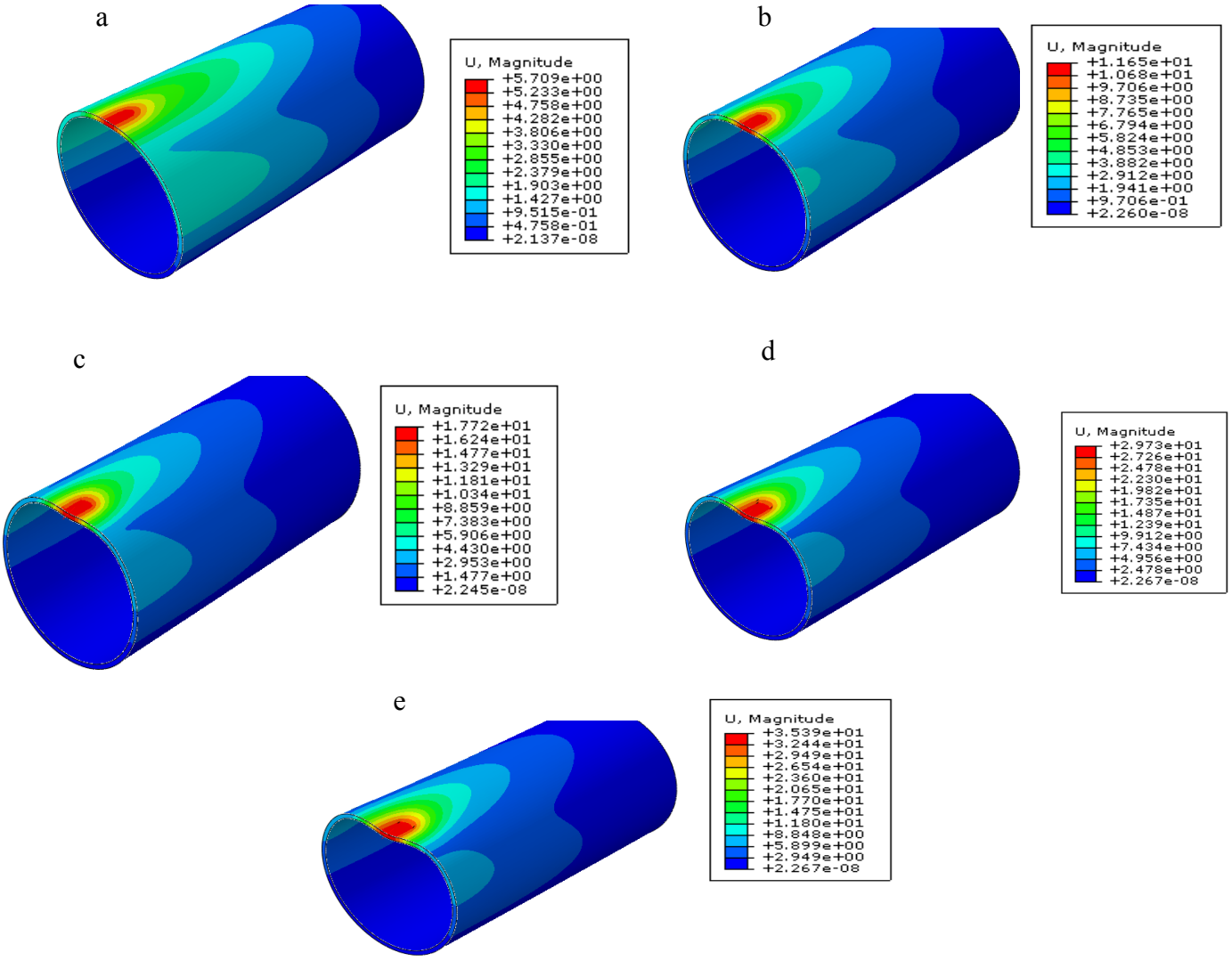

Figure 3-3: Numerical models generated for the study a. 2%, b. 4%, c. 6%, d. 10% and e. 12% OD

The data coordinates are extracted from the numerical models. B-Spline curves are then employed to interpolate the dent coordinates. The resulting surface from the interpolation of the 2% OD dent model is shown in the Figure 3- 4 below.

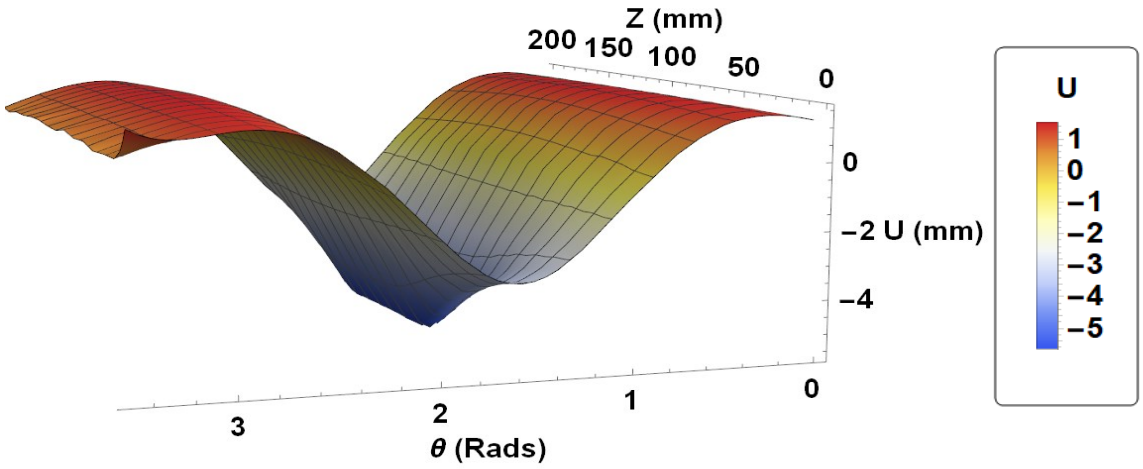

Figure 3-4: Analytical model of the dent surface for the 2% OD Model

The radius of curvatures in the longitudinal and the circumferential directions can be evaluated by performing derivatives on the spline functions that define the radial displacement of the pipeline.

The curvature, κ, of the deformed surface which is the inverse of the radius of curvature is a more descriptive representation of the deformation. The resulting directional curvatures obtained from the 2% OD model are shown in the figures (3-5 and 3-6) below.

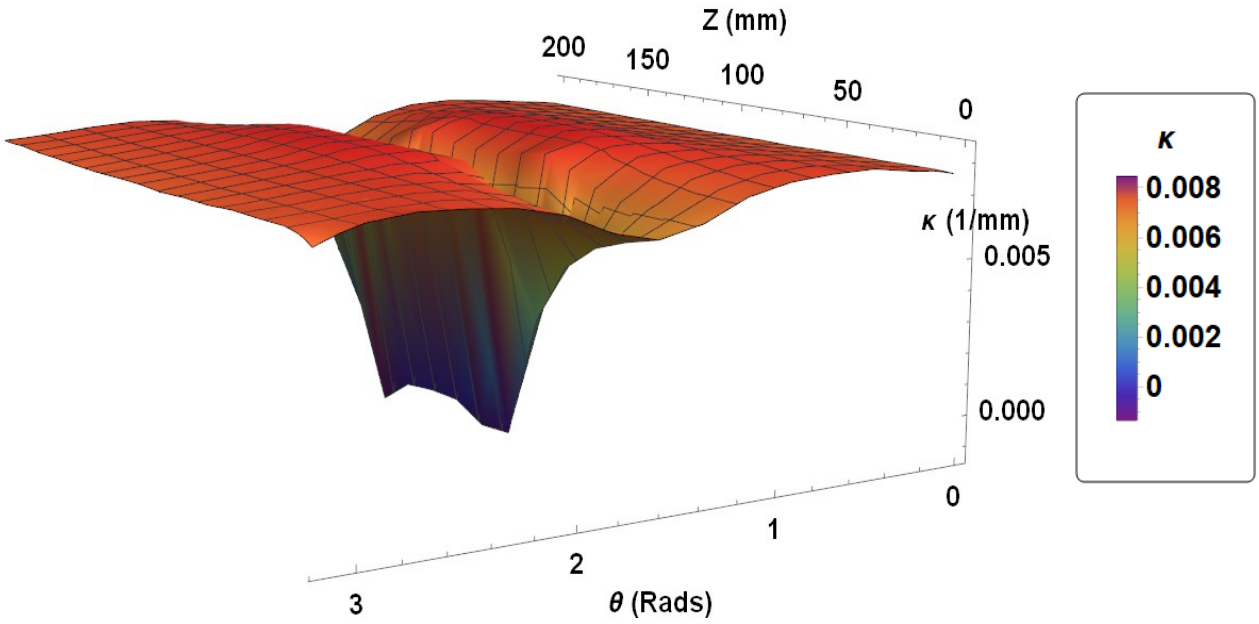

Figure 3-5: Curvature plot in the circumferential direction for the 2% OD model

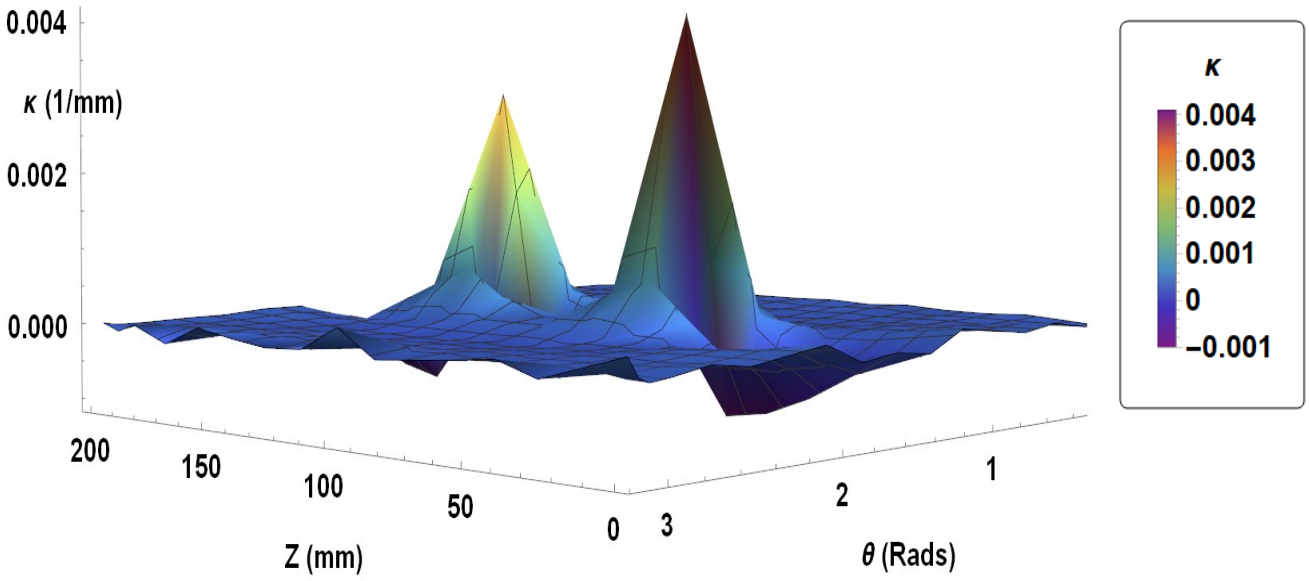

Figure 3-6: Curvature plot in the longitudinal direction for the 2% OD model

The curvatures plot above gives an indication of the positions of the strain concentrations of the dent. The circumferential curvature plot in figure has a minimum value along the peak of the

dent. This response implies that the peak circumferential strains would be generated along this region.

The longitudinal curvature plot in figure 3-6 shows two peaks which occur towards the shoulder of the dent and as such it is expected that a section that lies close to the shoulder of the dents would develop the peak longitudinal strains.

3.4.2 Strain Distribution

The normal strain components predicted from the numerical model and the ASME B31.8 equations are benchmarked. The pictorial comparison presented in this section of the study is for the dent model with a depth of 2% OD. The circumferential strains predicted by the numerical models and the analytical models are shown in figure 3-7.

From the plots in figure 3-7, the correlation in the strains predicted by the numerical models and the analytical model is observed in the similarities of the strain distributions shown in the contours. The circumferential strains in both the numerical model and the analytical model are seen to be concentrated at the dent effective region. This response is expected as from the curvature plots shown in figure 3-5, the minimum values for the curvature are concentrated along the dent effective region thus resulting in high concentrations of strains in this zone. The maximum strains predicted by the numerical model is 2.6% and this is a compressive strain developed at the external surface of the pipeline shown in figure 3-7a. The maximum compressive strain developed by the analytical model is 3.5% and this is developed at the external surface of the pipeline shown in figure 3-7b. The numerical models predict less conservative strains in the tensile zone of 1.7% in comparison to 3.5% tensile strains predicted at the internal surface of the pipeline by the ASME B31.8 equations as shown in figures 3-7c and 3-7d

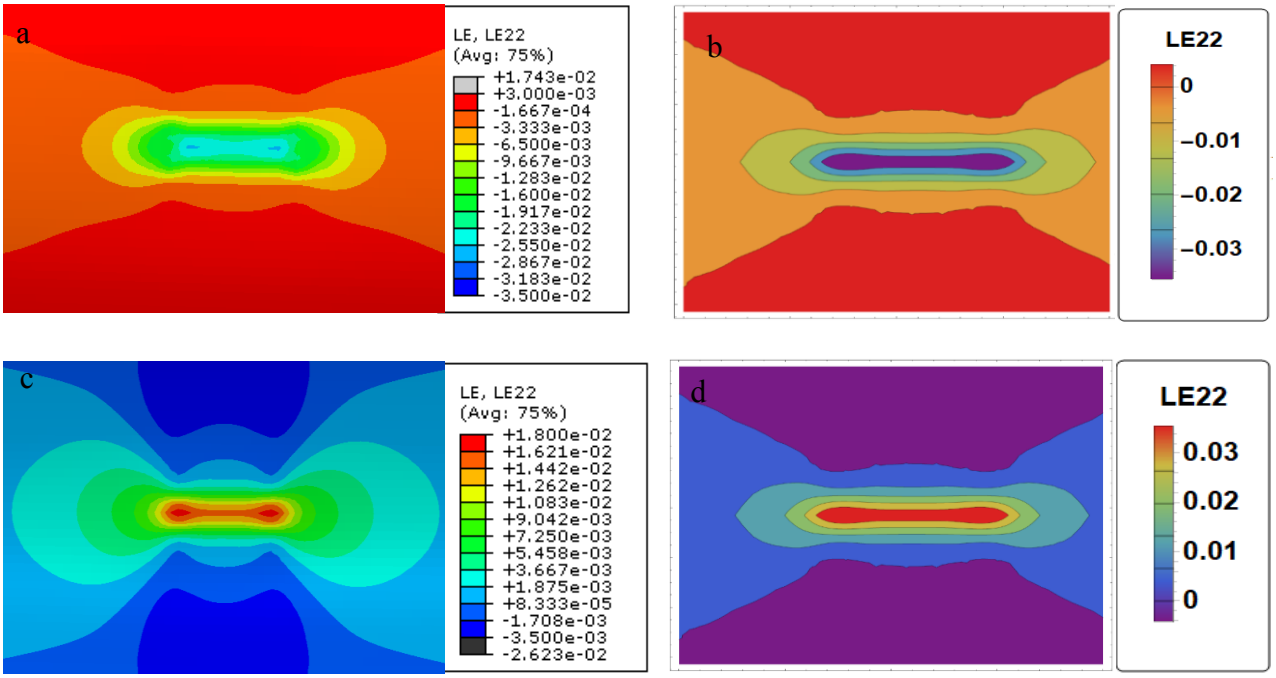

Figure 3-7: Circumferential Strains developed at a) external surface-numerical model, b) external surface-ASME B31.8. c) internal surface-numerical model and d) internal surface -ASME B31.8

The longitudinal strains are also evaluated for the 2% OD model. The results obtained from the analysis are shown in figure 3-8. From the plots in figure 3-8, it can be similarly deduced from visual inspection of the contour distribution that there is a good agreement in the predictions of the numerical model and the ASME B31.8 equations. The compressive strains distribution developed at the external surface of both the numerical and the analytical models are shown in figures (3-8a and 3-8b) respectively. The numerical model predicts a maximum strain value of 1.7% while the ASME B31.8 equations predict strain values of 1.6%. The maximum tensile strain values predicted by the numerical and the analytical models have a magnitude of 0.76% and 1.8% respectively as shown in the figures (3-8c and3- 8d) respectively.

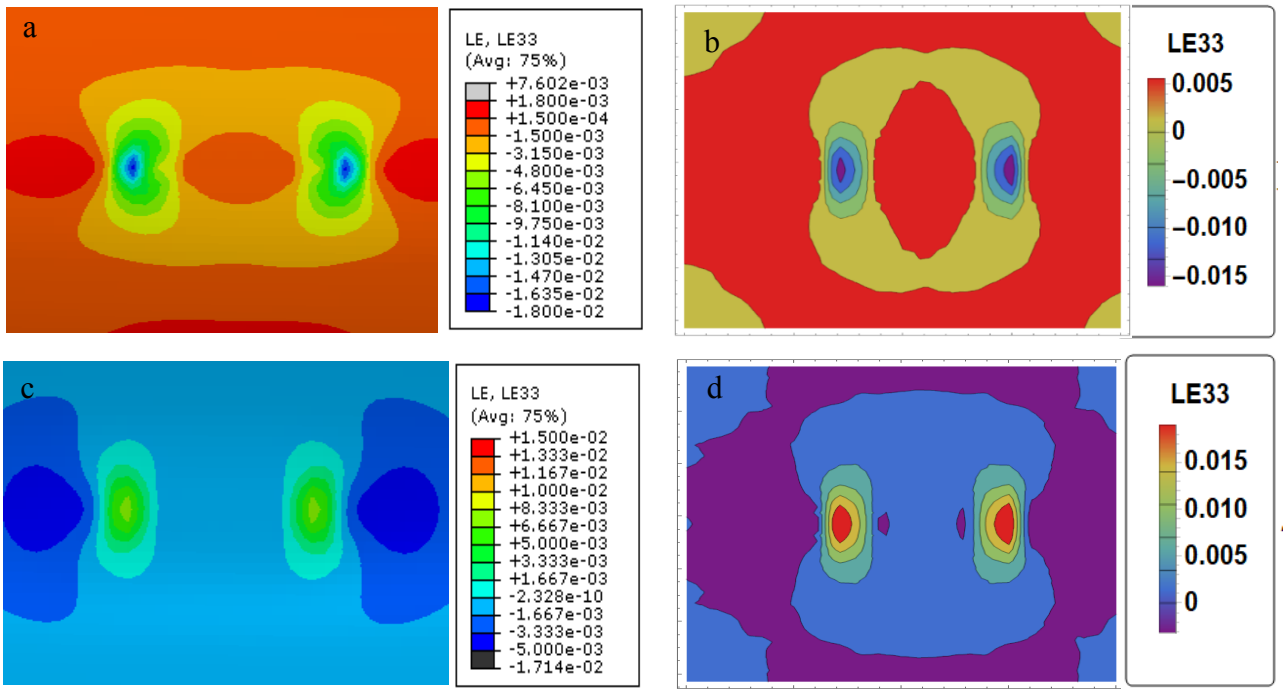

Figure 3-8: Longitudinal Strains developed at a) external surface-numerical model, b) external surface ASME B31.8, c) internal surface numerical model and d) internal surface –ASME B31.8

From figure 3.8, it can be seen that the longitudinal strains are not developed at the peak of the dent, which corresponds to the centroid of the contours, they are however developed towards the shoulder of the dent.

The equivalent plastic strains predicted by the numerical model and the ASME B31.8 equations are shown in figure 3-9. A similar trend is observed as the analytical model predicts a strain state comparable to the strain state of the numerical model in terms of the strain distribution. The maximum equivalent plastic strains developed in the numerical model are 3.5% and these are developed at the external surface of the pipeline while the analytical models predict a strain magnitude 4.3% at the external surface of the pipeline as shown in figures (3-9a and 3-9b). The maximum PEEQ strain magnitudes at the internal surface of the numerical and the analytical models shown in figures (3-9c and 3-9d) respectively are 2.6% and 4% respectively.

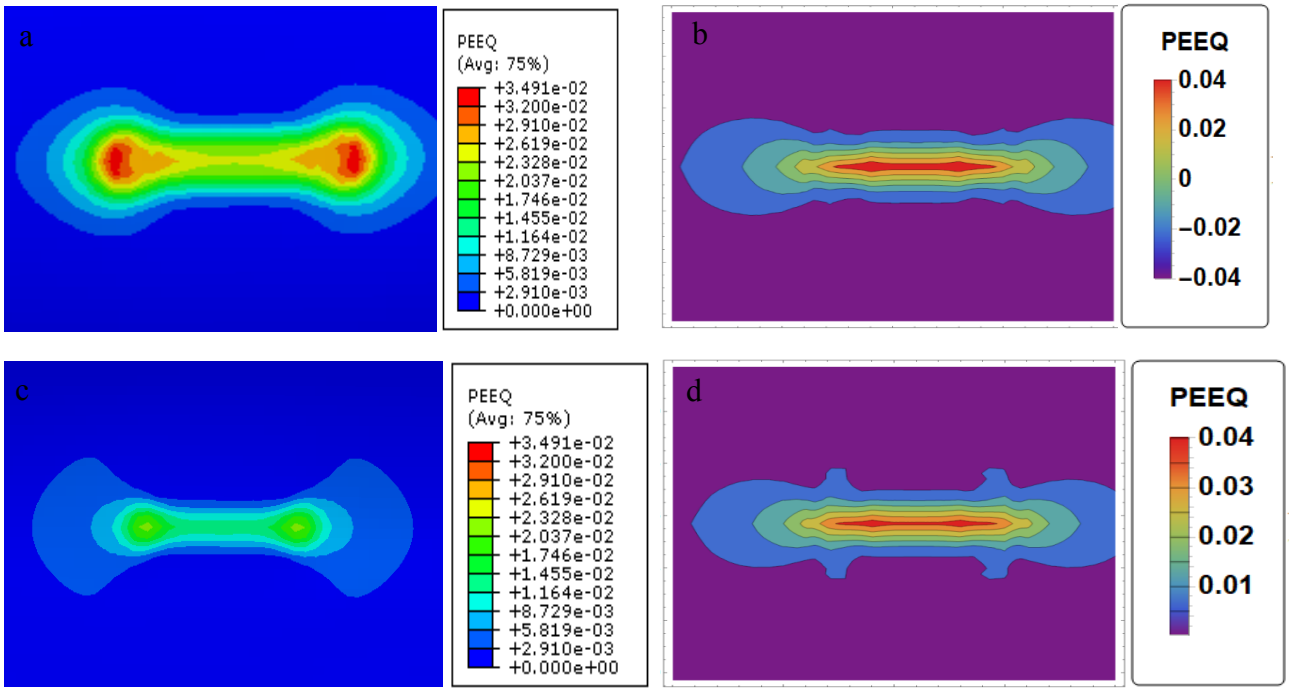

Figure 3-9: Equivalent Plastic Strains developed at a) external surface-numerical model, b) external surface ASME B31.8, c) internal surface numerical model and d) internal surface – ASME B31.8

A good correlation in the location and magnitude of the maximum plastic strains predicted by the numerical models and the analytical models was also observed in the other investigated pipeline models. The modified equations proposed by Lukasiewicz et al., (2006) are also investigated and the strain distribution predicted by the equations is shown in figure 3-10.

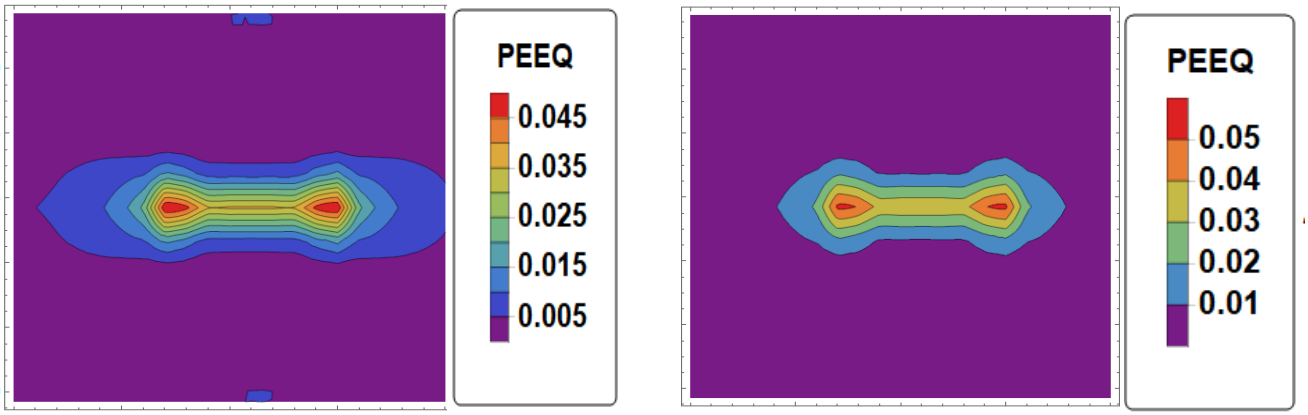

Figure 3-10: Equivalent Plastic Strains developed at a) external surface and b) internal surface – modified ASME B31.8 equations

From the contours presented in figure 3-10, it can be deduced that the modified equations predict more conservative strains when compared to the ASME B31.8 expressions. In terms of the geometric representation of the strain state, the modified equations seem to predict strain contours more comparable to the numerical models. The maximum strains are however developed at the internal surface of the pipeline. The distribution of the strains is similar as all the models show strain concentrations along the same region.

A parametric analysis is conducted to investigate these equations as regards the peak equivalent strains predicted.

Figure 3-11 is a chart showing the distribution of the PEEQ for the dent models with depths 2%-OD, 4% OD, 6%-OD, 10%-OD, and 12%-OD.

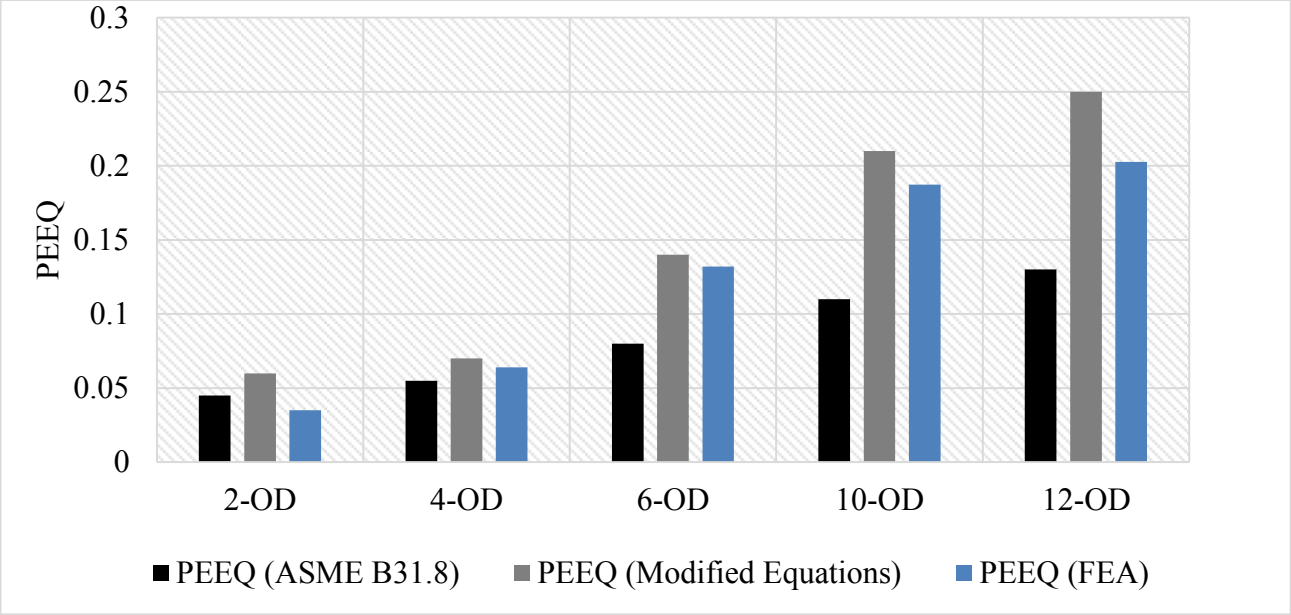

Figure 3-11: Equivalent Plastic Strains developed by the investigated dent models investigated

The plot above shows a good correlation on the peak plastic equivalent strains reported by the numerical model and the analytical models ranging from 3% to 20.27% for the dents generated with the numerical model. The plot also shows that the ASME B31.8 equations predict less conservative strains for the models analyzed in this study. The modified expressions which follow the constitutive relationship of deformation plasticity predicts strains similar in magnitude and more conservative than the strains predicted by the numerical model.

3.4.3 Sensor Investigation

For the previously analyzed models, the data coordinates used to develop the deformation contours were extracted at 64 points along the circumference of the pipeline. This degree of accuracy might, however, not attainable by all inline inspection devices and as such, the number of sensors required for predicting the strains effectively are also investigated. The different PEEQ strain contours were obtained considering the interpolation of the dent geometry with a

decreasing number of data points, corresponding to an inline inspection device with 64, 32, 16 and 8 sensors along the tools circumference. Figure 3-12 below shows the PEEQ strain contours developed at the external surface of the pipeline using the modified equivalent strain expressions in equation (6) in the 2%-OD dent model

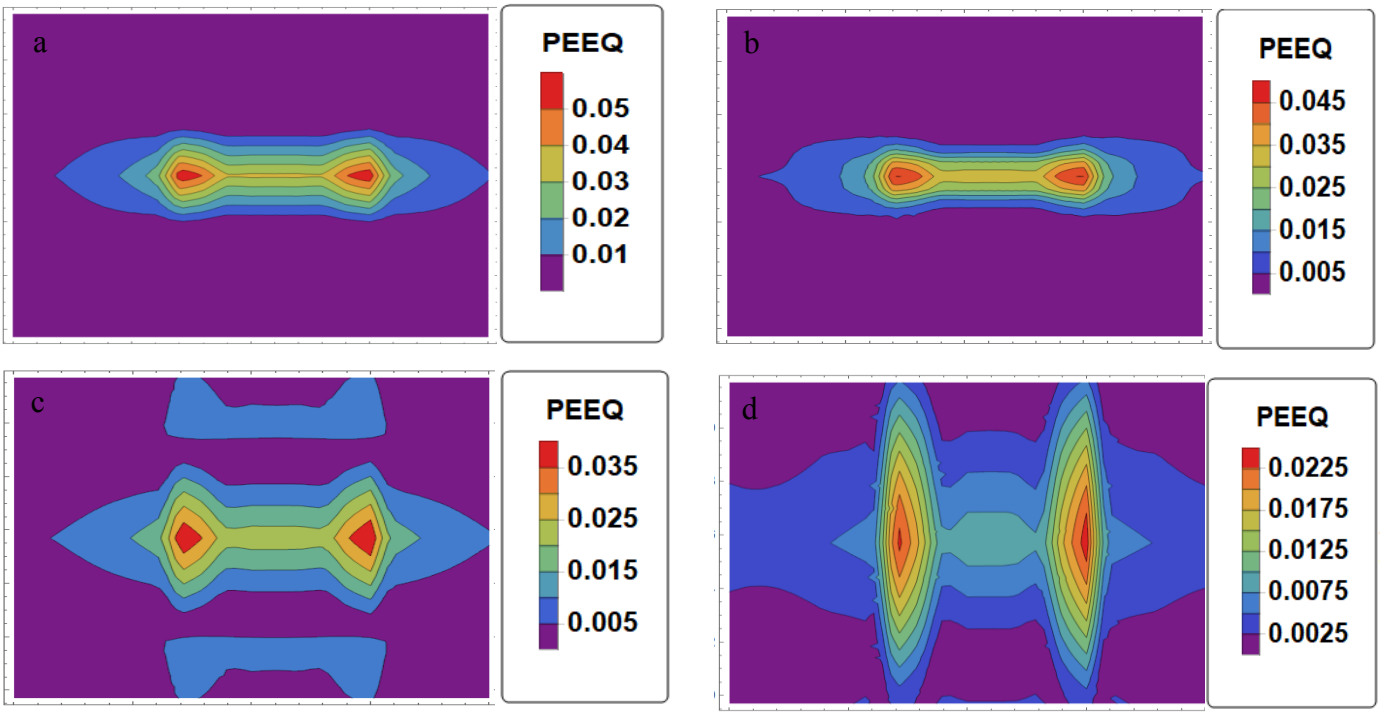

Figure 3-12: Equivalent Plastic Strains developed at a) 64-sensors, b) 32-sensors, c) 16-sensors and d) 8-sensors

From the contours presented in figure 3-12, it can be deduced that the PEEQ distributions predicted by the 64 and the 32 sensor tools are comparable with values of 3.75% and 4 % respectively. However, for the 16 sensor and the 8 sensors tools shown in figures (3-12c and 3-12d), the strain distribution is more distorted and the maximum values predicted are 3% and 2.3% respectively.

This analysis is also performed on the 12%-OD dent model. The distribution of the plastic strains is shown in figure 3-13. The contours show that the data obtained from the tool with 64 sensors

can be used to predict strains comparable with the numerical model as shown in the figures (3-13a. and 3-13e) respectively. The maximum equivalent strains predicted by the numerical model is 20% which occurs within the pipe wall, however, at the internal surface of the model, the maximum strains predicted are approximately 19% and the peak equivalent strains predicted by the analytical model is 23%. The strains predicted in these two models are comparable in magnitude and location. The results obtained from data with 32 sensors shown in figure 3-13b predicts a good representation of the strain state of the pipeline with the maximum strains predicted being 21%.

The results obtained from tools with 16 and 8 sensors shown in figures (3-13c and 3-13d) do not agree with the numerical model show in figure 3-13e. The magnitudes are similar, however, the location of the strain concentrations differ significantly.

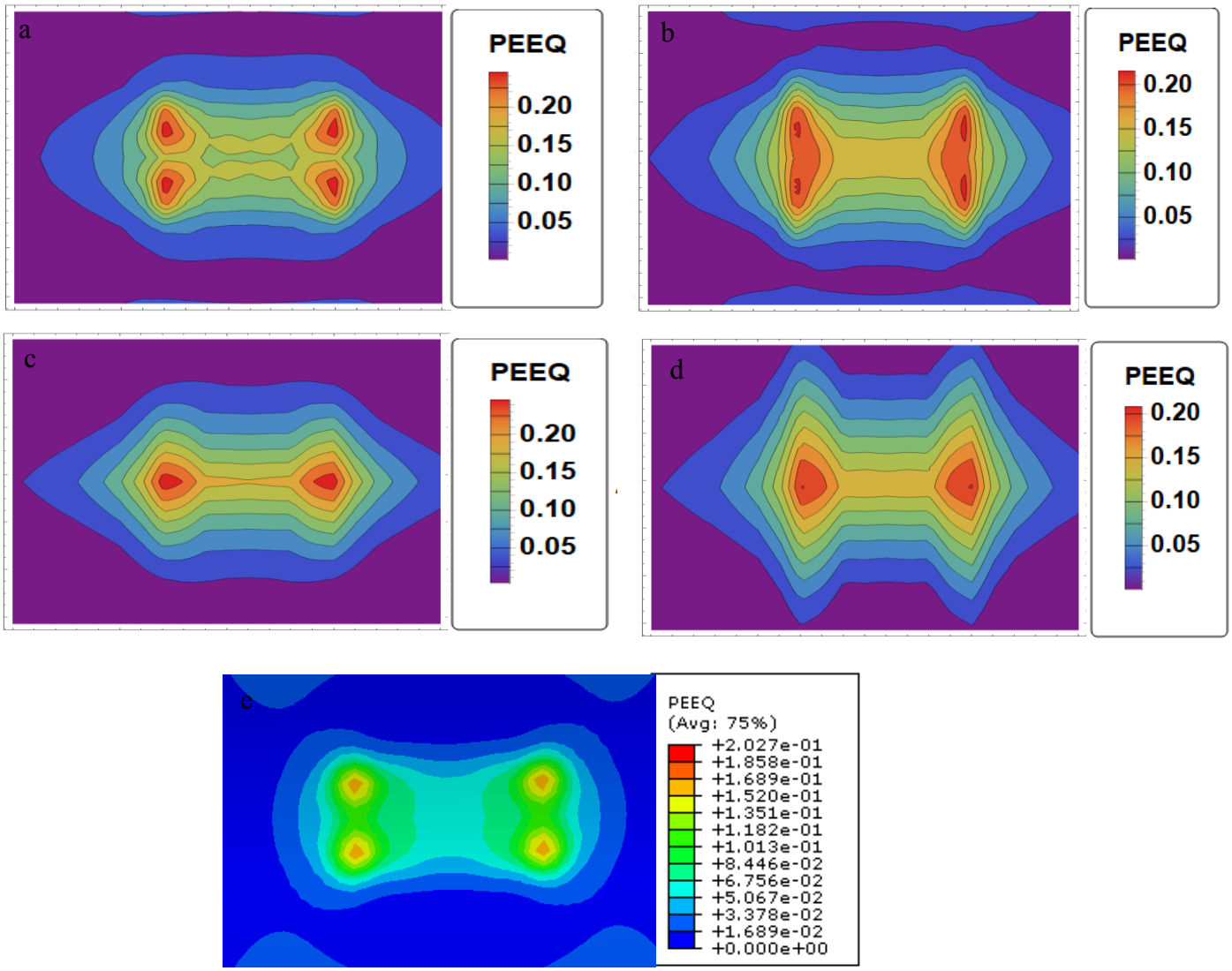

Figure 3-13: Equivalent Plastic Strains developed at a) 64-sensors, b) 32-sensors, c) 16-sensors, d) 8-sensors and e) numerical model.

A plot of all the models investigated is shown in figure 3-14.

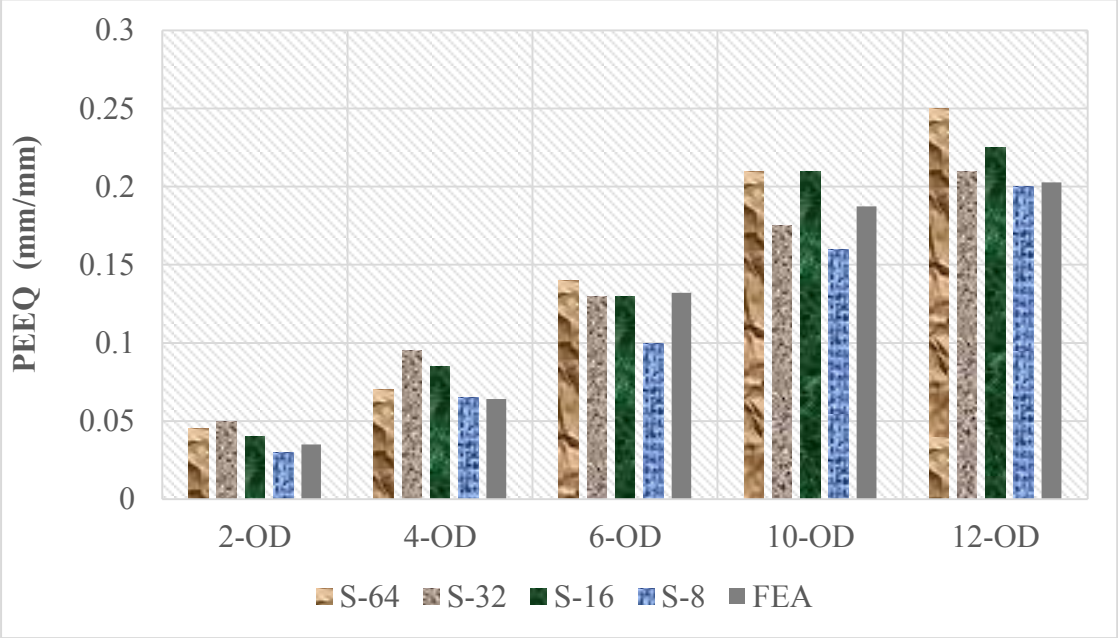

Figure 3-14: Equivalent Plastic Strains developed at a) 64-sensors, b) 32-sensors, c) 16-sensors, d) 8-sensors and e) numerical model.

The plot above shows that once the most serve point of the dent profile corresponding to the peak of the dent is included as a data point for the interpolation, the strain magnitudes are similar. However, from the contour plots developed, the locations could differ significantly.

3.5 Discussions

The work done herein is an extension of the already existing B-Spline technique to the interpolation of dented pipelines (Noronha et al., 2005) and the established ASME B31.8 directional strain component equations and the equivalent strain formulation that accounts for deformation plasticity (Lukasiewicz et al., 2006 and Noronha et al., 2010). The continuity of the B-Spline functions allows for the evaluation of the radius of curvature of the dented region of the pipeline. This approach to the three-dimensional strain evaluation could be implemented into

smart inline inspection tools such that the strain state of the deformed pipeline can be reported concurrently with the deformation profile.

While the ASME B31.8 codes state that the orientation of the radius of curvature for the reentrant dents should be negative while for dents that partially flatten the pipeline should be positive. A similar constraint is placed on the radius of curvature evaluated in the longitudinal direction, however, in the computation presented in this study, the radius of curvature is evaluated analytically using the expressions defined in equations (7 and 8) and the orientations of the curvatures used as is. A sign convention is, however, selected such that tensile strains are dominant in the internal surface of the pipeline and the compressive strains are dominant at the external surface of the pipeline.

The equivalent strains referred to in this study have been termed as "plastic" as the contribution of the elastic component of the deformation has been ignored. This was also done to ease the comparison of the analytical models and the numerical models. The ASME B31.8 equations provide a reasonable estimate of the strain state of the pipeline especially for the directional bending strain components. However, their predictions might underestimate the strain state of the pipeline as the circumferential membrane strains and the radial strains are ignored and these could be significant contributors the global strain state of the pipeline. The proposed equations in Noronha et.al. (2010) provide a good estimate of the strain distribution of the strains in the dented pipeline, while obeying the constitutive laws of deformation plasticity and could be better improved to account for the shear strains associated with the deformation as not all dent features are aligned in the principal directions. The investigation on the number of sensors revealed that 64 and 32 sensors along the circumference of the pipeline provides a good representation of the dent's surface and subsequently a strong correlation in the predicted values to the results from

nonlinear FEA, while data obtained from 8 and 16 sensors on the tool would result in erroneous strain values owing to the oscillations of the B-spline curves. The interpolation with few data points affects the mathematical dent surface generated and fails to capture the nodes that define the entire surface of the dent. It is however worth noting that the most severe point of the dent was always constrained to be a control point and as such the vector position of the most severe point of each dent surface was reported for each of the interpolated dent sections. The strain distribution predicted would vary significantly if this vector position were to be missed in the interpolation.

3.6 Conclusion

This study shows that the current implementation of the ASME B31.8 equations to the peak of the dent can lead to erroneous decisions as the location of the peak strains are hugely dependent on the geometry of the dent and while it might be considered common for the peak strains to be generated at the peak of the dent, it does not necessarily hold for all cases. The dents modelled predict peak strains towards the shoulder and these identified strain concentrations might not be captured by a two-dimensional strain analysis of the apex of the dent. The modeled dents are restrained dents and the pipelines are not pressurized, thus eliminating the concern of fatigue cycling of the dented surface and the rebounding of the dented surface. It will be interesting to investigate how these closed form expressions perform when used for the analysis of unrestrained dents subjected to internal pressure cycles.

References

ASME B31.8 Gas Transmission and Distribution Piping Systems. 2003. ASME International, New York, NY.

Baker, M., 2004. “Integrity Management Program–Dent Study.” Delivery Order DTRS56-02-D-70036, Final Report.

Cosham, A. and Hopkins, P., 2001. A New Industry Document Detailing Best Practices in Pipeline Defect Assessment. Proceedings of the International Onshore Pipeline Conference Amsterdam, The Netherlands.

Cosham, A. and Hopkins, P., 2003. The Pipeline Defect Assessment Manual (PDAM). A Report to the PDAM Joint Industry Project. Newcastle, UK.

CSA Z662, Oil and Gas Pipeline Systems. 2016.

Dawson, S.J., Russel, A. and Patterson, A., 2006. Emerging Techniques for Enhanced Assessment and Analysis of Dents. Proceedings of the International Pipeline Conference, Calgary, Alberta, Canada, Paper No. ASME, IPC2006-10264.

Deng, X. and Denney, T.S., 2002. 3D Myocardial Strain Strain Reconstruction from Tagged MRI using a Cylindrical B-Spline Model. In Biomedical Imaging. Proceedings of the IEEE International Symposium on (pp. 609-612).

Dinovitzer, A., Lazor, R., Carroll, L.B., Zhou, J., McCarver, F., Ironside, S., Raghu, D. and Keith, K., 2002. Geometric Dent Characterization. Proceedings of the International Pipeline Conference, Calgary, Alberta, Canada, (pp. 1589-1598). American Society of Mechanical Engineers.

Gao, M., McNealy, R., Krishnamurthy, R. and Colquhoun, I., 2008. Strain-Based Models for Dent Assessment-A Review. ASME Paper No. IPC2008-64565. Proceedings of the International Pipeline Conference, Paper No. ASME, IPC04-0061, Calgary, Alberta, Canada.

Iflefel, I.B., Moffat, D.G. and Mistry, J., 2005. The Interaction of Pressure and Bending on a Dented Pipe. International Journal of Pressure Vessels and Piping, 82(10), pp.761-769

Lukasiewicz, S.A., Czyz, J.A., Sun, C. and Adeeb, S., 2006. Calculation of Strains in Dents Based on High Resolution In-line Caliper Survey. Proceedings of the International Pipeline Conference, Calgary, Alberta, Canada, (pp. 129-134).

Maxey, W.A., 1986. Outside Force Defect Behaviour, Report to Linepipe. Research Supervisory Committee of the Pipeline Research Committee of the American Gas Association, NG-18 Report No. 162, AGA Catalogue No. L51518, Battelle.

Noronha, D.B., Martins, R.R., Jacob, B.P. and Souza, E., 2005. The use of B-splines in the Assessment of Strain Levels Associated with Plain Dents. Proceedings of the Rio Pipeline Conference and Exposition.

Orynyak, I.V. and Shlapak, L.S., 2001. Estimation of Ultimate Pressure for a Pipe with a Dent. Problemy Prochnosti, 5, pp.101-110.

Rafi, A.N.M., Das, S., Ghaednia, H., Silva, J., Kania, R. and Wang, R., 2012. Revisiting ASME Strain-Based Dent Evaluation Criterion. Journal of Pressure Vessel Technology, 134(4), p.041101.

Rosenfeld, M.J., Porter, P.C. and Cox, J.A., 1998. Strain Estimation using Vetco Deformation Tool Data. Proceedings of the International Pipeline Conference, Calgary, Alberta, Canada.

Weisstein, E., 2005. Wolfram Mathworld.

Chapter 4- Three Dimensional Strain Based Model for the Severity Characterization of Dented Pipelines

4.1 Abstract

Oil and gas pipelines traverse long distances and are often subjected to mechanical forces that result in permanent distortion of its geometric cross-section in the form of dents. In order to prioritize the repair of dents in pipelines, dents need to be ranked in order of severity. Numerical modeling via finite element analysis (FEA) to rank the dents based on strains is one approach that is considered to be computationally demanding. In order to reduce the computation time with minimal effect to the completeness of the strain analysis, an approach to the analytical evaluation of strains in dented pipelines based on the geometry of the deformed pipeline is presented herein. This procedure employs the use of B spline functions which are equipped with second order continuity and differentiability to generate displacement functions which define the surface of the dent. The strains associated with the deformation can be determined by evaluating the derivatives of the displacement functions. The mathematical model developed in three-dimensions allows pipeline operators to rapidly determine the severity of a dent with flexibility in the choice of strain measure so as to constrain or release the strain model from governing assumptions and account for the associated non-linearity in the deformation. The strain distribution predicted from the mathematical model proposed is benchmarked against the strains predicted by nonlinear FEA. A good correlation is observed in the strain contours predicted by the analytical and numerical models in terms of magnitude and location. A direct implication of the observed agreement is the possibility of performing concise strain analysis on dented pipelines with algorithms relatively easy to implement and not as computationally demanding as FEA.

Keywords-Pipeline, FEA, Strain.

4.2 Introduction

Pipeline systems form a major sector of the distribution and transmission network for oil and gas products. With use, environmental exposure, and third party interactions these structures are susceptible to damage. These damages include but are not limited to mechanical damages, corrosion, and wrinkles. Mechanical damages and corrosion have in recent time been identified as a major cause of pipeline failure (Cosham and Hopkins, 2004). The Canadian pipeline code, (CSA-Z662-2016) defines dents as depressions caused by mechanical damage that produces a visible disturbance in the curvature of the pipe or its component without reducing the wall thickness. The mechanism for the dent formation in piplines is a relatively simple phenomenon, as when subjected to heavy loads, pipes absorb the applied energy and transform it to plastic deformations (Karamanos and Andreadakis, 2006). These plastic deformations as a result of the formation of dents can indeed set up a sequence of events leading to eventual failure of the pipeline.

Dents in pipelines can be classified in terms of the rate of change of the curvature of the pipe wall as smooth or kinked, the former being used to described dents resulting in a smooth change in the curvature of the pipe wall and the latter used to describe dents that are associated with a sharp change in the pipe wall (Cosham and Hopkins, 2004). Dents are also classified by the response of the dented pipeline to internal pressure cycles as constrained or unconstrained. The constrained dents do not undergo the elastic rebound and inelastic reround of the pipeline after the indentation while the unconstrained dents can be pressure cycled after the indentation (Alexander,1999). Pipeline dents can further be classified by the consequence of contact and the timeframe of the consequence of contact (Leis, Forte and Zhu, 2004) in which the dents are categorized by their stability and failure timeframe respectively. The most common precedent for

judging the severity of dents is the depth based criterion, as adopted in many standards including the Canadian pipeline standards, CSA-Z662-16, which requires the repair of pipes with a plain dent deeper than 6% of the outside diameter (OD). Recent research has shown that the depth based criterion for discerning the severity of a dent is indeed not sufficient as it might be unduly conservative in its predictions leading to unnecessary excavations (Gao et al., 2008). It is also possible for failures to occur in shallow dents as reported in the National Energy Board safety advisory, (Erikson, 2010). The American standards, ASME B31.8-2007 presents closed form expressions that can be used to evaluate the strains in a dented pipeline by discretizing the strain into components. A schematic representation of the strain components in a pipeline is shown in figure 4-1.

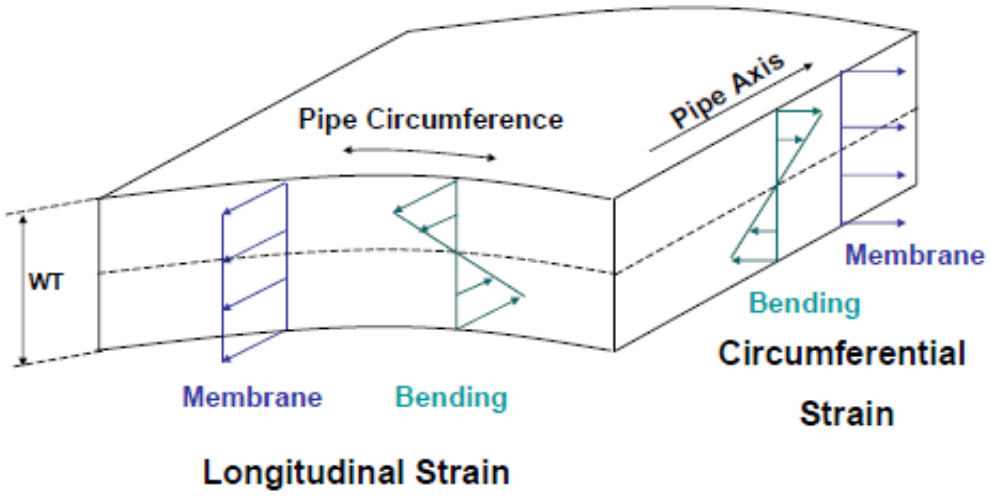

Figure 4-1: Strain components acting on a pipe wall (Lukasiewicz, et al 2006)

From figure 4-1, it can be seen that the bending strains represented in equations (1) and (2) vary linearly along the thickness of the pipe wall, while the longitudinal membrane strains, represented in equation (3) which are as due to the extension of the pipeline in the longitudinal direction remains constant along the thickness of the pipe wall. The expressions for the circumferential bending strain,(ε_1), the longitudinal bending strain,(ε_2), and the longitudinal

membrane strains (ε_3) at the peak of the dent as stipulated by ASME B 31.8-2007 standards are given in the equations (1-3)

$$\varepsilon_1 = \frac{t}{2}\left(\frac{1}{R_0} - \frac{1}{R_1}\right) \quad (1)$$

$$\varepsilon_2 = \frac{t}{2}\left(\frac{1}{R_2}\right) \quad (2)$$

$$\varepsilon_3 = \frac{1}{2}\left(\frac{d}{L}\right)^2 \quad (3)$$

where, t, is the pipe wall thickness, R_0 is the radius of the un-deformed pipeline, R_1 and R_2 are the external radii of curvature of the dent in the circumferential and longitudinal directions respectively, d is the depth of the dent and L is length of the dent.

These strain components are then combined accordingly to evaluate an equivalent total strain in the dented section as shown in equations (4) and (5).

$$\varepsilon_i = \sqrt{(\varepsilon_1)^2 - \varepsilon_1(\varepsilon_3 + \varepsilon_2) + (\varepsilon_3 + \varepsilon_2)^2} \quad (4)$$

$$\varepsilon_o = \sqrt{(\varepsilon_1)^2 + \varepsilon_1(\varepsilon_3 - \varepsilon_2) + (\varepsilon_3 - \varepsilon_2)^2} \quad (5)$$

where ε_i and $\varepsilon_o$are the strains in the inner and outer surfaces of the pipe wall respectively. The ASME B31.8 however does not clearly specify a method to be employed in the evaluation of the radius of the curvature of the dent. The study in Rosenfeld et al. (1998) presents the use of the half point osculating circle method and piecewise Bessel cubic interpolation for evaluating the radius of curvature. This technique, however, has its limitations when dents with complex geometries are being analyzed as identified by Noronha et al. (2005) whose work proposed the use of fourth order B-Spline interpolation for estimating the radii of curvature of the deformed

pipelines. The expressions outlined in the ASME B31.8 standards have also been subjected to criticism owing to the oversimplification of assumptions in their derivation and the ambiguity in the code stipulations regarding the definition of longitudinal membrane strains. The strain equations proposed in the 2003 edition of the ASME B-31.8 standard overestimates the bending strains by a factor of 2 as identified by (Noronha et al., 2005) this was corrected in the 2007 edition. However, with the current dent strain equations, the strain components in the dented region of a pipe are evaluated at the apex of the dent and combined based on the plane strain condition. It was also noted that longitudinal membrane strains presented in equations (3) is an empirical estimate benchmarked against a limited number of FEA models and as such is reported to have predicted erroneous strains (Baker et al., 2004). The codified dent strain equations are limited by its governing premise of assuming that the dent features are all aligned in the principal directions and also that the radial strains are ignored. The combined strain equations are derived using the plane strain assumption leading to incorrect equivalent strain predictions. Certain work by Lukasiewicz et al. (2006) presents an alternative method for evaluating the strains in deformed pipelines using mathematical algorithms and an FEA tool. The procedure is based on the shell theory as a shell model is used to define the mid-surface of the pipeline. The deflections in the longitudinal, circumferential directions are obtained from the numerical model while the radial displacements are obtained from high resolution inline inspection devices. The equivalent strain in the pipeline is evaluated by discretizing the strains into the bending and the membrane components. The strains are not also assumed to be aligned in the principal axis as the shear components are also evaluated. The equivalent strain can thus be evaluated using the closed form mathematical expressions shown in equation (6).

$$\epsilon_{eq} = \frac{2}{\sqrt{3}}\sqrt{\epsilon_x^2 + +\epsilon_y^2 + \epsilon_x\epsilon_y + \frac{\gamma_{xy}^2}{2}} \tag{6}$$

where, ϵ_x , ϵ_y and γ_{xy} are the longitudinal, circumferential and shear strains respectively .

It was suggested that the strains in a dented pipeline be split into the membrane and the bending strains, the membrane strains are to be evaluated using a finite element shell model with two degrees of freedom while the bending strains are evaluated analytically using the standard ASME –B31.8 equations. The results produced from the study were promising, however, the procedure still depends on the input of FEA which can increase the computation cost per dent analysis.

Noronha et. al. (2010) suggested two modifications to the strain evaluation technique, the first is based on the premise that the elastic strains developed in the deformed pipeline are negligible and the radial strains and the circumferential membrane strains are negligible. This premise allows the setting of the Poisson ratio of the pipeline to be 0.5. The expression for the equivalent strain state of the pipeline becomes equation (7)

$$\epsilon_{eqv} = \frac{\sqrt{2}}{3}\sqrt{[(\epsilon_I - \epsilon_{II})^2 + (\epsilon_{II} - \epsilon_{III})^2 + (\epsilon_{III} - \epsilon_I)^2} \quad (7)$$

where ϵ_I, ϵ_{II} and ϵ_{III} represent the principal strains in the longitudinal , circumferential and the radial directions. For the second suggested modification, it is assumed that the strains developed are not associated with a volume change and the radial component of the strains can be evaluated as the additive inverse of the sum of the longitudinal and the circumferential strain components. The resulting equation is shown in equation (8)

$$\epsilon_{eqv} = \frac{2}{\sqrt{3}}\sqrt{\epsilon_1^2 + \epsilon_{II}^2 + \epsilon_I\epsilon_{II}} \quad (8)$$

Comparing the strains predicted by these models revealed that while the ASME B31.8 equations shown in equations (4 and 5) and the first modification shown in equation (7) underestimate the

strains in a dented pipeline, the expressions in equation (8) performed reasonably better than the previous equivalent strain expressions predicting strain values comparable to results from nonlinear FEA.

As an optional technique to the analysis of dents, numerical methods via simulations can be used to characterize the severity of a dent feature on a pipeline. The numerical modelling technique with FEA provides a medium for predicting the stresses and strains in a dented pipeline from the material properties and shape functions of the mechanical-numerical model of a pipe defect of similar geometry (Belanger and Narayanan, 2008). The accuracy of this procedure is hinged on the representation of the material model of the pipeline and the geometry of the dent reported by the inline inspection devices with a numerical model (Woo et al., 2017). This numerical approach, with FEA to dent severity assessment is a more detailed technique to evaluating the developed strains when compared to the closed form expressions but it is however computationally prohibitive if used on the numerous dents reported from pipe inspections (Belanger and Narayanan, 2008). This study aims to derive an analytical technique for the strains developed during the indentation of a pipeline without considering the effect of initial imperfections of the pipeline, stress concentrator, discontinuities and internal pressure cycles. The deformation associated with the dent is discretized into the radial, circumferential, longitudinal directions in the cylindrical coordinate system. This discretization of the deformation allows operators the choice in the strain measure to be employed and offers more control on the constraining assumptions in the strain model. The result of the numerical procedure is the strain tensor that defines the strain state of the deformed pipeline.

4.3 Methods

4.3.1 Modeling of Dents

A series of generic nonlinear FEA pipeline indentation simulations was conducted using the commercially available numerical solver, ABAQUS 6.14. The numerical model was validated using the results from the experimental investigation performed in (Rafi et al., 2012). The full scale test specimen considered was a pipe of length 1100 mm, radius of 140 mm and a diameter to thickness ratio of 35. The pipe is an X-60 pipe having a yield stress, σ_y, of 400 MPa. The internal pressure corresponding to 20% of the yield pressure in the circumferential direction was applied with a hydro pump. The pipeline was restrained from global vertical displacement by supports and a rectangular indenter with dimensions 100mm by 36 mm and was displaced such that the final depth after is 10% of the pipeline's OD. The developed numerical model was generated to closely represent the experimental set up described above. The pipeline was modelled as an elastoplastic material and meshed with 8 node brick elements. The contact region between the pipeline and the indenter was defined using the master slave algorithm and a frictionless contact surface. Isotropic hardening was used to define the strain hardening response of the pipeline. A displacement controlled algorithm tracks the nonlinear equilibrium path of the deformed pipeline. This numerical model was validated with the load displacement response of the experimental study. However, for the generic models generated for this study, the pipes modeled were unpressurised and the dents formed were restrained. The parameters being investigated are 5 different dent depths and 3 different shapes of indenters and as such a total of 15 numerical models were generated. The dent depths investigated are 2%, 4%, 6%, 10% and 12% OD for each of the indenter shapes considered. The indenter shapes investigated were, a spherical indenter, a flat indenter and an irregular indenter which was unsymmetrical about one

of its axis. The diameter of the spherical indenter is 50 mm, the flat indenter has a length of 80 mm in contact with the pipeline's external surface and fillets of 10 mm, and the irregular indenter is asymmetrical along the longitudinal direction of the pipeline having a length of 100 mm and two peaks with a base length of 35 mm and 50 mm, respectively.

A unique name was chosen for each dent model, the SD models refer to the dents generated with the spherical indenter while FD and the AD models refer to the model generated using the flat and the asymmetric indenters respectively. The numerical suffix after the model name refers to the depth of the dent as a percentage of the OD.

4.3.2 Dent Profile Interpolation

The interpolation is done with the computing tool Mathematica which has inbuilt tools for the spline interpolation of surfaces. The data points that define the geometry of the dented surface of the pipeline are extracted from the numerical models and interpolated with B-spline curves as discussed in Noronha et al. (2005). The data points here refer to vector coordinates of the deformed pipeline which are extracted directly from the numerical model and converted into the cylindrical coordinate system as discussed in Luo and Chen (2000). The B-Spline curves are polynomials between a pair of data points with components defined in such a way that some level of smoothness up to a particular derivative is attained.

The coordinates are extracted at 64 points along the circumference of the pipeline at every 10 mm interval. The spline functions used for the surface interpolation are equipped with second order continuity so as to generate a differentiable mathematical surface for the dent.

4.3.3 Displacement Discretization

The morphology of the pipeline is well suited for the cylindrical coordinate system and as such the coordinates of the deformed pipeline can be obtained as described in (Okoloekwe, et al 2017). The transformation to this coordinate system is such that the coordinates of the deformed profile are thus represented in terms of the radial position, R, angular position, θ, and the longitudinal position, Z.

The schematic representation of this coordinate system is shown in figure 4-2.

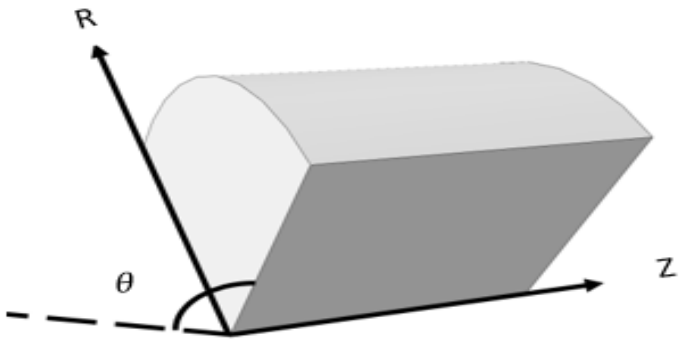

Figure 4-2: Schematic representation of the cylindrical coordinate system

The formulation of the global displacement field (u) of the pipeline in this coordinate system is such that the relationship shown in equation (9) holds.

$$u = u_r e_r + u_\theta e_\theta + u_z e_z \tag{9}$$

where u_r, u_θ, u_z represent the displacements in the local direction e_r, e_θ, and e_z respectively.

The gradient of the displacement vector can then be obtained taking into consideration that the basis vectors e_r and e_θ vary with the angular position, θ while e_z is independent of the angular position. Equation (10) shows the mathematical representation of the displacement gradient.

$$\nabla u = \begin{Bmatrix} \frac{\partial u_r}{\partial R} & \frac{\partial u_r}{R\partial\theta} - \frac{u_\theta}{R} & \frac{\partial u_r}{\partial z} \\ \frac{\partial u_\theta}{\partial R} & \frac{u_r}{R} + \frac{\partial u_\theta}{R\partial\theta} & \frac{\partial u_\theta}{\partial z} \\ \frac{\partial u_z}{\partial R} & \frac{\partial u_z}{R\partial\theta} & \frac{\partial u_z}{\partial z} \end{Bmatrix} \quad (10)$$

where, R is the radius of the mid-surface of the deformed pipeline. The local deformation of a pipeline is associated with geometric and material nonlinearities and as such it is difficult to obtain a theoretical solution without some simplifications in assumptions. In this formulation, it is also assumed that the normal to the pipe wall's midsurface prior to the deformation remains straight and normal and this implies that the thickness of the pipe wall remains unchanged during the deformation. A hypothetical radius of the mid-surface of the pipeline, R_{hyp} is evaluated such that the inextensibility of the pipes circumference is enforced. This is done by solving the expression in equation (11)

$$R_{hyp}(\theta, z) = \frac{\int_{-\Pi}^{\Pi} R_m(\theta,z)\partial\theta}{2\Pi} \quad (11)$$

where, R_m is the radius of the midsurface of the deformed pipeline.

Figure 4-3 shows a schematic representation of the cross-section of a deformed pipeline. Assuming a point moves from m in the un-deformed profile to m' in the deformed profile, the circumferential and radial displacements can be evaluated as a function of the mid-surface radius of the pipeline, R_m and the angular distortion of the deformed pipeline, ϕ

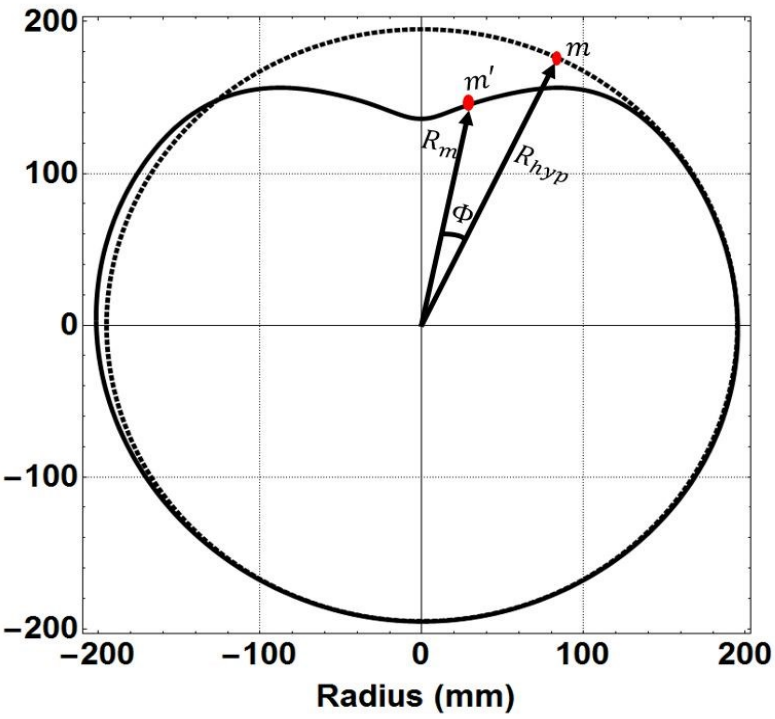

Figure 4-3: Schematic view of the cross sectional view of the mid-surface of a pipeline in the deformed and undeformed states

While the inline inspection devices report the radius of the inner surface of the pipeline, the radius of the mid-surface of the pipeline can be evaluated by considering the component of the thickness of the pipe wall and the associated slope in the deformed configuration. The radial displacement, u_r of the mid surface of the pipeline is evaluated as the difference between the radius of the deformed pipeline and the hypothetical radius. The radius of the mid-surface of the pipeline at the external and the internal surfaces are assumed to be the same and are evaluated using equation (12).

$$u_r = R_m(\theta, z)\mathrm{Cos}[\phi] - R_{hyp}(\theta, z) \quad (12)$$

The overall circumferential deformation of the pipeline is a function of both the deformation resulting from the ovalization of the pipe wall and the deformations as a result of the localized

distortion of the pipe wall owing to the slope of the pipe wall in the circumferential axis. Figure 4-4 below illustrates the deformation of the pipeline in the circumferential, (R-θ) plane.

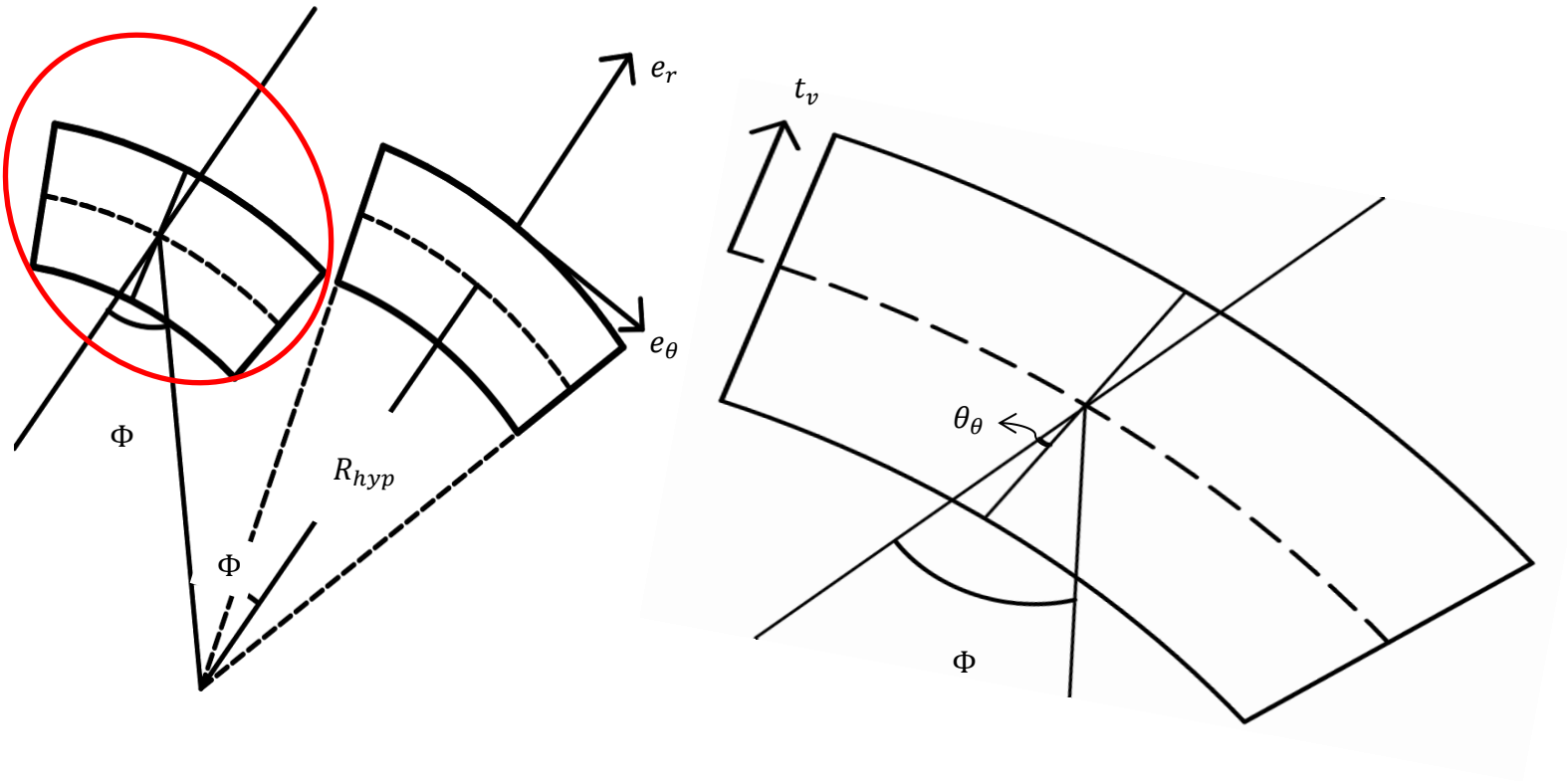

Figure 4-4: Schematic representation of deformation of the pipe wall in the circumferential direction (L) and a zoomed in section of the deformed pipeline (R)

The figure above represents the assumed deformation path of the pipe in the circumferential plane. The pipe deforms from the original configuration to the encircled section in the figure, this displacement is shown to be associated with the angular distortion, ϕ and a circumferential displacement of the mid-surface. However, the pipe wall also deflects locally and the slope developed in this local deformation is termed θ_θ. The circumferential displacement at of the pipeline can be evaluated using the expression in equation (13) below.

$$u_\theta = R_m Sin[\phi] - t_v Sin(\phi - \theta_\theta) \quad (13)$$

where, t_v is the variable thickness along the thickness of the pipe wall such that $(-\frac{t}{2} < t_v < \frac{t}{2})$ where t is the thickness of the pipe wall. The slope of the mid-surface of the pipeline is evaluated at each analyzed cross section of the pipeline using the equation (14).

$$\theta_\theta = \text{ArcTan}\left(\frac{\partial R_m}{R_m \partial \theta}\right) \quad (14)$$

The expression for the circumferential displacement is aligned such that the displacement at the internal surface of the pipeline is evaluated by replacing t_v in equation (13) with $-\frac{t}{2}$, at the mid-surface of the pipeline by replacing t_v with 0 and at the external surface of the pipeline by replacing t_v with $\frac{t}{2}$.

The longitudinal deformations associated with the indentation are evaluated by assuming a linear distribution of displacements along the thickness of the pipe wall. The longitudinal displacement is thus evaluated (while assuming large displacement and rotations) as a function of the longitudinal slope, θ_z of the pipe wall and is evaluated as shown in equation (15)

$$u_z = t_v Sin(\theta_z) \quad (15)$$

where, u_z is the longitudinal displacement. The slope of the deformed pipe wall in the longitudinal axis is evaluated across the circumference of the pipeline as shown in the equation (16) below.

$$\theta_z = \text{Arctan}\left(\frac{\partial u_r}{\partial z}\right) \quad (16)$$

A schematic representation of the deformation in the deformation of the pipeline on the longitudin

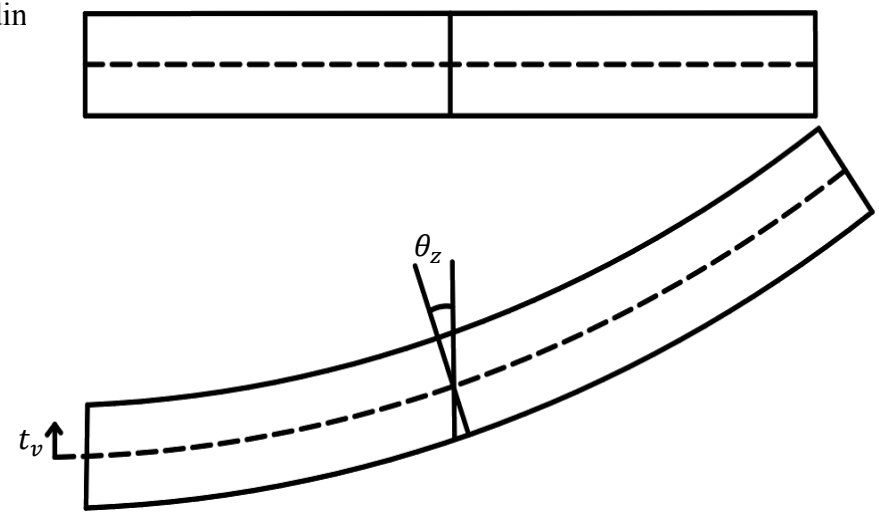

Figure 4-5: Schematic representation of deformation of the pipe wall in the longitudinal direction

4.3.4 Strain Measures

The strain formulation proposed in generating the strain state of the deformed pipeline is a combination of the linearized strain measure and the nonlinear strain measure. As discussed in Adeeb (2011), the linear strain or small strain measure, in its formulation assumes the displacement of the material particles of a deformed body are infinitesimal and as such no change occurs in the geometric and constitutive properties of the material during the deformation. It is mathematically represented in equation (17);

$$\varepsilon_L = \frac{1}{2}(\nabla u + \nabla u^T) \tag{17}$$

The Lagrangian strain measure contains nonlinear terms that account for large deformations and rotations associated with deformation. Equation (18) below represents the expression that defines the Lagrangian strain matrix.

$$\varepsilon_{NL} = \frac{1}{2}(\nabla u + \nabla u^T + \nabla u^T \nabla u) \tag{18}$$

The result of the analytical computation is the strain matrix that defines the strain state of the dented section of the pipe wall. The resulting matrix is shown in equation (19).

$$\varepsilon = \begin{Bmatrix} \varepsilon_{rr} & \varepsilon_{r\theta} & \varepsilon_{rz} \\ \varepsilon_{\theta r} & \varepsilon_{\theta\theta} & \varepsilon_{\theta z} \\ \varepsilon_{zr} & \varepsilon_{z\theta} & \varepsilon_{zz} \end{Bmatrix} \tag{19}$$

The diagonal strain components, ε_{rr}, $\varepsilon_{\theta\theta}$ and ε_{zz} represent the radial, circumferential and longitudinal strain components respectively. The out of plane shear strain components are represented $\varepsilon_{rz}, \varepsilon_{\theta z}, \varepsilon_{z\theta}$ and ε_{zr} and the in plane shear strain components are represented by $\varepsilon_{r\theta}$ and $\varepsilon_{\theta r}$. The restriction on the thickness of the pipe wall affects the accuracies of the strain components; $\varepsilon_{\theta r}$, $\varepsilon_{r\theta}$, ε_{rz} , ε_{zr} and ε_{rr}. It is assumed that the investigated features are aligned in the principal axis and thus the shear strain components $\varepsilon_{\theta r}$, $\varepsilon_{r\theta}$, ε_{rz} , ε_{zr} are not considered in this study.

The radial strain, ε_{rr}, is evaluated as recommended in Noronha et al. (2010), by enforcing compliance of the material model of the pipeline to deformation plasticity. This constraint implies that the sum of the trace of the active strain matrix should be zero. Hence, equation (20) holds.

$$\varepsilon_{rr} = -(\varepsilon_{\theta\theta} + \varepsilon_{zz}) \tag{20}$$

As it is assumed that the pipeline undergoes relatively large deformations in the longitudinal direction characterized by the extension of the membrane of the pipe wall, the trigonometric approximations of the Euler Bernoulli beam theory do not hold and the multiplicative decomposition of the displacement gradient contains nonlinear terms to take into account the expected non linearities. The circumferential strains are evaluated under the premise of the inextensibility of the pipeline's circumference and as such the linearized strain measure is more

appropriate for this axis. The equivalent strains are evaluated in compliance with deformation plasticity as proposed in Noronha et al. (2010).

4.4 Results

4.4.1 Validation of Numerical Models

The load–deformation response used to validate the numerically generated models is shown in figure 4-6. This load deformation plot obtained from the response from the study in Rafi et al. (2012) is benchmarked against the response obtained from the critical node of the numerical model generated.

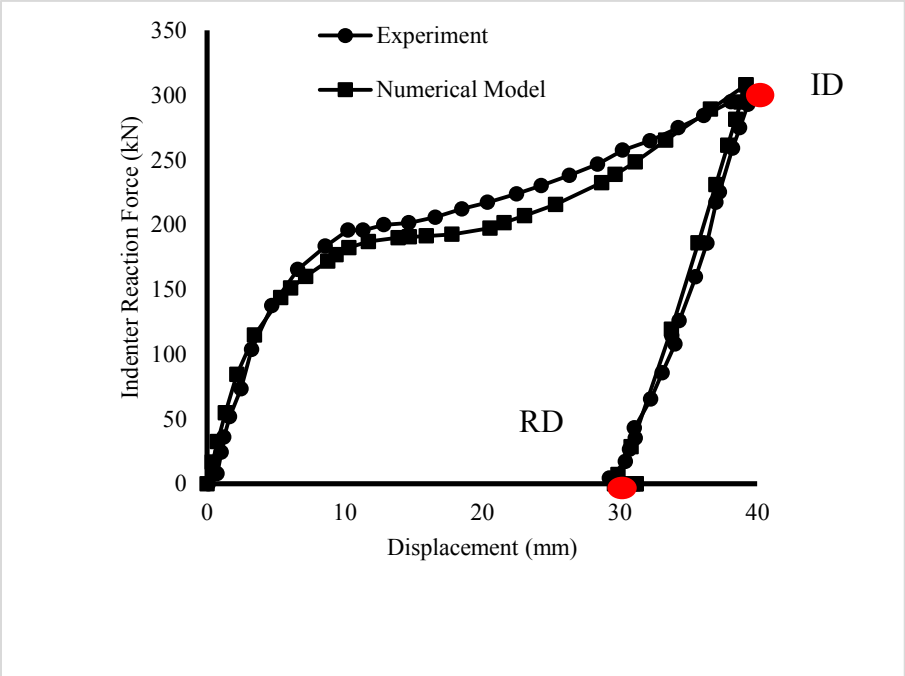

Figure 4-6: Load –Displacement plot

From figure 4-6, it can be seen that the initial load–displacement response is linear in the elastic regime as the forces vary linearly with the indentation depth. At the onset of yielding, the force-

displacement response becomes nonlinear as can be seen in the curve in the force-displacement response plot. This nonlinear response is due to the axial stretching along the length of the pipe local to the indenter. The peak of the force-displacement plot labelled, ID is the initial damage state which corresponds to the maximum indentation depth during contact. On release of the indenting body, the force tends to zero and the elastic portion of the displacement is recovered. The point in the plot tagged RD represents the residual damaged state of the pipeline corresponding to the state of damage after the indenting force has been removed. The flat line is as a result of the increase in the depth of the dent when the internal pressure is turned off. From the plot above it can be seen that both models had a displacement of 40mm at the initial damage state and a displacement of 28mm at the residual damaged state.

4.4.2 Numerical Models

The numerical models of the deformed pipes and the indenters are shown in figure 4-7 below.

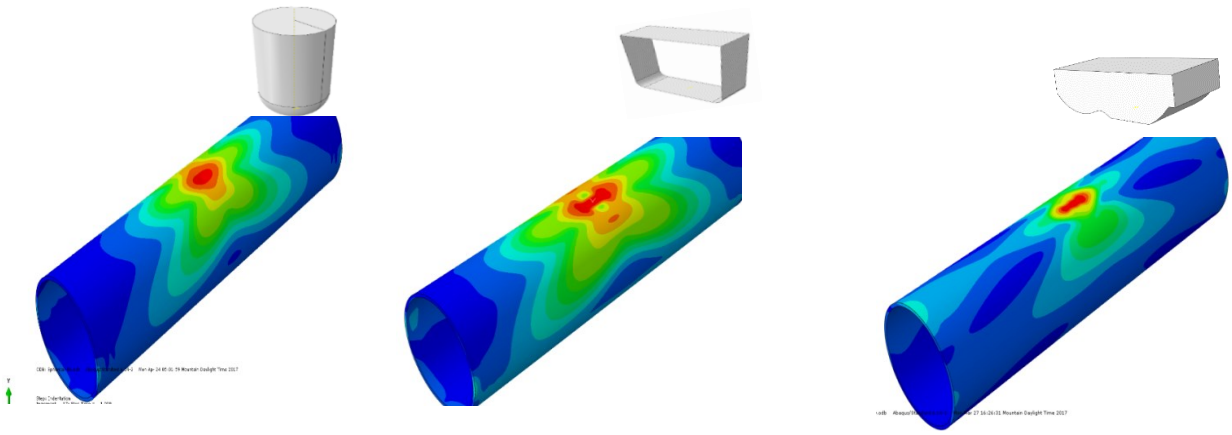

Figure 4-7: Numerical Models (SD, FD and AD)

4.4.3 Spline Interpolation

On extraction of the coordinates of the deformed pipe from the numerical model, B-spline curves were fit to the data set. Figure 4-8 shows the different profiles generated by the SD6 model.

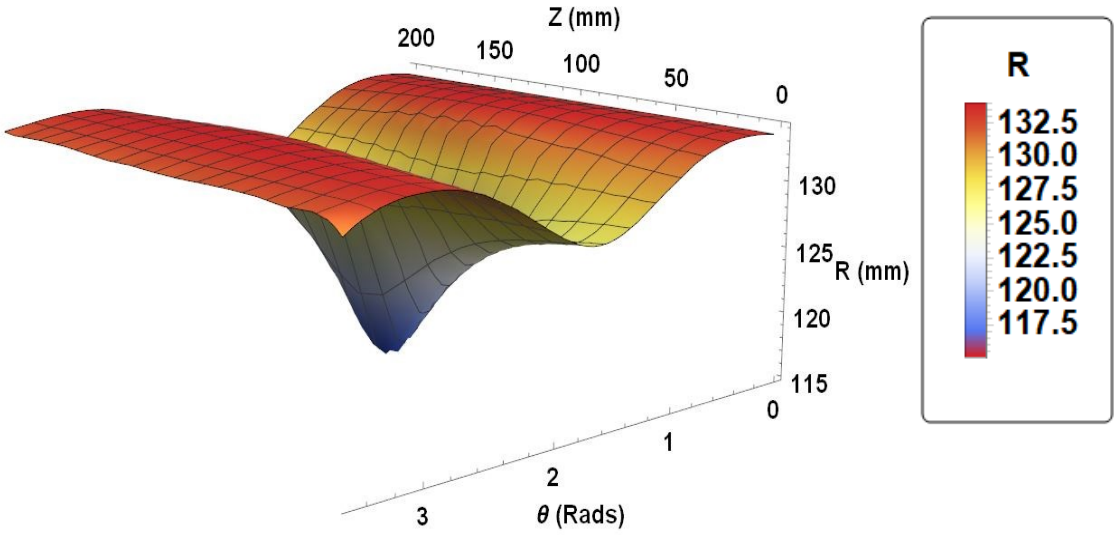

Figure 4-8: Interpolated dent surface of the SD6 model

4.4.4 Deformation Analysis

All contours presented in this study are planer view of the internal surface of the dent effective region of the pipeline, with the horizontal axis representing the longitudinal length of the pipeline and the vertical axis representing the pipeline's circumferential axis. The analytically evaluated radial displacement, (U1) of the SD6 model is obtained using the expressions shown in equation (12) and the radial displacement from the numerical model is obtained from the FEA simulation and the results are shown in the figure 4-9.

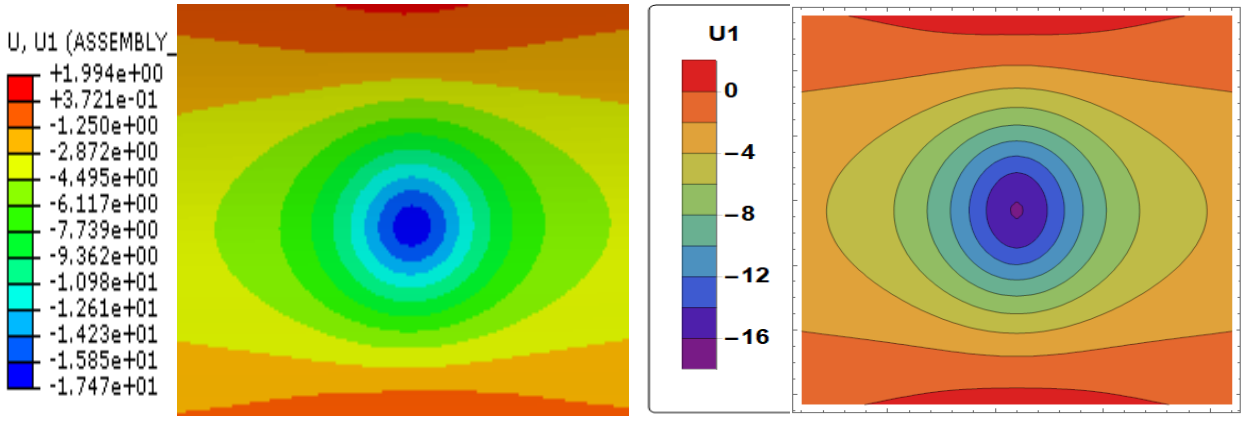

Figure 4-9: SD6- Radial displacement contours (Numerical model (L) Analytical model (R))

From the figure 4-9, the contours represent the U1 magnitudes in mm at the internal surface of the pipe wall. It is observed that the displacement is concentrated at the peak of the dent indicated by the heavy color concentrations at the middle of the planer section shown in the figure. The radial displacement softens further away from the peak of the dent as the pipeline returns to its original contour. A good correlation in the radial displacement predicted by both the analytical and the numerical model is observed with both techniques predicting a radial displacement of 17.5 mm respectively.

The contours of the circumferential displacement, (U2) in mm at the internal surface of the SD6 are shown in figure 4-10. The analytical circumferential displacement is evaluated using equation (13) and the circumferential displacement from the numerical model is obtained from the FEA simulation.

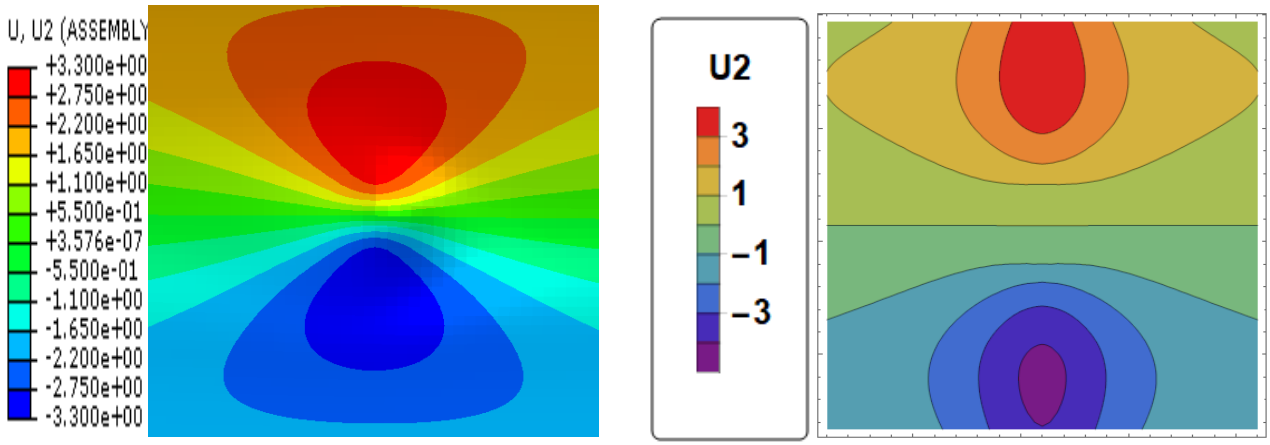

Figure 4-10: SD6-Circumferential displacement contours (Numerical model (L)

Analytical model (R))

A careful inspection of the circumferential deformation contours reveals that the deforming pipeline undergoes significant shape distortion in form of ovalization on both sides of the dent center characterized by the concentrations in the contour plots at the edges of the dent. This deformation mode reduces the amount of shear and extension of the pipe wall. The maximum circumferential displacement obtained by the numerical model and the analytical model at the internal surface of the dent is seen to be approximately 3.3 mm while the maximum circumferential displacement developed by the analytical model is 4.5 mm

The contour plot of the longitudinal displacement, (U3) in mm of SD6 at the internal surface of the dented section of the pipeline is shown in Figure 4-11. The displacements are evaluated assuming large deformations which allows for the associated membrane extension in the longitudinal axis and other nonlinearities associated with the deformation. The analytical longitudinal displacements are evaluated as per equation (15).

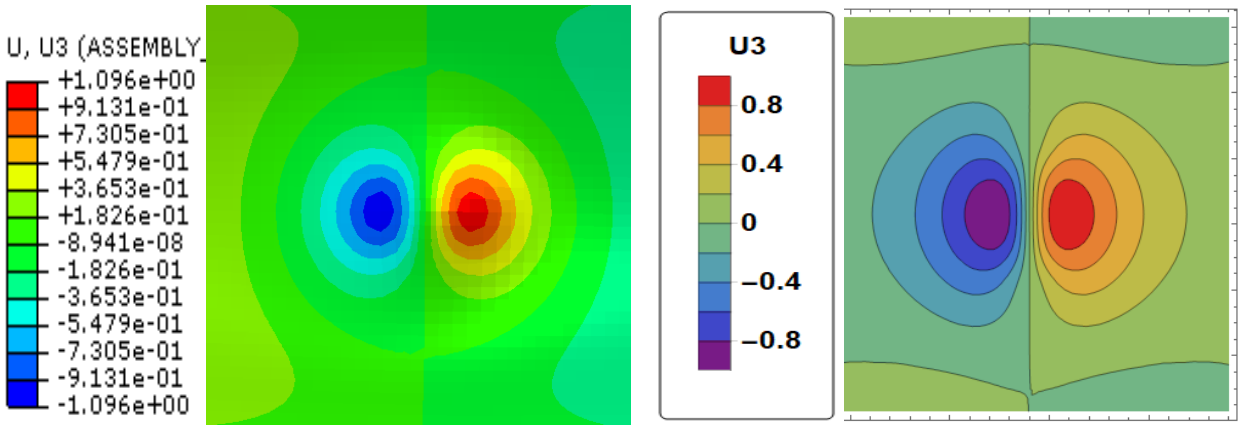

Figure 4-11: SD6-Longitudinal Displacement Contours (Numerical model (L) Analytical model (R))

The longitudinal displacements are concentrated at the shoulder as can be seen in figure 11. The numerical model and the analytical model both predict the peak displacements off the peak of the dent (the centroid of the contours). The longitudinal displacement at the peak of the dent which is the plane of symmetry is zero. An approximate peak value of 1mm is the maximum longitudinal displacement predicted by both the numerical model and the analytical model.

4.4.5 Strain Analysis

The contour plots of the circumferential strains, (LE 22) generated by the proposed technique and by the nonlinear FEA are shown in figure 4-12. It can be observed from figure 4-12 that the strain concentrations are at the peak of the dent and soften away further away from the dent's peak. The spherical geometry of the peak of the indenter is also well defined in the strain distribution. The result from the numerical model predicts a value of 9% while the proposed methodology predicts more conservative strain values having a peak of 10%. Visual inspection of the contours shows as expected, the circumferential strains predicted by both the proposed technique and the numerical models are aligned in the longitudinal axis of the pipe (the horizontal front of the planar section).

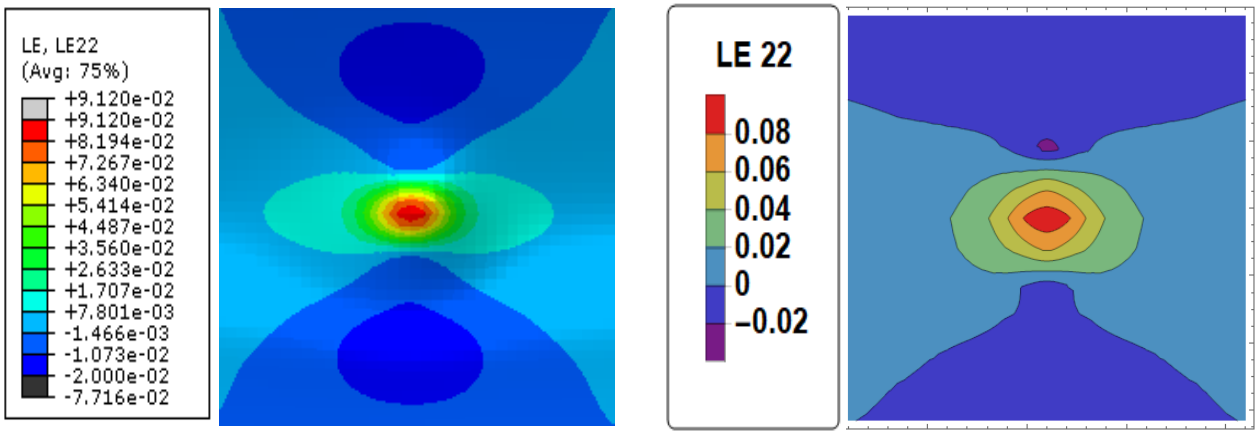

Figure 4-12: SD6-Circumferential strain contours (Numerical model (L) Analytical model (R))

The peak longitudinal strains (LE 33) generated at the internal surface of the pipeline by the numerical model and the proposed methodology are presented in figure 4-13.

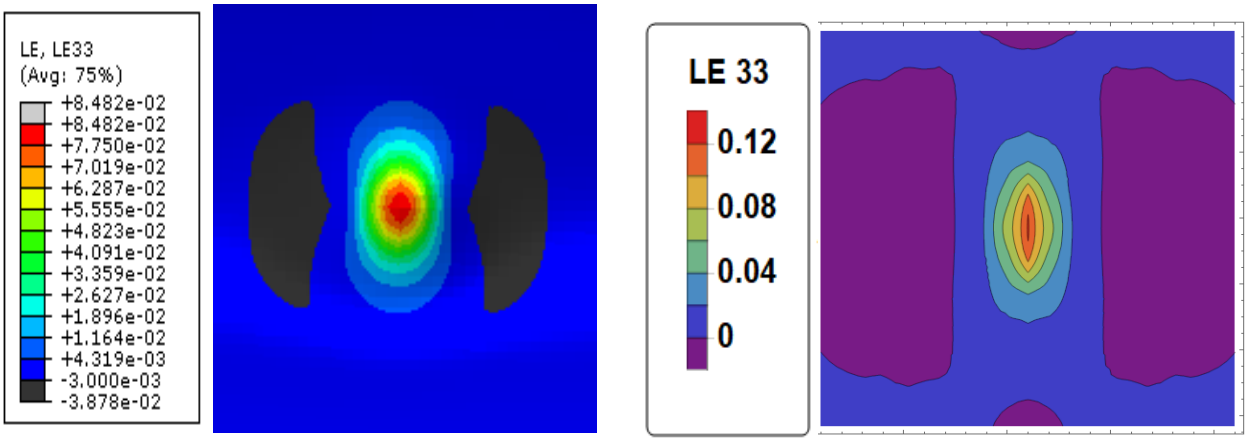

Figure 4-13: SD6-Longitudional strain contours - (Numerical model (L) model (R))

The nonlinear numerical modelling predicts a strain value of 8.5% while the analytical calculations predict a more conservative strain of 13.5%. The longitudinal strains are oriented along the circumferential direction (the vertical front of the planar section)

The peak radial strains predicted by the numerical simulations is 17.3% which is compressive and the analytical procedure predicts conservative strains of 22% compressive strains at the peak of the dent at the internal surface of the pipeline. Figure 4-14 shows the strain distributions obtained from the numerical and the analytical models.

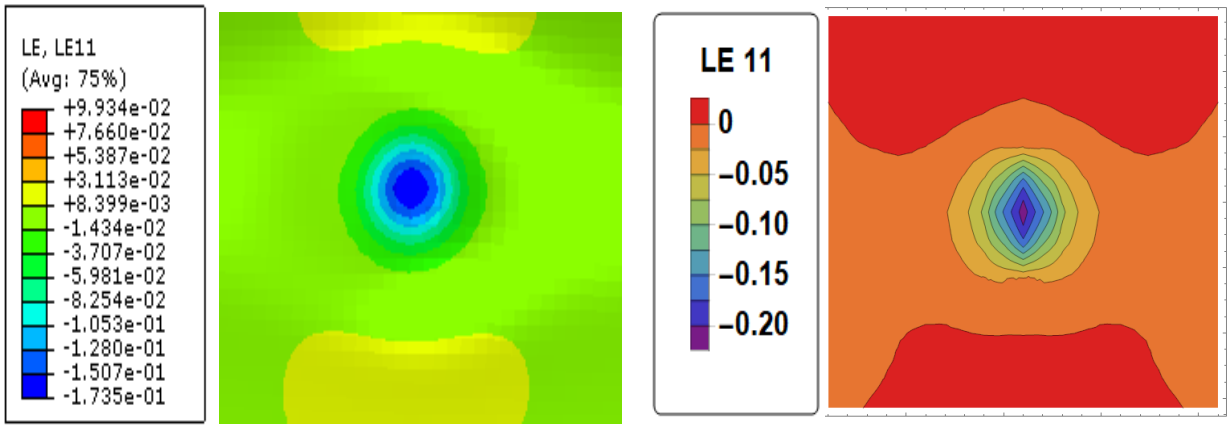

Figure 4-14: SD6-Radial strain contours - (Numerical model (L) Analytical model (R))

The equivalent strains, (PEEQ), evaluated analytically using equation (7) and that predicted by the numerical model are presented in figure 4-15. From figure 4-15, it is obvious a strong similarity in the strains predicted is obtained as while the numerical models predict maximum tensile strain value of 17.2%, the proposed method predicts strain values of 22.5%. The peak PEEQ strains are developed at the internal surface of the dent and occur at the peak of the dent profile.

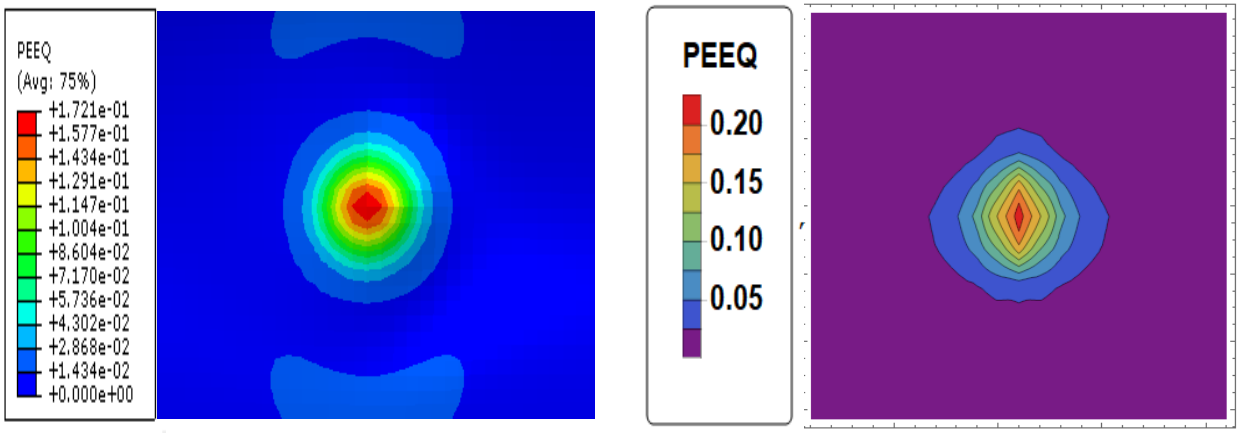

Figure 4-15: SD6- PEEQ Strain Contours (Numerical model (L) Analytical model (R))

The procedure discussed above was implemented on the other analytical models generated in this study and a similar correlation was obtained.

A similar trend was also observed for the other investigated models and the equivalent strains obtained for the FD6 and AD6 models are shown in the figure 4-16 and 4-17. A major difference in the strains predicted is the localization of the strain concentrations, while as expected for the SD models the plastic strains are concentrated at the peak of the dent effective region, for the FD and the AD models, the strain localization occurs at towards the shoulder of the dent.

For the FD models, a symmetrical strain distribution was generated with strain concentrations towards the shoulder of the dent. The numerical models predict a maximum PEEQ value of 13% while the analytical strain model predicts a maximum PEEQ strain value of 14%.

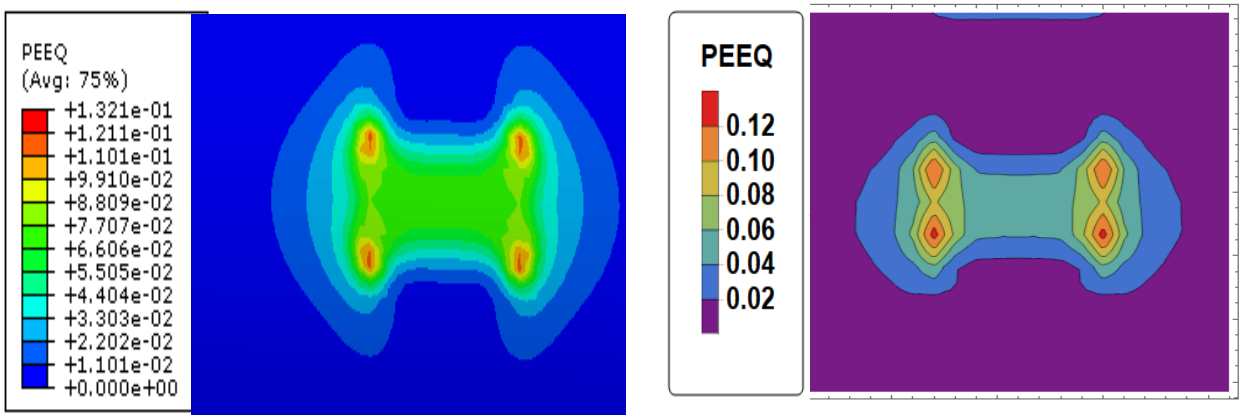

Figure 4-16: FD6- PEEQ Strain Contours (Numerical model (L) Analytical model (R))

For the equivalent strain distribution for the AD models, the maximum strains were located at the region of the sharper peak. The distribution is thus skewed. This is captured by the numerical model as well. The peak strain concentrations are predicted in the same region at the internal surface of the pipeline. The numerical model and the analytical models predict peak values of 10% strains at the internal surface of the pipeline for the AD6 models shown in figure 4-17.

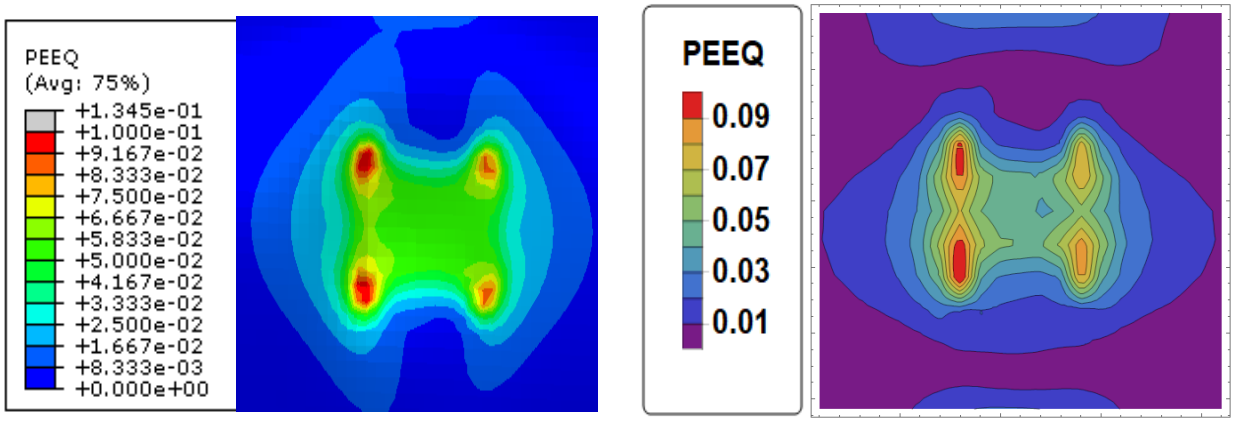

Figure 4-17: AD6- PEEQ Strain Contours (Numerical model (L) Analytical model (R))

4.4.6 Parametric Analysis

The parametric analysis is performed in order to investigate the correlation between the strain values and the dent depth and dent geometry. From the plots generated. fairly similar strain magnitudes and distribution to nonlinear FEA for all the models investigated. The response obtained from the SD, FD and AD models are shown in figure 4-18, 4-19 and 4-20 respectively.

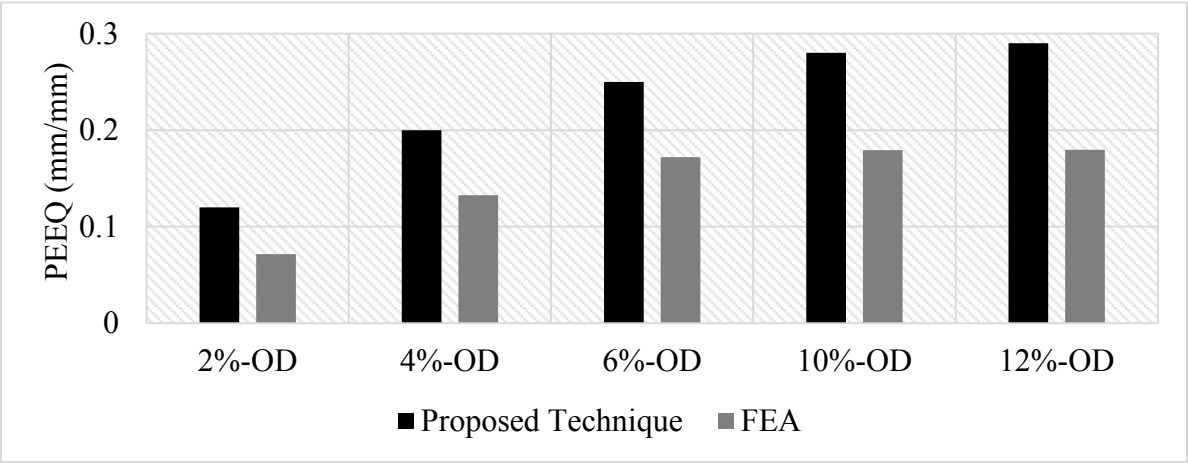

Figure 4-18: Plots of the SD models maximum equivalent strains

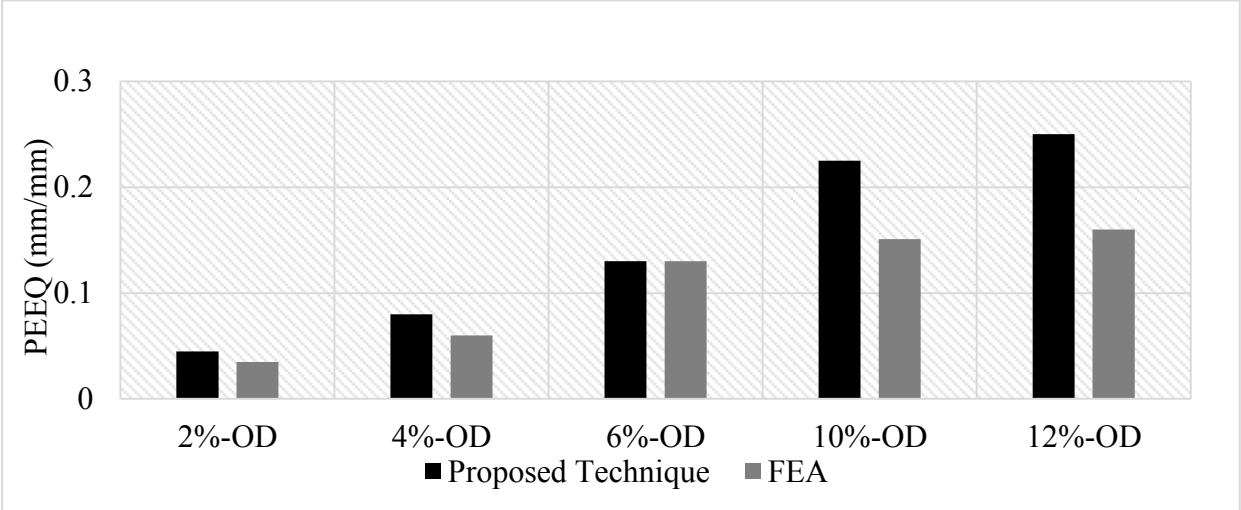

Figure 4-19: Plots of the FD models maximum equivalent strains

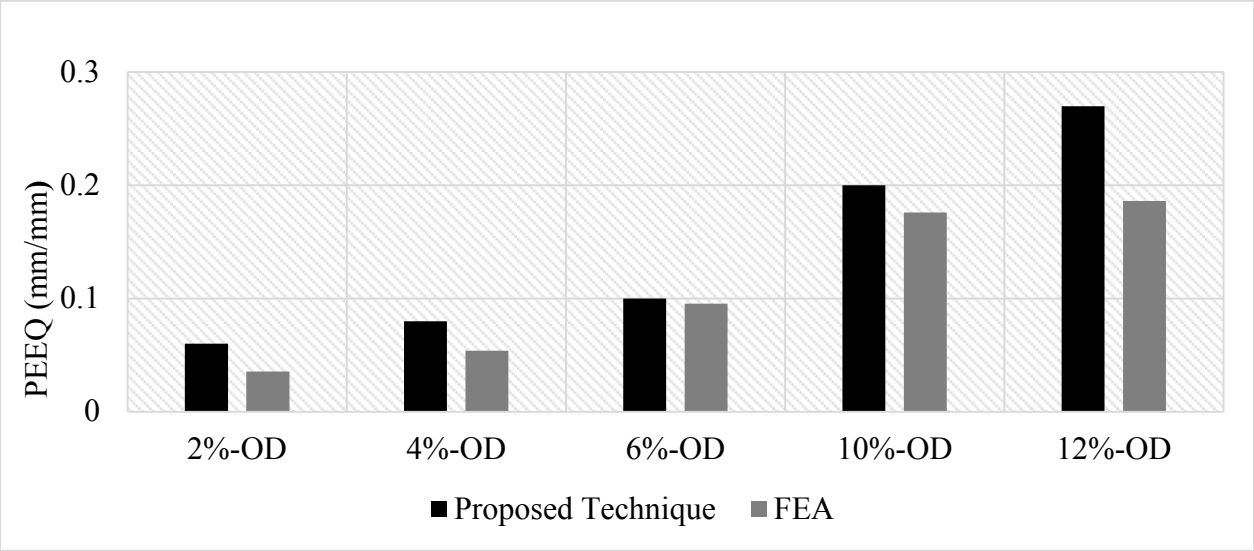

Figure 4-20: Plots of the AD models maximum equivalent strains

From the plots above, the proposed technique is seen to be more conservative than the nonlinear FEA. The strain level is also seen to have some correlation with the dent depth as the magnitude increases with increasing depths. The SD4 model is a typical case where the depth based criterion fails to identify a potential severe dent. As although the depth of the dent is less than 6% OD, the associated strains exceeds the codified threshold of 6% strain.

4.5 Discussions

This computational study is based on the premise that while the pipe might undergo severe ovalization, the response of the cross-sectional plane to the indenting force is predominantly bending rather than the extension of the membrane and as such the change of the length of the pipe in the circumferential direction is ignored. This premise is however valid for shallow dents as the membrane extensions are significant when the dent considered is acute (Rosenfeld et al., 1998).

The raw dent profile obtained from an actual inline inspection tool might have to be filtered using algorithms such as that described in (Hojjati and Lukaciewicz, 2008) to smoothen the data obtained, as unrealistic strains associated with the change in curvature owing to the noise in the dent profile. This concept is however beyond the scope of this study.

The trend in the results obtained so far shows that the technique can capture the associated displacements and the corresponding normal strain components. The shear strain components have however been ignored in this computation as they are believed to have a little effect on the global strain state of the pipeline.

The three dimensional analysis of dented pipelines becomes necessary when analyzing dents with off axis peaks (peaks not aligned with the most severe dent profile). As these analyses is performed by relatively easily programmable algorithms, it would be thus possible to have them implemented by smart inline inspection devices such that an estimate of the strain state of the pipeline is reported instantaneously. This would give operators an insight on how best to channel resources for implementing pipeline dent management strategies.

4.6 Conclusion

The global focus of the work done in this study is to develop a detailed analytical approach to the strain evaluation of dented pipelines so as to ensure effective resource allocation in pipeline dent repair schemes.

The model so developed is an ideal tool for the rapid characterization of dented pipelines. Its ability to be released from the underlying assumptions gives it an edge over the existing analytical models for strain evaluation. The simulations performed so far is targeted at increasing the confidence level in the analytical evaluation of strains in dented pipelines and also create a

platform for more comprehensive dent analysis. The loss of accuracy in the mathematical models is compensated for in terms of computation time, as several FEA runs will have to be performed to attain a geometric match with the reported ILI data.

On the other hand, the mathematical model proposed predicts a strain distribution instantaneously with the input of the coordinates of the dent profile. The major benefit of this proposed technique in comparison to the ASME codified equations are the flexibility in the strain measure and the all-encompassing nature of the methodology as it can be extended to include the effect of internal pressure cycles on the strain state of the pipeline and can be used as a good approximation in evaluating the strain state when deformation features which are not aligned in the principal direction are investigated. It is also necessary to point out that, at this point in time, the mathematical model developed is purely a severity ranking tool and further analysis needs to be carried out on dents identified to be unsuitable. More work should also be done on providing correcting factors to account for fatigue cycling and other possible interacting features.

References

Adeeb, S., 2011. Introduction to Solid Mechanics and Finite Element Analysis using Mathematica. Kendall Hunt.

Alexander, C.R., 1999. Analysis of Dented Pipeline Considering Constrained and Unconstrained Dent Configurations," Proceedings of the Energy Sources Technology Conference and Exhibition, Houston, Texas, USA.

ASME B31.8 Gas Transmission and Distribution Piping Systems. 2007. ASME International, New York, NY.

ASME B31.8 Gas Transmission and Distribution Piping Systems. 2016. ASME International, New York, NY.

Baker, M., 2004. Integrity Management Program–Dent Study, Department of Transportation, Office of Pipeline Safety, TTO Number 10, Delivery Order DTRS56-02-D-70036. Final Report.

Belanger, A.A. and Narayanan, R., 2008. Direct Strain Calculation of Pipe Line Dent from Knot Migration using a Kinematic Model Free of Material Properties. Proceedings of the International Pipeline Conference, Calgary, Alberta, Canada.

Cosham, A. and Hopkins, P., 2003, The Pipeline Defect Assessment Manual (PDAM). A Report to the PDAM Joint Industry Project. Newcastle, UK.

Cosham, A. and Hopkins, P., 2004. The Effect of Dents in Pipelines—Guidance in the Pipeline Defect Assessment Manual. International Journal of Pressure Vessels and Piping, 81(2), pp.127-139.

CSA Z662, Oil and Gas Pipeline Systems 2016.

Erickson, A., 2010, Fatigue Crack Failure Associated with Shallow Dents on Pipelines. NEB. File of-Surv-Inc-02.

Gao, M., McNealy, R., Krishnamurthy, R. and Colquhoun, I., 2008. Strain-Based Models for Dent Assessment—A Review. ASME Paper No. IPC2008-64565. Proceedings of the International Pipeline Conference, Paper No. ASME, IPC04-0061, Calgary, Alberta, Canada.

Hojjati, M.H. and Lukasiewicz, S.A., 2008. Filtering Algorithm for Radial Displacement Measurements of a Dented Pipe. International Journal of Pressure Vessels and Piping, 85(5),

pp.344-349.

Karamanos, S.A. and Andreadakis, K.P., 2006. Denting of Internally Pressurized Tubes under Lateral Loads. International Journal of Mechanical Sciences, 48(10), pp.1080-1094.

Leis, B.N., Forte, T.P. and Zhu, X., 2004. Integrity Analysis for Dents in Pipelines. Proceedings of the International Pipeline Conference, Calgary, Alberta, Canada.

Lukasiewicz, S.A., Czyz, J.A., Sun, C. and Adeeb, S., 2006, Calculation of Strains in Dents Based on High Resolution In-line Caliper Survey. Proceedings of the International Pipeline Conference, Calgary, Alberta, Canada, (pp. 129-134).

Luo, P.F. and Chen, J.N., 2000. Measurement of Curved-Surface Deformation in Cylindrical Coordinates. Experimental Mechanics, 40(4), pp.345-350.

Noronha, D.B., Martins, R.R., Jacob, B.P. and de Souza, E., 2010, Procedures for the Strain Based Assessment of Pipeline Dents. International Journal of Pressure Vessels and Piping, 87(5), pp.254-265.

Noronha, D.B., Martins, R.R., Jacob, B.P. and Souza, E., 2005. The use of B-Splines in the Assessment of Strain Levels Associated with Plain Dents. Proceedings of the Rio Pipeline Conference and Exposition.

Okoloekwe, C., Muntaseer, K., Langer, D., Hassanien, S., Cheng, R., and Adeeb, S. 2017. Deformation Analysis of Dented Pipelines via Surface Interpolation. Proceedings of the Pressure Vessels and Piping Conference, Waikoloa, Hawaii, USA.

Rafi, A.N.M., Das, S., Ghaednia, H., Silva, J., Kania, R. and Wang, R., 2012. Revisiting ASME

Strain-Based Dent Evaluation Criterion. Journal of Pressure Vessel Technology, 134(4), p.041101.

Rosenfeld, M.J., Porter, P.C. and Cox, J.A., 1998, "Strain Estimation using Vetco Deformation Tool Data," Proceedings of the International Pipeline Conference, Calgary, Alberta, Canada.

Woo, J., Muntaseer, K. and Adeeb, S. 2017. Development of a Profile Matching Criteria to Model Dents in Pipelines using Finite Element Analysis. Proceedings of the Pressure Vessels and Piping Conference, Waikoloa, Hawaii, USA.

Chapter 5- Summary and Conclusion

The key focus of this thesis was on improving the strain based criterion for accessing the severity of dents in pipelines.

The academic publication presented as paper 1 in this study, discusses the governing equations used to define the directional displacements associated with the indentation of a pipeline and the evaluation of the strains from the obtained directional displacements. The strains developed along the pipe wall in the mathematical model was benchmarked against results from a nonlinear finite element model. The outcome of this study revealed that the analytical evaluation of the strains from the deformation profile by discretizing the directional displacement were comparable in magnitude and location to the numerically generated models. The ASME B31.8-2016 non mandatory equations for evaluating the directional strains in dented pipelines also predicted comparable strain distributions along the thickness of the pipe wall.

The study presented as paper 2 was focused on improving the implementation of the codified equations. In this study, the ASME B31.8-2016 equations were extended to calculate strain at any point in the dented section of the pipeline. The extension to the three-dimensional continuum is done by interpolating the dented surface with spline functions which allows for the evaluation of the radius of curvature at each point on the dented surface. This procedure makes it possible for considering strain concentrations which might not necessarily be aligned with the deepest point of the dent profile. The three-dimensional render of the strain state is thus more informative and provides a suitable platform for the characterization on dents in order of severity as from this analysis. It will be possible to identify the location of the peak strain values relative to the strain concentrations in the dent effective area and also to a reasonable extent the magnitude of the peak strain value.

Paper 3 presented in this study is focused on extending the technique on displacement discretization technique to a three-dimensional continuum which provides a medium for the concise strain analysis of dented pipelines. By implementing this technique, it thus becomes possible to generate a strain matrix at each vector position of the deformed pipeline and ultimately the strain distribution on the dented section of the pipeline.

However, the cases considered in this study were restrained, unpressurized dents of which the final indentation depth was known. For cases of unrestrained dents, the indentation is accompanied by a rebound and a reround of the pipeline. As such the technique presented here in might fail to capture the actual strain state of the pipeline. The mathematical models presented here in also assumes that the membrane strains developed during the indentation are negligible as the pipeline remains inextensible in the circumferential direction which cannot be generalized for all dent scenarios.

The attempts at improving the existing analytical techniques for evaluating the strains in dented pipelines presented in this study has, however, produced promising results and can be seen as a step in the right direction in optimizing the structural integrity assessment of pipelines. The techniques discussed in this study can easily be implemented by inline inspection devices such that the strain state of dent can be evaluated in real-time. This would go a long way in reducing the computation time required to ascertain the severity of a dent feature in a pipeline.

The scope of this procedure is also not limited to pipelines as the principles used in formulating the expressions are hinged on the fundamentals of the Kirchhoff -Love's Hypothesis and as such is applicable to the strain analysis of thin walled structures. Further work on this subject matter would include developing an analytical model for pressurized pipelines, this inclusion would

thus allow for the analytical fatigue analysis of dented pipelines and thus a more thorough fitness-for-purpose assessment of the defected pipeline.

Bibliography

Adeeb, S.,2011. Introduction to Solid Mechanics and Finite Element Analysis Using Mathematica. Kendall Hunt.

Alexander, C.R., 1999, Analysis of Dented Pipeline Considering Constrained and Unconstrained Dent Configurations," Proceedings of the Energy Sources Technology Conference and Exhibition, Houston, Texas, USA.

ASME B31.8 Gas Transmission and Distribution Piping Systems. 2003. ASME International, New York, NY.

ASME B31.8 Gas Transmission and Distribution Piping Systems. 2007. ASME International, New York, NY.

ASME B31.8 Gas Transmission and Distribution Piping Systems. 2016. ASME International, New York, NY.

Baker, M., 2004. Integrity Management Program–Dent Study. Department of Transportation, Office of Pipeline Safety, TTO Number 10.

Barbian, A. and Beller, M., 2012, In-line Inspection of High Pressure Transmission Pipelines: State-of-the-Art and Future Trends. Proceedings of the 18th World Conference on Nondestructive Testing, Durban, South Africa.

Belanger, A.A. and Narayanan, R., 2008, Direct Strain Calculation of Pipe Line Dent from Knot Migration using a Kinematic Model Free of Material Properties. Proceedings of the International Pipeline Conference.

Bitter, N.P. and Shepherd, J.E., 2013. On the Adequacy of Shell Models for Predicting Stresses and Strains in Thick-Walled Tubes Subjected to Detonation Loading. Pressure Vessels and Piping Conference, Paris, France.

Ciarlet, P.G. and Mardare, C., 2008. An Introduction to Shell Theory. Differential Geometry: Theory and Applications, 9, pp.94-184.

Cosham, A. and Hopkins, P., 2003. The Pipeline Defect Assessment Manual (PDAM) – A Report to the PDAM Joint Industry Project. Newcastle, UK.

Cosham, A. and Hopkins, P., 2004, The Effect of Dents in Pipelines - Guidance in the Pipeline Defect Assessment Manual. International Journal of Pressure Vessels and Piping, 81(2), pp.127-139.

CSA Z662, Oil and Gas Pipeline Systems 2016.

Dawson, S.J., Russell, A. and Patterson, A., 2006. Emerging Techniques for Enhanced Assessment and Analysis of Dents. Proceedings of the International Pipeline Conference, Calgary, Alberta, Canada.

Dinovitzer, A., Lazor, R., Carroll, L.B., Zhou, J., McCarver, F., Ironside, S., Raghu, D. and Keith, K., 2002, Geometric Dent Characterization. 4th International Pipeline Conference (pp. 1589-1598). Calgary, Canada.

Erickson, A., 2010. Fatigue Crack Failure Associated with Shallow Dents on Pipelines. NEB. File of-Surv-Inc-02.

Foroughi, H., Moen, C.D., Myers, A., Tootkaboni, M., Vieira, L. and Schafer, B.W., 2014. Analysis and Design of Thin Metallic Shell Structural Members-Current Practice and Future

Research Needs. in Proc. of Annual Stability Conference Structural Stability Research Council, Toronto, Canada.

Fowler, J.R., 1993, Criteria for Dent Acceptability in Offshore Pipeline. Offshore Technology Conference. Offshore Technology Conference, Houston, Texas, USA.

Gao, M., McNealy, R., Krishnamurthy, R. and Colquhoun, I., 2008. Strain-Based Models for Dent Assessment—A Review. ASME Paper No. IPC2008-64565. Proceedings of the International Pipeline Conference, Paper No. ASME, IPC04-0061, Calgary, Alberta, Canada.

Ghaednia, H., Das, S., Wang, R. and Kania, R., 2015. Safe Burst Strength of a Pipeline with Dent–Crack Defect: Effect of Crack Depth and Operating Pressure. Engineering Failure Analysis, 55, pp.288-299.

Hanif, W. and Kenny, S., 2014, Mechanical Damage and Fatigue Assessment of Dented Pipelines using FEA. Proceedings of the 10th International Pipeline Conference, Calgary, Canada.

Hojjati, M.H. and Lukasiewicz, S.A., 2008. Filtering Algorithm for Radial Displacement Measurements of a Dented Pipe. International Journal of Pressure Vessels and Piping, 85(5), pp.344-349.

Ironside, S.D. and Carroll, L.B., 2002, Pipeline Dent Management Program 2002 4th International Pipeline Conference (pp. 1859-1864). Calgary, Canada.

Karamanos, S.A. and Andreadakis, K.P., 2006. Denting of Internally Pressurized Tubes under Lateral Loads. International Journal of Mechanical Sciences, 48(10), pp.1080-1094.

Koiter, W.T., 1970. The Stability of Elastic Equilibrium. Stanford Univ Ca Dept. of Aeronautics and Astronautics.

Leis, B.N., Forte, T.P. and Zhu, X., 2004. Integrity Analysis for Dents in Pipelines. Proceedings of the International Pipeline Conference, Paper No. ASME, IPC04-0061, Calgary, Alberta, Canada.

Love, A.E.H., 1888. The Small Free Vibrations and Deformation of a Thin Elastic Shell. Philosophical Transactions of the Royal Society of London. A, 179, pp.491-546.

Lukasiewicz, S.A., Czyz, J.A., Sun, C. and Adeeb, S., 2006, Calculation of Strains in Dents Based on High Resolution In-line Caliper Survey. Proceedings of the International Pipeline Conference, Calgary, Alberta, Canada, (pp. 129-134).

Luo, P.F. and Chen, J.N., 2000. Measurement of Curved-Surface Deformation in Cylindrical Coordinates. Experimental Mechanics, 40(4), pp.345-350.

Macdonald, K.A. and Cosham, A., 2005. Best Practice for the Assessment of Defects in Pipelines – Gouges and Dents. Engineering Failure Analysis, 12(5), pp.720-745.

Naghdi, P.M. and Nordgren, R.P., 1963. On The Nonlinear Theory of Elastic Shells under the Kirchhoff Hypothesis. Quarterly of Applied Mathematics, 21(1), pp.49-59.

Noronha, D.B., Martins, R.R., Jacob, B.P. and de Souza, E., 2010, Procedures for the Strain Based Assessment of Pipeline Dents. International Journal of Pressure Vessels and Piping, 87(5), pp.254-265.

Noronha, D.B., Martins, R.R., Jacob, B.P. and Souza, E., 2005. The use of B-Splines in the Assessment of Strain Levels Associated with Plain Dents. Proceedings of the Rio Pipeline Conference and Exposition.

Okoloekwe, C., Muntaseer, K., Langer, D., Hassanien, S., Cheng, R., and Adeeb, S. 2017. Deformation Analysis of Dented Pipelines via Surface Interpolation. Proceedings of the Pressure Vessels and Piping Conference, Hawaii, USA.

Ong, L.S., Soh, A.K. and Ong, J.H., 1992. Experimental and Finite Element Investigation of a Local Dent on a Pressurized Pipe. The Journal of Strain Analysis for Engineering Design, 27(3), pp.177-185.

Panetta, P.D., Diaz, A.A., Pappas, R.A., Taylor, T.T., Francini, R.B. and Johnson, K.I., 2001. Mechanical Damage Characterization in Pipelines. Pacific Northwest National Lab. Richland WASA35467

Race, J.M., Haswell, J.V., Owen, R. and Dalus, B., 2010. UKOPA Dent Assessment Algorithms: A Strategy for Prioritising Pipeline Dents. Proceedings of the 8th International Pipeline Conference, Calgary, Alberta, Canada.

Rafi, A.N.M., Das, S., Ghaednia, H., Silva, J., Kania, R. and Wang, R., 2012. Revisiting ASME Strain-Based Dent Evaluation Criterion. Journal of Pressure Vessel Technology, 134(4), p.041101.

Rafi, A.N.M., Das, S., Ghaednia, H., Silva, J., Kania, R. and Wang, R., 2012. Revisiting ASME Strain-Based Dent Evaluation Criterion. Journal of Pressure Vessel Technology, 134(4).

Reissner, E., 1952. Stress-Strain Relations in the Theory of Thin Elastic Shells. Studies in Applied Mathematics, 31(1-4), pp.109-119.

Rogers, D.F. and Adams, J.A., 1990. Mathematical Elements for Computer Graphics, McGraw-Hill Book Co. New York.

Rosenfeld, M.J., Porter, P.C. and Cox, J.A., 1998, "Strain Estimation using Vetco Deformation Tool Data," Proceedings of the International Pipeline Conference, Calgary, Alberta, Canada.

Rosenfeld, M.J., Porter, P.C. and Cox, J.A., 1998. Strain Estimation using Vetco Deformation Tool Data. International Pipeline Conference, Calgary, Alberta, Canada.

Sanders Jr, J.L., 1963. Nonlinear Theories for Thin Shells. Quarterly of Applied Mathematics, 21(1), pp.21-36.

Ventsel, E. and Krauthammer, T., 2001. Thin Plates and Shells: Theory: Analysis and Applications. CRC press.

Woo, J., Muntaseer, K. and Adeeb, S. 2017. Development of A Profile Matching Criteria to Model Dents in Pipelines using Finite Element Analysis Pressure Vessels and Piping Conference, Hawaii, USA.

Wu, Y.Z.P. and Han, X., 2013. Analysis of Pipe Size Influence on Pipeline Displacement with Plain Dent Based on FE Calculation. International Journal of Computer Science Issues, 10(1), pp.507-510.